Aspects of Supersymmetric Gauge Theories in Two and Three Dimensions

RENWICK, MATTHEW

Aspects of Supersymmetric Gauge Theories in Two and Three Dimensions

Matthew Renwick

A Thesis presented for the degree of
Doctor of Philosophy

Department of Mathematical Sciences
Durham University
United Kingdom

September 2020

Aspects of Supersymmetric Gauge Theories in Two and Three Dimensions

Matthew Renwick

Submitted for the degree of Doctor of Philosophy

September 2020

Abstract: In this thesis we study two- and three-dimensional supersymmetric gauge theories, in particular 2d $\mathcal{N} = (2, 2)$ and 3d $\mathcal{N} = 4$ theories. The techniques of supersymmetric localization and the Jeffrey-Kirwan residue are applied to compute correlation functions in these theories. Using the localization result for the correlation functions of 2d $\mathcal{N} = (2, 2)$ Gauged Linear Sigma Models (GLSMs) on the Omega-deformed two-sphere, we examine the correlation functions of a GLSM describing a non-compact geometry. We investigate the ambiguity in the results for three-point correlators using twisted masses and the Omega deformation, and we compare with previous evaluations of these correlation functions in the literature. For 3d $\mathcal{N} = 4$ $U(N)$ theories, by combining inputs from supersymmetric localization and brane constructions in type IIB string theory, we compute correlation functions of monopole operators that are inserted in an Omega background. We study various examples of correlators involving the product of monopoles of minimal positive and negative charges, and investigate the effects of monopole bubbling and wall-crossing phenomena. Our results are successfully tested using the non-commutative Moyal (star) product and the action of Parity-Time (PT) symmetry.

Declaration

The work in this thesis is based on research carried out in the Department of Mathematical Sciences at Durham University. No part of this thesis has been submitted elsewhere for any degree or qualification.

Acknowledgements

Firstly, I would like to thank my supervisor, Stefano Cremonesi, for his time, patience, enthusiasm, and sharing of knowledge. This thesis would not be possible without his guidance.

I would also like to thank everyone that I have shared an office with throughout my time here and the rest of the Department of Mathematical Sciences for a friendly and supportive working environment. In particular, I would like to thank Philip Glass and Alastair Stewart for interesting discussions, their advice, answering my questions, and being a general sounding board for me. I also thank everyone that I have had the pleasure of being on a pub quiz team with during the past three and a half years.

In addition, I thank the Engineering and Physical Sciences Research Council for providing funding via a PhD studentship.

Finally, I would like to thank my parents for their undying support and my partner Katie for her love, encouragement, and basically putting up with me.

Dedicated to

My Parents

Contents

List of Figures

List of Tables

Chapter 1

Introduction

In the 20$^{\text{th}}$ century, the marriage of special relativity and quantum mechanics was established through the theoretical framework of quantum field theory (QFT). This resulted in the development of the Standard Model, a theory describing the fundamental building blocks of the Universe and their interactions. This theory has had great success, including, most notably, the prediction of the Higgs boson, whose existence was experimentally verified in 2012 at the Large Hadron Collider, CERN. However, the Standard Model is incomplete. Issues include the absence of gravity, the origin of neutrino mass, the asymmetry between matter and anti-matter, the nature of Dark Matter, and the Hierarchy problem. One proposed extension to the Standard Model is supersymmetry.

Supersymmetry is a spacetime symmetry that exchanges bosons (particles of integer spin) with fermions (particles of half-integer spin). It predicts that every particle has a superpartner, with the same mass and quantum numbers, but a different spin. The work of Haag, Łopuszanski, and Sohnius [1], generalising the Coleman-Mandula theorem [2], implies that supersymmetry is the most general spacetime symmetry of an interacting QFT.[1] As a mathematical structure, supersymmetry first appeared in the early 1970s in the context of string theory, which paved the way for Wess and

[1]The maximal group of symmetry is (SuperPoincaré) $\times$ (Compact internal symmety). Relaxing the requirement of particle finiteness allows us to replace SuperPoincaré with SuperConformal symmetry.

Zumino (1974) to write down a supersymmetric field theory in four dimensions [3].

The idea of symmetry has been a key guiding principle throughout the development of physics. Although supersymmetry has not been observed in Nature, there are many theoretical reasons for studying supersymmetric QFTs. Such theories can be viewed as theoretical laboratories for obtaining exact results, even at strong coupling, where the usual tricks of Feynman break down. Supersymmetry provides enhanced theoretical control, allowing the structure of QFTs to be probed, and the non-perturbative behaviour of systems to be studied. It is hoped that by analysing supersymmetric theories we can learn more generic details about QFTs, which would help us to improve our understanding of the real world.

Additionally, string theory, the framework that proposes to unite general relativity and quantum mechanics by replacing point-like particles by one-dimensional objects called strings, relies on supersymmetry for consistency. String theory also contains extended objects called branes, these are dynamical objects that are defined by imposing boundary conditions for open strings. Type IIA (IIB) string theory has Dp branes with p even (odd), where the D refers to Dirichlet boundary conditions. These objects are useful for studying supersymmetric gauge theories because a stack of N coincident Dp branes realises a $(p+1)$-dimensional maximally supersymmetric Yang-Mills (SYM) theory with gauge group $U(N)$. For the case $p = 3$, we have four-dimensional $\mathcal{N} = 4$ $U(N)$ SYM, with 16 Poincaré supercharges. The study of string theory and supersymmetric field theories is also important due to connections with research in mathematics, in particular the areas of geometry and topology. Over recent years, advancements in physics have led to new insights and developments in mathematics.[2]

Dualities have played a central role in the developments of superstring theory and supersymmetric gauge theories. The basic reason for studying dualities is that a difficult question to answer from one perspective can turn into an easier question to answer from another perspective. Electric-magnetic duality, which exchanges electric

[2]Of course physics and mathematics have a long and illustrious history.

and magnetic fields, is an example of a strong-weak duality. By exploiting the idea that the strong coupling limit of one theory is equivalent to the weak coupling limit of another theory, we can learn about the non-perturbative aspects of a given theory by studying its dual theory.

Localization is a technique whose full power has only been exploited recently in the study of supersymmetric field theories. It is a useful tool applied to reduce infinite-dimensional path integrals to finite-dimensional integrals, allowing the exact non-perturbative computation of partition functions. Localization formulae can be used to extract physical and mathematical information about field theories, and provide a method to perform detailed tests of non-perturbative dualities. The localization procedure has been successfully applied to a range of supersymmetric field theories defined on curved backgrounds of various dimensions. Alongside the evaluation of partition functions, the insertion of local and non-local operators has been studied, including order and disorder operators, which are defined as functions of the fundamental fields in the theory and defined through boundary conditions, respectively.

1.1 Thesis Outline

The aim of this thesis is to explore the correlation functions of two- and three-dimensional supersymmetric gauge theories. The computation of such correlation functions, which would be difficult to evaluate by standard methods, is made possible by exploiting the power of supersymmetric localization, and, in the case of 3d theories, inputs from brane constructions in string theory.

The outline of this thesis is as follows.

In chapter 2 we review background material on supersymmetric gauge theories. We recap some basic features of four-dimensional $\mathcal{N} = 1$ supersymmetry. We then discuss the supersymmetry algebra and field content of two-dimensional $\mathcal{N} = (2, 2)$

gauge theories, which are related to 4d $\mathcal{N} = 1$ theories by dimensional reduction. We write down the gauge-invariant Lagrangian for a $U(1)$ gauge symmetry and discuss how topological theories with $\mathcal{N} = (2, 2)$ supersymmetry are obtained through twisting. By minimising the scalar potential appearing in the theory, we study the classical geometry of some examples. We then examine the Coulomb branch vacua and the dualisation of sigma models. Furthermore, we discuss three-dimensional $\mathcal{N} = 4$ gauge theories and focus on the Coulomb branch structure of the moduli space of supersymmetric vacua. Finally, the type IIB brane construction of 3d $\mathcal{N} = 4$ $U(N)$ gauge theories is presented.

In chapter 3 we explain how the technique of supersymmetric localization is used to compute the path integral of a supersymmetric field theory. We then discuss the defining properties and constructive definition of the Jeffrey-Kirwan (JK) residue, whose importance in localization computations has been recognised in the last few years. Finally, we present explicit examples to demonstrate how the JK prescription is applied to compute JK integrals.

In chapter 4 we review the result from supersymmetric localization for the correlation functions of two-dimensional $\mathcal{N} = (2, 2)$ Gauged Linear Sigma Models (GLSMs) on the Omega-deformed two-sphere. We then examine the computation of the correlation functions of a GLSM describing a non-compact geometry. We compare with the previous evaluations of these correlation functions in the literature, discuss some issues with mass regulation, and highlight the ambiguity of the result for three-point correlators.

In chapter 5 we present new results from our paper [4] on the computation of correlators of monopole operators in three-dimensional $\mathcal{N} = 4$ $U(N)$ supersymmetric quantum chromodynamics (SQCD) in the Omega background. We use inputs from supersymmetric localization and brane constructions. Our method is illustrated by presenting several examples of the computations of two- and three-point correlators in $U(2)$ SQCD. We also study various examples of correlators containing products of monopole operators of minimal positive and negative charge in $U(N)$ theories.

Along the way we investigate wall-crossing phenomena and make connection with the non-commutative Moyal (star) product.

Finally, we conclude in chapter 6 by summarising our work and discussing the possible directions for future research. Additional details are collected in appendices.

Chapter 2

Review of Supersymmetric Gauge Theories

We begin this chapter on the familiar ground of 4d $\mathcal{N} = 1$ theories, four-dimensional theories with four Poincaré supercharges. We then discuss the ingredients of lower-dimensional supersymmetric gauge theories. We review Witten's construction of two-dimensional $\mathcal{N} = (2, 2)$ Gauged Linear Sigma Models [5], theories that become strongly coupled in the infrared and flow to Non-Linear Sigma Models. Finally, we present an overview of three-dimensional $\mathcal{N} = 4$ gauge theories and discuss their realisation using a brane construction from type IIB string theory [6].

2.1 Four-dimensional $\mathcal{N} = 1$

We work in Minkowski spacetime with metric $\eta_{\mu\nu} = \text{diag}\,(+1, -1, -1, -1)$, where Greek indices $\mu, \nu, \ldots = 0, 1, 2, 3$ represent spacetime coordinates and Latin indices are used for the spatial directions $i, j, \ldots = 1, 2, 3$. The material presented in this section is standard textbook and lecture material, see for example [7, 8].

The 4d $\mathcal{N} = 1$ supersymmetry algebra is a $\mathbb{Z}_2$ graded algebra $L = L_0 \oplus L_1$. The bosonic even L_0 sector comprises the usual generators of the Poincaré algebra: P_μ

for translations, and $M_{\mu\nu}$ for rotations and boosts. These satisfy the commutation relations

$$\begin{aligned}
[P_\mu, P_\nu] &= 0 \ , \\
[M_{\mu\nu}, P_\lambda] &= -i\eta_{\mu\lambda}P_\nu + i\eta_{\nu\lambda}P_\mu \ , \\
[M_{\mu\nu}, M_{\rho\sigma}] &= -i\eta_{\mu\rho}M_{\nu\sigma} + i\eta_{\nu\rho}M_{\mu\sigma} - i\eta_{\nu\sigma}M_{\mu\rho} + i\eta_{\mu\sigma}M_{\nu\rho} \ .
\end{aligned} \tag{2.1.1}$$

The generators of the fermionic odd L_1 sector are the spin 1/2 complex supercharges Q_α and $\overline{Q}_{\dot\alpha}$, where the Weyl spinor indices are $\alpha, \beta, \ldots = 1, 2$ and $\dot\alpha, \dot\beta, \ldots = 1, 2$, and we have the additional commutation relations[1]

$$\begin{aligned}
&[P_\mu, Q_\alpha] = \left[P_\mu, \overline{Q}_{\dot\alpha}\right] = 0 \ , \\
&[M_{\mu\nu}, Q_\alpha] = i(\sigma_{\mu\nu})_\alpha{}^\beta Q_\beta \ , \\
&\left[M_{\mu\nu}, \overline{Q}^{\dot\alpha}\right] = i(\overline{\sigma}_{\mu\nu})^{\dot\alpha}{}_{\dot\beta}\overline{Q}^{\dot\beta} \ , \\
&\left\{Q_\alpha, \overline{Q}_{\dot\beta}\right\} = 2(\sigma^\mu)_{\alpha\dot\beta}P_\mu \ , \\
&\{Q_\alpha, Q_\beta\} = \left\{\overline{Q}_{\dot\alpha}, \overline{Q}_{\dot\beta}\right\} = 0 \ ,
\end{aligned} \tag{2.1.2}$$

with $(\sigma^\mu)_{\alpha\dot\beta} = (\mathbb{1}, -\sigma_i)_{\alpha\dot\beta}$, and

$$(\sigma_{\mu\nu})_\alpha{}^\beta = \frac{1}{4}\left(\sigma^\mu\overline{\sigma}^\nu - \sigma^\nu\overline{\sigma}^\mu\right)_\alpha{}^\beta \quad , \quad (\overline{\sigma}_{\mu\nu})^{\dot\alpha}{}_{\dot\beta} = \frac{1}{4}\left(\overline{\sigma}^\mu\sigma^\nu - \overline{\sigma}^\nu\sigma^\mu\right)^{\dot\alpha}{}_{\dot\beta} \ , \tag{2.1.3}$$

where σ_i are the Pauli matrices, which satisfy $\sigma_i\sigma_j = \delta_{ij}\mathbb{1} + i\epsilon_{ijk}\sigma_k$, and ϵ_{ijk} is the anti-symmetric Levi-Civita symbol, with $\epsilon_{123} = 1$. The spinor indices are raised and lowered with the Levi-Civita tensors

$$\epsilon^{\alpha\beta} = \epsilon^{\dot\alpha\dot\beta} = \begin{pmatrix} 0 & 1 \\ -1 & 0 \end{pmatrix} \quad , \quad \epsilon_{\alpha\beta} = \epsilon_{\dot\alpha\dot\beta} = \begin{pmatrix} 0 & -1 \\ 1 & 0 \end{pmatrix} \ , \tag{2.1.4}$$

which gives

$$\psi^\alpha = \epsilon^{\alpha\beta}\psi_\beta \quad , \quad \psi_\alpha = \epsilon_{\alpha\beta}\psi^\beta \quad , \quad \overline{\psi}^{\dot\alpha} = \epsilon^{\dot\alpha\dot\beta}\overline{\psi}_{\dot\beta} \quad , \quad \overline{\psi}_{\dot\alpha} = \epsilon_{\dot\alpha\dot\beta}\overline{\psi}^{\dot\beta} \ . \tag{2.1.5}$$

[1]This is the case for minimal generators of the supersymmetry. If we have extended supersymmetry, we introduce an index $I = 1, \ldots, N$ to count the supercharges and the commutation relations are modified. Significantly, the anti-commutator of two supercharges, Q^I_α and Q^J_β or $\overline{Q}_{I\dot\alpha}$ and $\overline{Q}_{J\dot\beta}$, does not necessarily vanish due to the presence of central charges.

We follow the convention that undotted indices are contracted from North-West to South-East, $\psi\chi = \psi^{\alpha}\chi_{\alpha} = \epsilon^{\alpha\beta}\psi_{\beta}\chi_{\alpha}$, whilst dotted indices are contracted from South-West to North-East, $\overline{\psi}\overline{\chi} = \overline{\psi}_{\dot{\alpha}}\overline{\chi}^{\dot{\alpha}} = \epsilon^{\dot{\alpha}\dot{\beta}}\overline{\psi}_{\dot{\alpha}}\overline{\chi}_{\dot{\beta}}$.

It is also possible to have a scalar charge R that generates a $U(1)_R$ symmetry and acts non-trivially on the supercharges

$$[R, Q_{\alpha}] = -Q_{\alpha} \quad , \quad \left[R, \overline{Q}_{\dot{\alpha}}\right] = \overline{Q}_{\dot{\alpha}} \ . \tag{2.1.6}$$

Finally, there can be a global non-R symmetry, a flavour symmetry F, generated by scalar charges that commutes with the generators of the supersymmetry algebra.

To write down supersymmetric actions we introduce superspace, where the bosonic and fermionic fields are components that are packaged into a superfield. Superspace, an extension to (bosonic) Minkowski space x^{μ}, is formulated by introducing the Grassmann odd coordinates θ_{α} and $\overline{\theta}_{\dot{\alpha}}$. The supercharges Q_{α} ($\overline{Q}_{\dot{\alpha}}$) generate translations in θ_{α} ($\overline{\theta}_{\dot{\alpha}}$) and x^{μ}.

The supercharge generators, written as differential operators, are

$$Q_{\alpha} = -i\left(\partial_{\alpha} - i\left(\sigma^{\mu}\overline{\theta}\right)_{\alpha}\partial_{\mu}\right) \quad , \quad \overline{Q}_{\dot{\alpha}} = i\left(\overline{\partial}_{\dot{\alpha}} - i\left(\theta\sigma^{\mu}\right)_{\dot{\alpha}}\partial_{\mu}\right) \ , \tag{2.1.7}$$

where

$$\partial_{\mu} = \frac{\partial}{\partial x^{\mu}} \quad , \quad \partial_{\alpha} = \frac{\partial}{\partial\theta^{\alpha}} \quad , \quad \overline{\partial}_{\dot{\alpha}} = \frac{\partial}{\partial\overline{\theta}^{\dot{\alpha}}} \ . \tag{2.1.8}$$

These derivatives satisfy the following relations

$$\begin{aligned} &\{\partial_{\alpha}, \partial_{\beta}\} = \left\{\overline{\partial}_{\dot{\alpha}}, \overline{\partial}_{\dot{\beta}}\right\} = \left\{\partial_{\alpha}, \overline{\partial}_{\dot{\alpha}}\right\} = 0 \ , \\ &\left\{\partial_{\alpha}, \theta^{\beta}\right\} = \delta_{\alpha}{}^{\beta} \ , \\ &\left\{\overline{\partial}_{\dot{\alpha}}, \overline{\theta}^{\dot{\beta}}\right\} = \delta_{\dot{\alpha}}{}^{\dot{\beta}} \ , \\ &\left\{\partial_{\alpha}, \overline{\theta}^{\dot{\alpha}}\right\} = \left\{\overline{\partial}_{\dot{\alpha}}, \theta^{\alpha}\right\} = 0 \ . \end{aligned} \tag{2.1.9}$$

In addition, the supercovariant derivatives are

$$D_{\alpha} = \partial_{\alpha} + i\left(\sigma^{\mu}\overline{\theta}\right)_{\alpha}\partial_{\mu} \quad , \quad \overline{D}_{\dot{\alpha}} = \overline{\partial}_{\dot{\alpha}} + i\left(\theta\sigma^{\mu}\right)_{\dot{\alpha}}\partial_{\mu} \ , \tag{2.1.10}$$

which satisfy the anti-commutation relations

$$\{D_\alpha, D_\beta\} = \left\{\overline{D}_{\dot\alpha}, \overline{D}_{\dot\beta}\right\} = 0 \quad , \quad \left\{D_\alpha, \overline{D}_{\dot\alpha}\right\} = -2(\sigma^\mu)_{\alpha\dot\alpha} P_\mu \ . \tag{2.1.11}$$

A generic superfield $Y\left(x, \theta, \overline{\theta}\right)$ can be Taylor expanded in terms of its components

$$\begin{aligned} Y(x,\theta,\overline{\theta}) = y(x) + \theta\psi(x) + \overline{\theta}\overline{\chi}(x) + \theta\theta m(x) + \overline{\theta}\overline{\theta}\overline{n}(x) \\ + \theta\sigma^\mu\overline{\theta} v_\mu(x) + \theta\theta\overline{\theta}\overline{\lambda}(x) + \overline{\theta}\overline{\theta}\theta\rho(x) + \theta\theta\overline{\theta}\overline{\theta} D(x) \ , \end{aligned} \tag{2.1.12}$$

which terminates due to the Grassmann nature of the $\theta, \overline{\theta}$ coordinates. The spinor indices in this expression have been contracted and so are suppressed in the notation, for instance $\theta\sigma^\mu\overline{\theta} = \theta^\alpha(\sigma^\mu)_{\alpha\dot\beta}\overline{\theta}^{\dot\beta}$.

A general superfield has too many components to be an irreducible representation of the supersymmetry algebra. Consequently, we must impose constraints to reduce the number of components consistently with the supersymmetry algebra. This can be achieved by using a reality condition or a differential constraint.

A chiral superfield Φ is obtained by imposing the constraint $\overline{D}_{\dot\alpha}\Phi = 0$. The component expansion of this superfield, using the coordinate change $y^\mu = x^\mu + i\theta\sigma^\mu\overline{\sigma}$, is

$$\Phi(y) = \phi(y) + \sqrt{2}\theta\psi(y) - \theta\theta F(y) \ , \tag{2.1.13}$$

where ϕ is a complex scalar, ψ is a Weyl fermion, and F is a complex auxiliary scalar. The supersymmetry transformations of these components are

$$\begin{aligned} \delta\phi &= \sqrt{2}\zeta\psi \ , \\ \delta\psi_\alpha &= -\sqrt{2}\zeta_\alpha F + 2i(\sigma^\mu\overline{\zeta})_\alpha\partial_\mu\phi \ , \\ \delta F &= -i\sqrt{2}\partial_\mu\psi\sigma^\mu\overline{\zeta} \ , \end{aligned} \tag{2.1.14}$$

where $\zeta, \overline{\zeta}$ are the supersymmetry transformation parameters. Similarly, the anti-chiral superfield $\overline{\Phi}$, the conjugate to the chiral superfield, is obtained from the constraint $D_\alpha\overline{\Phi} = 0$.

The supersymmetry transformations in (2.1.14) are obtained from

$$\delta\Phi(y) = i\left(\zeta Q + \overline{\zeta Q}\right)\Phi(y) = \left[\zeta^\alpha \partial_\alpha + 2i\left(\theta\sigma^\mu\overline{\zeta}\right)\partial_\mu\right]\Phi(y)\ , \tag{2.1.15}$$

where the two terms in the square brackets in the last step are the supercharges from (2.1.7) changed to the y coordinate basis and now $\partial_\mu = \frac{\partial}{\partial y^\mu}$. Acting with the appropriate derivatives, (2.1.15) becomes

$$\delta\Phi(y) = \sqrt{2}\zeta\psi - 2\zeta\theta F + 2i\left(\theta\sigma^\mu\overline{\zeta}\right)\left[\partial_\mu\phi + \sqrt{2}\theta\partial_\mu\psi\right]\ . \tag{2.1.16}$$

The term that comes with no θ gives us the expression for $\delta\phi$ in (2.1.14). Likewise, collecting the terms with $\sqrt{2}\theta$ and $-\theta\theta$ we find the transformations $\delta\psi_\alpha$ and δF in (2.1.14), respectively, after applying the helpful identity $\theta^\alpha\theta^\beta = -\frac{1}{2}\epsilon^{\alpha\beta}\theta\theta$.

The most general supersymmetric action involving (anti-)chiral superfields with at most two derivatives is given by

$$S = \int \mathrm{d}^4x\mathrm{d}^2\theta\mathrm{d}^2\overline{\theta}K\left(\Phi,\overline{\Phi}\right) + \left(\int \mathrm{d}^4x\mathrm{d}^2\theta W(\Phi) + c.c.\right)\ , \tag{2.1.17}$$

where $\mathrm{d}^2\theta = \frac{1}{2}\mathrm{d}\theta^1\mathrm{d}\theta^2$ and $\mathrm{d}^2\overline{\theta} = \frac{1}{2}\mathrm{d}\overline{\theta}^{\dot{2}}\mathrm{d}\overline{\theta}^{\dot{1}}$. Integration over a Grassmann coordinate θ satisfies

$$\int \mathrm{d}\theta\,(a + \theta b) = b\ , \tag{2.1.18}$$

which is equivalent to differentiating the integrand with respect to θ. Due to the anti-commuting nature of these coordinates we have

$$\int \mathrm{d}\theta^1\mathrm{d}\theta^2\theta^2\theta^1 = 1\ \ ,\ \ \int \mathrm{d}\theta^1\mathrm{d}\theta^2\theta^1\theta^2 = -1\ . \tag{2.1.19}$$

The first term in (2.1.17) is the D-term, where $K\left(\Phi,\overline{\Phi}\right)$ is the Kähler Potential, a real function of $\Phi,\overline{\Phi}$. This governs the kinetic terms for chiral multiplets. The Grassmann integral $\int \mathrm{d}^2\theta\mathrm{d}^2\overline{\theta}$ picks out the top component of $K\left(\Phi,\overline{\Phi}\right)$, i.e. the term that comes with $\theta\theta\overline{\theta}\overline{\theta}$ in its component expansion. The action is invariant under a Kähler transformation

$$K\left(\Phi,\overline{\Phi}\right) \to K\left(\Phi,\overline{\Phi}\right) + \Lambda(\Phi) + \overline{\Lambda}(\overline{\Phi})\ , \tag{2.1.20}$$

where $\Lambda(\Phi)$ $\left(\overline{\Lambda}(\overline{\Phi})\right)$ is an arbitrary (anti-)chiral superfield.

The second term in (2.1.17) is the F-term, where $W(\Phi)$ is the superpotential, a holomorphic function of Φ. The Grassmann integral $\int \mathrm{d}^2\theta$ picks out the top component, $\theta\theta$, of $W(\Phi)$. To ensure that the action is invariant under a global $U(1)_R$ symmetry, the Kähler Potential and superpotential must carry R charges 0 and 2, respectively.[2]

We can consider a renormalisable theory with a set of chiral superfields Φ^i, where $i = 1, \ldots, N$. In this case, the Kähler Potential and superpotential are restricted to the form

$$K\left(\Phi^i, \overline{\Phi}_i\right) = \overline{\Phi}_i \Phi^i \quad , \quad W(\Phi^i) = a_i \Phi^i + \frac{1}{2} m_{ij} \Phi^i \Phi^j + \frac{1}{3} g_{ijk} \Phi^i \Phi^j \Phi^k \ , \tag{2.1.21}$$

for some arbitrary coefficients a_i, m_{ij}, g_{ijk}. Consequently, the action (2.1.17) becomes

$$\begin{aligned} S = & \int \mathrm{d}^4x \mathrm{d}^2\theta \mathrm{d}^2\overline{\theta} \overline{\Phi}_i \Phi^i + \left(\int \mathrm{d}^4x \mathrm{d}^2\theta W(\Phi^i) + c.c. \right) \\ = & \int \mathrm{d}^4x \left[\left| \partial_\mu \phi^i \right|^2 - i\psi^i \sigma^\mu \partial_\mu \overline{\psi}_i + \overline{F}_i F^i - \left(\partial_i W\right) F^i - \left(\overline{\partial}^i \overline{W}\right) \overline{F}_i \right. \\ & \left. - \frac{1}{2} \left(\partial_i \partial_j W\right) \psi^i \psi^j - \frac{1}{2} \left(\overline{\partial}^i \overline{\partial}^j \overline{W}\right) \overline{\psi}_i \overline{\psi}_j \right] \ , \end{aligned} \tag{2.1.22}$$

where

$$\partial_i W = \frac{\partial W}{\partial \Phi^i} \quad , \quad \overline{\partial}^i \overline{W} = \frac{\partial \overline{W}}{\partial \overline{\Phi}_i} \ . \tag{2.1.23}$$

The auxiliary fields, F^i and $\overline{F}_i$, can be integrated out and the solution to their equations of motion are

$$F^i = \frac{\partial \overline{W}}{\partial \overline{\phi}_i} \quad , \quad \overline{F}_i = \frac{\partial W}{\partial \phi^i} \ . \tag{2.1.24}$$

Substituting these back into the action (2.1.22), we obtain the scalar potential

$$U(\phi^i, \overline{\phi}_i) = \overline{F}_i F^i = \sum_{i=1}^{N} \left| \frac{\partial W}{\partial \phi^i} \right|^2 \ . \tag{2.1.25}$$

The moduli space of supersymmetric vacua $\mathcal{M}$ is given by the solutions to $U(\phi^i, \overline{\phi}_i) = 0$. In this case, the zeros of the scalar potential are simply given by

$$\frac{\partial W}{\partial \phi^i} = 0 \quad \Rightarrow \quad \left\langle \phi^i \right\rangle = \text{constant} \ , \tag{2.1.26}$$

[2]Since the Grassmann coordinates θ^α and $\overline{\theta}^{\dot{\alpha}}$ have R charges 1 and -1, respectively.

and so we can write

$$\mathcal{M} = \left\{ \left\langle \phi^i \right\rangle = \text{constant} \middle| \frac{\partial W}{\partial \phi^i} = 0 \ \forall i \right\} \ . \tag{2.1.27}$$

Relaxing the requirement of renormalisability allows for theories with a general Kähler Potential of degree greater than 2. These theories are called Non-Linear Sigma Models (NLSMs). In section 2.2 we will consider supersymmetric gauge theories (with $\mathcal{N}=(2,2)$ supersymmetry), where a vector superfield V is introduced, which is obtained by taking the generic superfield (2.1.12) and imposing the constraint $Y = Y^\dagger$.

The moduli space of supersymmetric vacua is an object of physical and mathematical interest. We now study an explicit example involving the computation of a moduli space, where we see that the space is comprised of a union of branches that intersect at a point.

Consider a model of three chiral superfields, X, Y, and Z, with the homogeneous superpotential $W(X,Y,Z) = XYZ$. The scalar potential is given by

$$U = |\partial_X W|^2 + |\partial_Y W|^2 + |\partial_Z W|^2 = |YZ|^2 + |XZ|^2 + |XY|^2 \ . \tag{2.1.28}$$

The moduli space of vacua, the set of constant field configurations that minimise the potential, is

$$\mathcal{M} = \{ X, Y, Z \in \mathbb{C} \,|\, YZ = XZ = XY = 0 \} \ . \tag{2.1.29}$$

These F-term equations are solved by setting any two of X, Y, Z to zero. Therefore, there are three possibilities

$$\begin{aligned} \mathcal{M}_X &= \{ X \in \mathbb{C}, Y = Z = 0 \} \ , \\ \mathcal{M}_Y &= \{ Y \in \mathbb{C}, X = Z = 0 \} \ , \\ \mathcal{M}_Z &= \{ Z \in \mathbb{C}, X = Y = 0 \} \ . \end{aligned} \tag{2.1.30}$$

Consequently, the moduli space is given by $\mathcal{M} = \mathcal{M}_X \cup \mathcal{M}_Y \cup \mathcal{M}_Z$, which we illustrate in Figure 2.1. This figures highlights that this moduli space is composed of

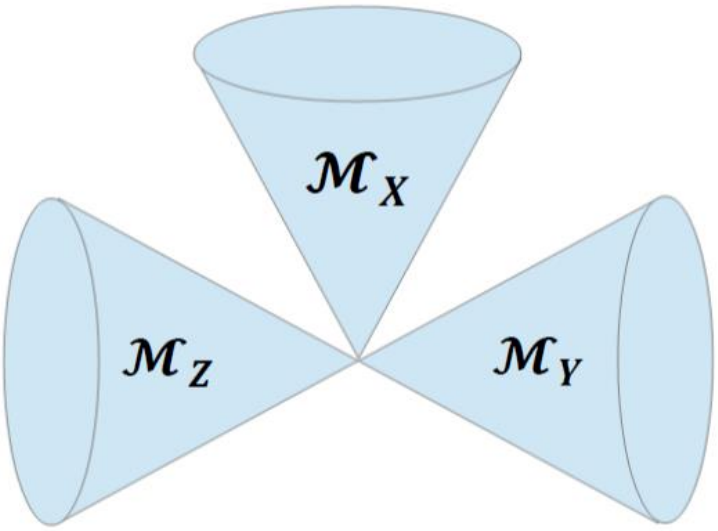

Figure 2.1: The moduli space for a model with three chiral superfields X, Y, Z and the superpotential $W(X, Y, Z) = XYZ$.

three branches that intersect at the origin, which is the singular point where X, Y, and Z vanish.

2.2 Two-dimensional $\mathcal{N} = (2, 2)$

The study of two-dimensional theories is particularly significant due to the shared dynamical and quantum properties with four-dimensional theories and links to string theory. 2d $\mathcal{N} = (2, 2)$ supersymmetry is obtained from the dimensional reduction of 4d $\mathcal{N} = 1$ supersymmetry. In this section, we follow the conventions of [9]. We restrict to the case of abelian gauge theories and write down the generic gauge-invariant supersymmetric Lagrangian for a single $U(1)$ gauge group.

2.2.1 Supersymmetry Algebra

The $\mathcal{N} = (2, 2)$ supersymmetry algebra is generated by the four real supercharges $Q_\pm$ and $\overline{Q}_\pm$, the Hamiltonian H for time translations, the momentum P for spatial translations, and the Lorentz generator M. In addition, there are two kinds of $U(1)$ symmetries, vector and axial R symmetries, which are generated by F_V and F_A,

respectively. These obey the following (anti-)commutation relations

$$\begin{aligned}
&Q_\pm^2 = \overline{Q}_\pm^2 = 0 \ , \\
&\{Q_\pm, \overline{Q}_\pm\} = (H \pm P) \ , \\
&\{\overline{Q}_+, \overline{Q}_-\} = \{Q_+, Q_-\} = 0 \ , \\
&\{Q_-, \overline{Q}_+\} = \{Q_+, \overline{Q}_-\} = 0 \ , \\
&[M, Q_\pm] = \mp Q_\pm \ , \ \left[M, \overline{Q}_\pm\right] = \mp \overline{Q}_\pm \ , \\
&[F_V, Q_\pm] = -Q_\pm \ , \ \left[F_V, \overline{Q}_\pm\right] = \overline{Q}_\pm \ , \\
&[F_A, Q_\pm] = \mp Q_\pm \ , \ \left[F_A, \overline{Q}_\pm\right] = \pm \overline{Q}_\pm \ ,
\end{aligned} \tag{2.2.1}$$

where $\pm$ are left/right handed spinor indices. Under the $U(1)$ vector and axial R rotations, the Grassmann coordinates transform as

$$\begin{aligned}
&U(1)_V : \theta^\pm \to e^{-i\alpha}\theta^\pm \quad , \quad \overline{\theta}^\pm \to e^{i\alpha}\overline{\theta}^\pm \ , \\
&U(1)_A : \theta^\pm \to e^{\mp i\beta}\theta^\pm \quad , \quad \overline{\theta}^\pm \to e^{\pm i\beta}\overline{\theta}^\pm \ .
\end{aligned} \tag{2.2.2}$$

The algebra (2.2.1) is invariant under an automorphism, which is described by the exchange of the generators

$$Q_- \leftrightarrow \overline{Q}_- \quad , \quad F_V \leftrightarrow F_A \ . \tag{2.2.3}$$

This symmetry is called two-dimensional mirror symmetry [10, 11]. Two theories that are equivalent under the exchange of these generators are said to be mirror to each other.

2.2.2 Field Content

Gauge theories with $\mathcal{N} = (2,2)$ supersymmetry in two dimensions contain the following ingredients.

Firstly, we have a real vector superfield V, with the gauge transformation $V \to V + i\left(\overline{\Lambda} - \Lambda\right)$, for some arbitrary chiral superfield Λ and its conjugate $\overline{\Lambda}$. The vector

superfield $V = \left(v_\mu, \sigma, \overline{\sigma}, \lambda_\mu, \overline{\lambda}_\mu, D\right)$ contains a real gauge field v_μ, the complex conjugate scalars $\sigma, \overline{\sigma}$, Dirac fermions $\lambda_\mu, \overline{\lambda}_\mu$, and a real auxiliary scalar D, transforming in the adjoint representation of the gauge group. In Wess-Zumino (WZ) gauge, the component expansion of this superfield is given by

$$\begin{aligned} V = {} & \theta^-\overline{\theta}^-(v_0 - v_1) + \theta^+\overline{\theta}^+(v_0 + v_1) - \theta^-\overline{\theta}^+\sigma - \theta^+\overline{\theta}^-\overline{\sigma} \\ & + i\theta^-\theta^+\left(\overline{\theta}^-\overline{\lambda}_- + \overline{\theta}^+\overline{\lambda}_+\right) + i\overline{\theta}^+\overline{\theta}^-\left(\theta^-\lambda_- + \theta^+\lambda_+\right) + \theta^-\theta^+\overline{\theta}^+\overline{\theta}^- D \ , \end{aligned} \tag{2.2.4}$$

and the supersymmetry variations of the component fields are

$$\begin{aligned} \delta v_\pm &= i\overline{\zeta}_\pm\lambda_\pm + i\zeta_\pm\overline{\lambda}_\pm \ , \\ \delta\sigma &= -i\overline{\zeta}_+\lambda_- - i\zeta_-\overline{\lambda}_+ \ , \\ \delta\overline{\sigma} &= -i\zeta_+\overline{\lambda}_- - i\overline{\zeta}_-\lambda_+ \ , \\ \delta\lambda_+ &= i\zeta_+\left(D + iF_{01}\right) + 2\zeta_-\partial_+\overline{\sigma} \ , \\ \delta\lambda_- &= i\zeta_-\left(D - iF_{01}\right) + 2\zeta_+\partial_-\sigma \ , \\ \delta\overline{\lambda}_+ &= -i\overline{\zeta}_+\left(D - iF_{01}\right) + 2\overline{\zeta}_-\partial_+\sigma \ , \\ \delta\overline{\lambda}_- &= -i\overline{\zeta}_-\left(D + iF_{01}\right) + 2\overline{\zeta}_+\partial_-\overline{\sigma} \ , \\ \delta D &= -\overline{\zeta}_+\partial_-\lambda_+ - \overline{\zeta}_-\partial_+\lambda_- + \zeta_+\partial_-\overline{\lambda}_+ + \zeta_-\partial_+\overline{\lambda}_- \ , \end{aligned} \tag{2.2.5}$$

where $F_{01} = \partial_0 v_1 - \partial_1 v_0$, and we have the supersymmetry transformation

$$\delta = \zeta_+ Q_- - \zeta_- Q_+ - \overline{\zeta}_+\overline{Q}_- + \overline{\zeta}_-\overline{Q}_+ \ , \tag{2.2.6}$$

with supersymmetry parameters $\zeta_\pm, \overline{\zeta}_\pm$.

Additionally, there is a chiral superfield Φ, which satisfies the constraint $\overline{D}_\pm\Phi = 0$. This has charge Q under an abelian gauge group and its gauge transformation is given by $\Phi \to e^{iQ\Lambda}\Phi$. The chiral multiplet $\Phi = (\phi, \psi_-, \psi_+, F)$ contains a complex scalar ϕ, a complex Dirac spinor ψ, and a complex auxiliary scalar F, transforming in a representation $\mathcal{R}_\Phi$ of the gauge group. The component expansion of this superfield takes the form

$$\Phi = \phi(y) + \theta^+\psi_+(y) + \theta^-\psi_-(y) + \theta^+\theta^- F(y) \ , \tag{2.2.7}$$

where $y^{\pm} = x^{\pm} - i\theta^{\pm}\overline{\theta}^{\pm}$. The supersymmetry transformations of the component fields are

$$\begin{aligned}
\delta\phi &= \zeta_+\psi_- - \zeta_-\psi_+ \ , \\
\delta\psi_+ &= i\overline{\zeta}_- \left(D_0 + D_1\right)\phi + \zeta_+ F - \overline{\zeta}_+\overline{\sigma}\phi \ , \\
\delta\psi_- &= -i\overline{\zeta}_+ \left(D_0 - D_1\right)\phi + \zeta_- F + \overline{\zeta}_-\sigma\phi \ , \\
\delta F &= -i\overline{\zeta}_+ \left(D_0 - D_1\right)\psi_+ - i\overline{\zeta}_- \left(D_0 + D_1\right)\psi_- \\
&\quad + \overline{\zeta}_+\overline{\sigma}\psi_- + \overline{\zeta}_-\sigma\psi_+ + i\left(\overline{\zeta}_-\overline{\lambda}_+ - \overline{\zeta}_+\overline{\lambda}_-\right)\phi \ ,
\end{aligned} \tag{2.2.8}$$

where the covariant derivative is $D_\mu = \partial_\mu + iv_\mu$.

Finally, the gauge-invariant field strength of the vector superfield is $\Sigma = \overline{D}_+ D_- V$, which is a twisted chiral superfield satisfying $\overline{D}_+\Sigma = D_-\Sigma = 0$. The fact that we can write the gauge-invariant field strength in this form is unique to two dimensions. In component form we have

$$\Sigma = \sigma(\widetilde{y}) + i\theta^+\overline{\lambda}_+(\widetilde{y}) - i\overline{\theta}^-\lambda_-(\widetilde{y}) + \theta^+\overline{\theta}^- \left[D - iF_{01}\right](\widetilde{y}) \ , \tag{2.2.9}$$

where $\widetilde{y}^{\pm} = x^{\pm} \mp i\theta^{\pm}\overline{\theta}^{\pm}$.

We will see in section 2.2.6 that the two-dimensional mirror symmetry (2.2.3) has the effect of exchanging chiral and twisted chiral superfields.

2.2.3 Supersymmetric Lagrangian

The gauge-invariant Lagrangian for the theory of a single charged chiral multiplet with a $U(1)$ gauge symmetry, described by a vector multiplet V, is given by a sum of terms

$$\mathcal{L} = \mathcal{L}_{\text{kin}} + \mathcal{L}_{\text{gauge}} + \mathcal{L}_{\widetilde{W}} + \mathcal{L}_W \ . \tag{2.2.10}$$

The kinetic term for the chiral multiplet of charge 1 is

$$\begin{aligned}\mathcal{L}_{\text{kin}} =& \int \mathrm{d}^4\theta \overline{\Phi} e^V \Phi \\ =& -D^\mu\overline{\phi}D_\mu\phi + i\overline{\psi}_-(D_0+D_1)\psi_- + i\overline{\psi}_+(D_0-D_1)\psi_+ \\ &+ D\left|\phi\right|^2 + \left|F\right|^2 - \left|\sigma\right|^2\left|\phi\right|^2 - \overline{\psi}_-\sigma\psi_+ - \overline{\psi}_+\overline{\sigma}\psi_- \\ &- i\overline{\phi}\lambda_-\psi_+ + i\overline{\phi}\lambda_+\psi_- + i\overline{\psi}_+\overline{\lambda}_-\phi - i\overline{\psi}_-\overline{\lambda}_+\phi \ .\end{aligned} \tag{2.2.11}$$

The kinetic term for the vector multiplet, written in terms of the field strength Σ, is

$$\begin{aligned}\mathcal{L}_{\text{gauge}} =& -\frac{1}{2e^2}\int \mathrm{d}^4\theta \overline{\Sigma}\Sigma \\ =& \frac{1}{2e^2}\left(-\partial^\mu\overline{\sigma}\partial_\mu\sigma + i\overline{\lambda}_-\left(\partial_0+\partial_1\right)\lambda_- + i\overline{\lambda}_+\left(\partial_0-\partial_1\right)\lambda_+ + F_{01}^2 + D^2\right) \ ,\end{aligned} \tag{2.2.12}$$

where e^2 is the gauge coupling, with mass dimension one.

In addition, the twisted superpotential term is given by

$$\mathcal{L}_{\widetilde{W}} = -\frac{t}{2}\int \mathrm{d}^2\overline{\theta}\Sigma + c.c. = -rD + \theta F_{01} \ , \tag{2.2.13}$$

where t is the complexified Fayet–Iliopoulos (FI) term

$$t = r - i\theta \ , \tag{2.2.14}$$

r is the FI parameter, and θ is the theta angle, which are dimensionless parameters.

Finally, one can also add a superpotential F-term

$$\mathcal{L}_W = \int \mathrm{d}^2\theta W(\Phi) + c.c. \ , \tag{2.2.15}$$

where $W(\Phi)$ is a gauge-invariant holomorphic function of Φ.

After eliminating the auxiliary fields, D and F, in (2.2.10), the potential for the scalar fields ϕ and σ is

$$U = \left|\sigma\right|^2\left|\phi\right|^2 + \frac{e^2}{2}\left(\left|\phi\right|^2 - r\right)^2 + \left|\frac{\partial W}{\partial\phi}\right|^2 \ . \tag{2.2.16}$$

The general Lagrangian for the case with multiple charged chiral multiplets Φ_i, with

charge Q_i under the $U(1)$, where $i = 1, \ldots, N$, is

$$\mathcal{L} = \int \mathrm{d}^4\theta \left(\sum_{i=1}^{N} \overline{\Phi}_i e^{Q_i V} \Phi_i - \frac{1}{2e^2} \overline{\Sigma}\Sigma \right) - \frac{t}{2} \int \mathrm{d}^2\overline{\theta}\Sigma + c.c + \mathcal{L}_W \ , \tag{2.2.17}$$

and hence the scalar potential becomes

$$U = \sum_{i=1}^{N} |Q_i \sigma|^2 |\phi_i|^2 + \frac{e^2}{2} \left(\sum_{i=1}^{N} Q_i |\phi|^2 - r \right)^2 + \sum_{i=1}^{N} \left| \frac{\partial W}{\partial \phi_i} \right|^2 \ . \tag{2.2.18}$$

This system demonstrates a decoupling of the parameters, the chiral and twisted chiral sectors do not talk to each other. t is a twisted chiral parameter, associated to the twisted superpotential $\widetilde{W}$, while the superpotential W depends on chiral superfields only. There is no mixing of parameters between W and $\widetilde{W}$.

The classical system exhibits both $U(1)_V$ and $U(1)_A$ R symmetries. The Lagrangian (2.2.17) is invariant under the vector and axial R rotations upon assigning the $U(1)_V \times U(1)_A$ charges $(0, 2)$ to Σ. To ensure that the superpotential term is invariant under the R symmetries, it must obey the quasi-homogeneous condition

$$W(\lambda\Phi) = \lambda^2 W(\Phi) \ , \tag{2.2.19}$$

where $\lambda \in \mathbb{C}^\times$, since θ^2 has vector R charge -2 and axial R charge 0.

We must also consider quantum effects. For the case of a single $U(1)$ gauge theory with one chiral superfield Φ of charge 1, the FI parameter runs as

$$r(\mu) = r(\Lambda_{UV}) - \log\left(\frac{\Lambda_{UV}}{\mu} \right) \ , \tag{2.2.20}$$

where Λ_{UV} is the UV renormalisation scale and μ is some finite energy scale. There is another quantum effect called the axial R symmetry anomaly. The measure in the path integral is not invariant under the axial R symmetry, which has the effect of shifting the theta angle

$$\theta \to \theta - 2\alpha \ . \tag{2.2.21}$$

Consequently, the classical system is no longer invariant under $U(1)_A$, the symmetry is broken to $\mathbb{Z}_2$ in the quantum theory. A shift in the theta angle can be absorbed by an axial R symmetry transformation. Hence, the two parameters describing the

classical theory, r and θ, are replaced by a single complex scale parameter Λ in the quantum theory.[3]

Repeating this argument for N chiral superfields Φ_i of charge Q_i, where $i = 1, \ldots, N$, (2.2.20) and (2.2.21) become

$$r(\mu) = r(\Lambda_{UV}) - b \log\left(\frac{\Lambda_{UV}}{\mu}\right) \quad , \quad \theta \to \theta - 2b\alpha \ , \tag{2.2.22}$$

where $b = \sum_{i=1}^{N} Q_i$. We must consider two scenarios. If $b = 0$, the FI parameter does not run, the theta angle is not shifted, and the system is invariant under the $U(1)_A$ R symmetry. As such, the quantum theory is described in terms of the two parameters r and θ. On the other hand, if $b \neq 0$, the $U(1)_A$ symmetry is anomalously broken to $\mathbb{Z}_{2b}$ and the quantum theory has the single parameter Λ. This is a renormalisation group invariant dynamical scale, which is defined by

$$\Lambda^b = \mu^b e^{-t(\mu)} = \Lambda_{UV}^b e^{-t(\Lambda_{UV})} \ . \tag{2.2.23}$$

There are two distinct topological supersymmetric backgrounds for 2d $\mathcal{N} = (2,2)$ theories, which are called the A- and B-model and are obtained by twisting the theory [12, 13]. After Wick rotating to Euclidean space, the spacetime symmetry is the rotation group $SO(2) = U(1)_E$. Twisting of the theory is achieved by combining either of the vector or axial R symmetries with the $U(1)_E$ symmetry. This results in the two different models, which are described by

$$\begin{aligned} &\text{A-model}: \ U(1)_E \to U(1)_E \times U(1)_V \ , \\ &\text{B-model}: \ U(1)_E \to U(1)_E \times U(1)_A \ . \end{aligned} \tag{2.2.24}$$

For both of these models, the scalar ϕ (the lowest component) of the chiral superfield Φ remains a scalar, however the spin of the fermionic fields is modified. In the A-model, ψ_- and $\overline{\psi}_+$ become scalars, whereas ψ_+ and $\overline{\psi}_-$ become anti-holomorphic and holomorphic one-forms, respectively. On the other hand, in the B-model, $\overline{\psi}_\pm$ become scalars, and ψ_+ and ψ_- become anti-holomorphic and holomorphic one-

[3] This effect is called dimensional transmutation.

	Before Twisting			After Twisting	
	$U(1)_V$	$U(1)_A$	$U(1)_E$	A-model	B-model
ϕ	0	0	0	0	0
ψ_-	-1	1	1	0	2
$\overline{\psi}_+$	1	1	-1	0	0
$\overline{\psi}_-$	1	-1	1	2	0
ψ_+	-1	-1	-1	-2	-2

Table 2.1: Charges for the component fields of a chiral superfield. The A- and B-model are obtained by twisting with the $U(1)_V$ and $U(1)_A$ R symmetry, respectively.

forms, respectively. We summarise this in Table 2.1, which contains the charges of the fields under the various symmetries, before and after twisting. Two-dimensional mirror symmetry, which was proved by Hori and Vafa [14], can be used to study these models since the A- and B-models are interchanged under this symmetry.

Defining the supercharges

$$Q_A = \overline{Q}_+ + Q_- \quad , \quad Q_B = \overline{Q}_+ + \overline{Q}_- \ , \tag{2.2.25}$$

which satisfy $Q_A^2 = Q_B^2 = 0$, an operator $\mathcal{O}$ is called a chiral operator if it satisfies

$$[Q_B, \mathcal{O}] = 0 \ , \tag{2.2.26}$$

and a twisted chiral operator if it satisfies

$$[Q_A, \mathcal{O}] = 0 \ . \tag{2.2.27}$$

The scalar ϕ (σ) in the chiral superfield Φ (twisted chiral superfield Σ) is an example of a chiral (twisted chiral) operator.

In the A-model (B-model), the supercharge Q_A (Q_B) is a scalar. Hence, each of these models preserves 1/2 of the supersymmetry on any curved background. The A- and B-models are both topological because the correlation functions are independent of the choice of the worldsheet metric. Correlations functions in the A-model depend holomorphically on twisted chiral operators and receive instanton corrections, whereas B-model correlators depend holomorphically on chiral operators

and are classically exact.

2.2.4 Non-Linear Sigma Models from Gauge Theories

In the early 1990s, Witten [5] studied the geometry of Gauged Linear Sigma Models (GLSMs) with $\mathcal{N} = (2,2)$ supersymmetry. These are theories that flow to Non-Linear Sigma Models (NLSMs) of Kähler or Calabi-Yau manifolds at low-energy scales. The classical geometry of these gauge theories can be studied by minimising the scalar potential. This is achieved by setting the D- and F-terms to zero and quotienting by the gauge group. We now discuss the classical supersymmetric vacua for a couple of examples, firstly in the absence of a superpotential term, and then with the presence of such a term. For more examples see [15, 16].

Example 1: $\mathbb{CP}^{N-1}$

Consider the case of a single $U(1)$ gauge theory with N chiral superfields Φ_i of charge 1, where $i = 1, \ldots, N$, and no superpotential. The potential energy of this theory is given by

$$U = \sum_{i=1}^{N} |\sigma|^2 |\phi_i|^2 + \frac{e^2}{2} \left(\sum_{i=1}^{N} |\phi_i|^2 - r \right)^2 . \tag{2.2.28}$$

We wish to study the classical supersymmetric vacua given by the configurations where U vanishes. This depends on the FI parameter:

- $\mathbf{r < 0}$: the potential energy U is positive and there is no supersymmetric vacua.
- $\mathbf{r = 0}$: $U = 0$ is obtained by setting $\phi_i = 0$ and leaving σ arbitrary.
- $\mathbf{r > 0}$: $U = 0$ is given by $\sigma = 0$ and $\sum_{i=1}^{N} |\phi_i|^2 = r$.

We will study the $r > 0$ scenario in more detail. The vacuum manifold is described by the set of all supersymmetric vacua modulo the $U(1)$ gauge group action,

$$\left\{ \sum_{i=1}^{N} |\phi_i|^2 = r \right\} / U(1) . \tag{2.2.29}$$

This tells us that the vacuum manifold is the complex projective space $\mathbb{CP}^{N-1}$, which can be generalised to some weighted projective space by considering chiral superfields of different charges. Thus, at low-energies, the classical theory reduces to a Non-Linear Sigma Model on $\mathbb{CP}^{N-1}$. This is the theory of the massless modes of ϕ_i, which are tangent to the vacuum manifold.

How do we obtain this vacuum manifold? The metric on the space of vacua is computed after taking the quotient by the gauge group. One method to obtain this relies on the fact that as we flow to the infrared, the GLSM reduces to the NLSM and the gauge field is no longer dynamical. As a result we can take the kinetic terms for the lowest component of the chiral multiplets and integrate out the gauge field by imposing its equation of motion.

The general kinetic term for N chiral fields ϕ_i of charge Q_i is

$$\sum_{j=1}^{N} D^{\mu}\overline{\phi}_j D_{\mu}\phi_j \ , \tag{2.2.30}$$

where $D_{\mu}\phi_j = \partial_{\mu}\phi_j + iv_{\mu}Q_j\phi_j$. Integrating out the gauge field v_{μ}, the kinetic term becomes

$$\sum_{j=1}^{N} \partial^{\mu}\overline{\phi}_j\partial_{\mu}\phi_j - \frac{j_{\mu}j^{\mu}}{4\sum\limits_{j=1}^{N} Q_j^2|\phi_j|^2} \ , \tag{2.2.31}$$

where $j^{\mu} = i\sum\limits_{j=1}^{N} Q_j\left(\partial^{\mu}\overline{\phi}_j\phi_j - \overline{\phi}_j\partial^{\mu}\phi_j\right)$ and the gauge field has been set to

$$v_{\mu} = -\frac{j_{\mu}}{2\sum\limits_{j=1}^{N} Q_j^2|\phi_j|^2} \ , \tag{2.2.32}$$

by its equation of motion.

Consequently, the metric on the space of vacua, which is obtained from (2.2.31), is

$$\mathrm{d}s^2 = rg^{FS} \ . \tag{2.2.33}$$

This is the metric of $\mathbb{CP}^{N-1}$, where g^{FS} denotes the Fubini-Study metric,

$$g^{FS} = \frac{\sum_{i=1}^{N-1} |dz_i|^2}{1 + \sum_{i=1}^{N-1} |z_i|^2} - \frac{\sum_{i=1}^{N-1} |\overline{z}_i \mathrm{d}z_i|^2}{\left(1 + \sum_{i=1}^{N-1} |z_i|^2\right)^2} \ , \tag{2.2.34}$$

which is expressed in terms of the coordinates $z_i = \frac{\phi_i}{\phi_N}$, where $i = 1, \ldots, N-1$.

Alternatively, the metric on the space of vacua can be computed from the derivative of the Kähler Potential $K(z, \overline{z})$, since

$$g_{i\overline{j}} = \frac{\partial^2}{\partial z^i \partial \overline{z}^j} K(z, \overline{z}) \ , \tag{2.2.35}$$

where $z, \overline{z}$ are local complex coordinates. For the case of $\mathbb{CP}^{N-1}$, the Kähler Potential is $K = r \log\left(1 + z_1\overline{z}_1 + z_2\overline{z}_2 + \ldots + z_{N-1}\overline{z}_{N-1}\right)$, and performing (2.2.35) we recover (2.2.33).

Example 2: Hypersurfaces in $\mathbb{CP}^{N-1}$

We can now examine an example with a superpotential. Consider the case of a single $U(1)$ gauge theory with $N+1$ chiral superfields $\Phi_1, \ldots, \Phi_N, P$, of charge $1, \ldots, 1, -d$, and the gauge-invariant superpotential

$$W = PG(\phi_1, \ldots, \phi_N) \ , \tag{2.2.36}$$

where $G(\phi_1, \ldots, \phi_N)$ is a homogeneous polynomial of degree d. The polynomial G is generic, which means

$$G = \frac{\partial G}{\partial \phi_1} = \cdots = \frac{\partial G}{\partial \phi_N} = 0 \ \Rightarrow \ \phi_1 = \cdots = \phi_N = 0 \ . \tag{2.2.37}$$

The condition $G = 0$ defines the hypersurface M in $\mathbb{CP}^{N-1}$, which is a smooth complex manifold of complex dimension $N-2$. When $d = N$, we have the Calabi-Yau (CY) case, where the sum of the $U(1)$ charges vanishes. The famous Quintic model occurs when $N = 5$.

The potential energy of the theory is given by

$$U = \sum_{i=1}^{N} |\sigma|^2 |\phi_i|^2 + |\sigma|^2 d^2 |p|^2 + \frac{e^2}{2} \left(\sum_{i=1}^{N} |\phi_i|^2 - d|p|^2 - r \right)^2 + |G|^2 + \sum_{i=1}^{N} |p|^2 |\partial_i G|^2 \ . \tag{2.2.38}$$

The structure of the vacuum manifold is again different for $r > 0$, $r = 0$, and $r < 0$:

- $\mathbf{r > 0}$: $U = 0$ is given by

$$\sigma = p = 0 \quad , \quad \sum_{i=1}^{N} |\phi_i|^2 = r \quad , \quad G = 0 \ . \tag{2.2.39}$$

  The vacuum manifold is the set of all fields satisfying these equations modulo the $U(1)$ gauge group action. This gives the complex hypersurface M of $\mathbb{CP}^{N-1}$, which is a CY manifold when $d = N$.

- $\mathbf{r = 0}$: The vacuum manifold is the complex σ-plane, with $p = \phi_i = 0$ from the requirement $U = 0$.

- $\mathbf{r < 0}$: $U = 0$ is described by

$$\sigma = \phi_i = 0 \quad , \quad |p|^2 = \frac{|r|}{d} \ , \tag{2.2.40}$$

  and hence the vacuum manifold is a point. Taking the limit where the gauge coupling $e \to \infty$, the classical theory is the Landau-Ginzburg (LG) model with the superpotential

$$W = \langle p \rangle G(\phi_1, \ldots, \phi_N) \ , \tag{2.2.41}$$

  where $\langle p \rangle = \sqrt{\frac{|r|}{d}}$ is the vacuum expectation value. Actually, there is a slight subtlety. The choice of the vacuum value for p breaks the $U(1)$ gauge symmetry into $\mathbb{Z}_d$. The presence of this residual symmetry, which acts non-trivially on Φ_i, means that the low-energy theory is not the ordinary LG model but its $\mathbb{Z}_d$-orbifold/LG orbifold.

This example is particularly neat because it demonstrates that the Calabi-Yau sigma model and the Landau-Ginzburg orbifold are two phases of the same system. These

two descriptions are interpretations of different regions of the same moduli space of theories.

Following on from the work of Witten, [17] explicitly computed the quantum-exact A-model correlation functions (including instanton contributions) with target space a toric variety or a Calabi-Yau hypersurface. The GLSM construction was used to prove an equivalence between an $\mathcal{N} = (2,2)$ theory with a cigar geometry and Liouville theory [18]. Further direct GLSM computations have been carried out in [19, 20], where the contribution of discrete Coulomb branch vacua to A-model correlators was investigated for models with compact and non-compact geometry. Recently, [21] investigated generalised Kähler geometries by considering new ingredients and structures for GLSMs whose target spaces are compatible with $\mathcal{N} = (2,2)$ supersymmetry.

In this section we have only discussed theories with a single $U(1)$ gauge group but the generalisation to higher rank or non-abelian gauge groups is possible. The quantum dynamics of $\mathcal{N} = (2,2)$ non-abelian gauge theories have also been studied, see for example [22, 23]. We will consider quantum effects in the next subsection.

2.2.5 Coulomb Branch Vacua

In $\mathcal{N} = (2,2)$ gauge theories, Coulomb branch vacua arise when the scalars in the field strength multiplets Σ_a gain a non-zero expectation value, $\langle \Sigma_a \rangle \neq 0$. When this happens the chiral superfields ϕ_i charged under the gauge symmetries become massive and can be integrated out. This leads to a quantum correction to the twisted superpotential in the theory. For the general case of a $U(1)^k = \prod_{a=1}^{k} U(1)_a$ gauge group with N chiral superfields Φ_i of charge Q_i^a, the effective twisted superpotential is

$$\widetilde{W}_{\text{eff}}(\Sigma_1, \ldots, \Sigma_k) = -\sum_{a=1}^{k} \Sigma_a \left(\sum_{i=1}^{N} Q_i^a \left[\log \left(\frac{\sum_{b=1}^{k} Q_i^b \Sigma_b}{\mu} \right) - 1 \right] + t^a(\mu) \right) , \quad (2.2.42)$$

where the renormalised complexified FI parameter for each $U(1)_a$ gauge group factor is

$$t_a(\mu) = t_a(\Lambda_{\rm UV}) + \sum_{i=1}^{N} Q_i^a \log\left(\frac{\mu}{\Lambda_{\rm UV}}\right) \ . \tag{2.2.43}$$

The supersymmetric vacua on the Coulomb branch are determined by the solutions to

$$\exp\left(-\frac{\partial\widetilde{W}_{\rm eff}}{\partial\Sigma_a}\right) = 1 \ , \tag{2.2.44}$$

for all the field strength multiplets Σ_a, where $a = 1, \dots, k$. We set $\exp\left(-\frac{\partial\widetilde{W}_{\rm eff}}{\partial\Sigma_a}\right) = 1$, rather than $\frac{\partial\widetilde{W}_{\rm eff}}{\partial\Sigma_a} = 0$, because we must take into account the 2π period of the theta angle θ^a, which is contained in the complexified FI parameter t^a in (2.2.42). Hence, for the effective twisted superpotential (2.2.42), the vacuum equations are given by

$$\prod_{i=1}^{N}\left(\frac{\sum_{b=1}^{k} Q_i^b\Sigma_b}{\mu}\right)^{Q_i^a} = \exp\left(-t_a(\mu)\right) \ . \tag{2.2.45}$$

The $\mathbb{CP}^{N-1}$ model

For the previously discussed $\mathbb{CP}^{N-1}$ model, with N chiral fields Φ_i of charge 1 and a single Σ field, the effective twisted superpotential is

$$\widetilde{W}_{\rm eff}(\Sigma) = -\Sigma\left(N\left[\log\left(\frac{\Sigma}{\mu}\right) - 1\right] + t(\mu)\right) \ . \tag{2.2.46}$$

Imposing (2.2.44), there are N distinct Coulomb branch vacua described by

$$\frac{\partial\widetilde{W}_{\rm eff}}{\partial\Sigma} = -N\log\left(\frac{\Sigma}{\mu}\right) - t(\mu) = 0 \quad\Rightarrow\quad \Sigma^N = \mu^N\exp\left(-t(\mu)\right) \ . \tag{2.2.47}$$

2.2.6 Dual Descriptions

It is important to discuss duality. A basic example of dualisation is T-duality in string theory. This tells us that the sigma model on the circle of radius R is equivalent to the sigma model on the circle of radius $\frac{1}{R}$, where the momentum of one theory is exchanged with the winding number of the other theory.

Applying T-duality to the $\mathcal{N} = (2,2)$ supersymmetric sigma model on the cylinder $\mathbb{C}^\times = \mathbb{R} \times S^1$ results in the sigma model on another cylinder $\widetilde{\mathbb{C}}^\times = \mathbb{R} \times \widetilde{S}^1$, where S^1 and $\widetilde{S}^1$ have radius R and $\frac{1}{R}$, respectively. To see this we consider the system described by the Lagrangian

$$\mathcal{L} = \int \mathrm{d}^4\theta \left(\frac{R^2}{4} B^2 - \frac{1}{2}(Y + \overline{Y})B \right) , \tag{2.2.48}$$

where B is a real superfield (an unconstrained field) and Y is a periodic twisted chiral superfield, satisfying $Y = Y + 2\pi i$.

Firstly, integrating out B imposes the constraint

$$B = \frac{1}{R^2}(Y + \overline{Y}) , \tag{2.2.49}$$

and substituting this back into the original Lagrangian gives

$$\mathcal{L}_1 = \int \mathrm{d}^4\theta \left(-\frac{1}{2R^2} \overline{Y} Y \right) . \tag{2.2.50}$$

This is the sigma model on the cylinder with radius $\frac{1}{R}$ for the circle, which is described in terms of the twisted chiral superfield Y.

What happens if we integrate out Y and $\overline{Y}$? Integrating out these fields yields the constraints $\overline{D}_+ D_- B = D_+ \overline{D}_- B = 0$, which are solved by

$$B = \Phi + \overline{\Phi} , \tag{2.2.51}$$

where Φ is a periodic chiral superfield, $\Phi = \Phi + 2\pi i$, whose periodicity matches the period of the dual field Y. Substituting this solution for B into the original Lagrangian gives

$$\mathcal{L}_2 = \int d^4\theta \left(\frac{R^2}{2} \overline{\Phi} \Phi \right) . \tag{2.2.52}$$

This is the sigma model on the cylinder with radius R for the circle, which is described in terms of the chiral superfield Φ.

Consequently, these two theories are equivalent, with the duality map

$$R^2(\Phi + \overline{\Phi}) = Y + \overline{Y} . \tag{2.2.53}$$

The $R \to \frac{1}{R}$ duality on the S^1 transforms a theory of a chiral multiplet to another theory of a twisted chiral multiplet. This is an example of the two-dimensional mirror symmetry (2.2.3), where the supercharges Q_- and $\overline{Q}_-$ are exchanged under this equivalence.

To end this section we discuss the mirror theory of the $\mathbb{CP}^{N-1}$ sigma model. For $\mathbb{CP}^{N-1}$, realised as the $U(1)$ gauge theory with $i = 1, \ldots, N$ chiral superfields Φ_i of charge 1, we saw in section 2.2.4 that the system reduces to the sigma model described by the quotient (2.2.29).

Dualising the phase of the N chiral fields, one obtains N twisted chiral superfields Y_i, with periodicity $Y_i = Y_i + 2\pi i$. The dual theory, described in terms of (Σ, Y_i), has the exact twisted superpotential

$$\widetilde{W} = \left(\sum_{i=1}^{N} Y_i - t(\mu)\right)\Sigma + \sum_{i=1}^{N} \mu e^{-Y_i} \ , \tag{2.2.54}$$

where the dual fields Y_i couple to the gauge field as a dynamical Theta angle, and the final term is the instanton correction needed to ensure that the theories are quantum mechanically equivalent [14].

Taking the strong coupling (sigma model) limit, the Σ field becomes heavy and can be integrated out, which results in the constraint

$$\sum_{i=1}^{N} Y_i = t \ , \tag{2.2.55}$$

and the twisted superpotential becomes

$$\widetilde{W} = e^{-Y_1} + \ldots + e^{-Y_N} \ . \tag{2.2.56}$$

The constraint (2.2.55) is solved by

$$\begin{aligned} Y_i &= \Theta_i \quad \text{for} \quad i = 1, \ldots, N-1 \ , \\ Y_N &= t - \sum_{i=1}^{N-1} \Theta_i \quad . \end{aligned} \tag{2.2.57}$$

Consequently, the mirror theory is the LG model on the $(N-1)$-dimensional cylinder

parameterised by the periodic coordinates Θ_i with the superpotential

$$\widetilde{W} = e^{-\Theta_1} + \ldots + e^{-\Theta_{N-1}} + e^{-t+\Theta_1+\ldots+\Theta_{N-1}} \ . \tag{2.2.58}$$

2.3 Three-dimensional $\mathcal{N} = 4$

Three-dimensional $\mathcal{N} = 4$ gauge theories, with 8 supercharges, are completely specified by the choice of a gauge group G, associated with a vector multiplet, and some matter content, associated to hypermultiplets. 3d $\mathcal{N} = 4$ theories are related to 4d $\mathcal{N} = 2$ and 6d $\mathcal{N} = (1, 0)$ theories by dimensional reduction.

2.3.1 Field Content

The vector multiplet contains a gauge field A_μ and three real scalars (ϕ^1, ϕ^2, ϕ^3), transforming in the adjoint representation of G, plus fermions. The matter fields are contained in hypermultiplets, which transform under a pseudo-real representation $\mathcal{R}_{\text{p-r}}$ of G. We will only consider matter hypermultiplets, which come in pairs of chiral multiplets transforming in complex conjugate representations, $\mathcal{R}_{\text{p-r}} = \mathcal{R} \oplus \mathcal{R}^*$.

In three dimensions, the gauge field A_μ is dual to a scalar γ, which is called the dual photon, since

$$F_{\mu\nu} = \epsilon_{\mu\nu\rho}\partial^\rho\gamma \ , \tag{2.3.1}$$

where $F_{\mu\nu}$ is the gauge field strength. The dual photon γ is a scalar that we normalise to have period 2π, which is compact due to the flux quantization of the field strength.

The R symmetry group is $SU(2)_C \times SU(2)_H$. The three real scalars in the vector multiplet transform as a triplet under the $SU(2)_C$, whereas the pair of complex scalars in each hypermultiplet $(Q, \widetilde{Q}^\dagger)$, transform as a doublet under the $SU(2)_H$. There also exists twisted vector and twisted hypermultiplets, where the roles of $SU(2)_C$ and $SU(2)_H$ are exchanged.

2.3.2 Branches

Examining the moduli space of supersymmetric vacua of these theories, the set of zero energy field configurations, is a rich and interesting subject. The space of vacua is comprised of a union of intersecting subspaces, which are called branches, analogous to Figure 2.1. There are two important branches, the Higgs branch $\mathcal{M}_H$ and the Coulomb branch $\mathcal{M}_C$. Mixed branches are obtained by products of subspaces of these branches. Mirror symmetry in three dimensions informs us that dual theories exist, where in the infrared limit, the Higgs branch of one theory is the Coulomb branch of the dual theory, and vice versa [24].

2.3.3 Higgs Branch

The Higgs branch $\mathcal{M}_H$ is parameterised by the vacuum expectation values (VEVs) of the scalars in the hypermultiplets. These are subject to D- and F-term constraints and the classical description can be worked out from the level of the Lagrangian since there are no quantum corrections [25]. $\mathcal{M}_H$ is classically exact and is described as the hyper-Kähler quotient $\mathbb{R}^{4\dim\mathcal{R}}////G$ [26]. The R symmetry group $SU(2)_H$ acts non-trivially on $\mathcal{M}_H$, whereas the $SU(2)_C$ R symmetry acts trivially.

2.3.4 Coulomb Branch

On the other hand, the Coulomb branch is parameterised by the VEVs of both the scalars in the vector multiplet and the dual photons. The R symmetry group $SU(2)_H$ acts trivially on $\mathcal{M}_C$, whereas the $SU(2)_C$ R symmetry acts non-trivially.

It is not an easy task to characterise the geometry of Coulomb branches. For abelian theories, the metric on the Coulomb branch receives one-loop quantum corrections and has been directly evaluated [27, 28]. However, the metric on the Coulomb branch of non-abelian theories receives non-perturbative quantum corrections, which are notably hard to compute.

In recent years, significant progress has been made by utilising the description of the Coulomb branch as a complex algebraic variety, hence bypassing difficulties related to the metric. The key players in this description are chiral operators, including standard Casimir-invariant operators and monopole operators [29]. The VEVs of these chiral operators parameterise the Coulomb branch and the algebraic relations that they satisfy give the chiral ring relations.[4]

The potentials in the action impose that only scalars valued in a Cartan subalgebra can take vacuum expectation value. At a generic point on the Coulomb branch, the gauge group G is broken to its maximal torus $U(1)^{\mathrm{rank}(G)}$. $\mathcal{M}_C$ is classically described by

$$(\mathbb{R}^3 \times S^1)^{\mathrm{rank}(G)}/\mathcal{W} \ , \tag{2.3.2}$$

where the $\mathbb{R}^3$ factors are parameterised by the Cartan components of the three real scalars ϕ_a^i, and the S^1 factors are parameterised by the dual photons γ_a, with $a = 1, \ldots, \mathrm{rank}(G)$. The Weyl group of G is denoted by $\mathcal{W}$.

Two out of the three real scalars in the vector multiplet can be combined to create the complex scalars $\varphi_a = \phi_a^1 + i\phi_a^2$. The remaining real scalars ϕ_a^3 can be combined with the dual photons γ_a to form the complex scalars

$$u_a^{\pm} = \exp\left(\pm\chi_a\right) = \exp\left(\pm\left[\frac{2\pi}{g^2}\phi_a^3 + i\gamma_a\right]\right) \ , \tag{2.3.3}$$

where g^2 is the Yang-Mills coupling of the gauge group factor. These complex scalars $u_a^{\pm}$ satisfy the classical relations

$$u_a^+ u_a^- = 1 \ \ \forall \ a \ . \tag{2.3.4}$$

Consequently, the classical Coulomb branch is alternatively described as a complex algebraic variety, which is given by

$$(\mathbb{C} \times \mathbb{C}^*)^{\mathrm{rank}(G)}/\mathcal{W} \ . \tag{2.3.5}$$

[4]It is believed that the Coulomb branch is finitely generated, namely that every Coulomb branch admits a finite basis of generators.

This classical description of the Coulomb branch is valid when all of the hypermultiplets are massive and the theory is that of free abelian vector multiplets.

The coordinates $u_a^{\pm}$, appearing in the description of the Coulomb branch as a complex algebraic variety, are chiral 't Hooft monopole operators [30]. Monopole operators in three-dimensional Euclidean gauge theories are local disorder operators, which are defined by requiring the gauge field to have a Dirac monopole singularity at a certain insertion point x. As such, the integral of the field strength around a sphere S_x^2 enclosing the point x obeys

$$\frac{1}{2\pi}\oint_{S_x^2} F_a = n_a \ , \tag{2.3.6}$$

where $n_a \in \mathbb{Z}$ arises from the Dirac quantization condition. These monopole operators are point-like objects in three dimensions, so monopole operators in three dimensions are like instantons in four dimensions.

In addition, to ensure that half of the supersymmetry is preserved, we require a corresponding singularity for the real scalar ϕ_a^3. Consequently, the insertion of a half-BPS monopole of charge B is defined by requiring in the path integral the singular profile

$$F = -\frac{B}{2} \star \mathrm{d}(\frac{1}{r}) \quad , \quad \phi_3 = \frac{B}{2r} \ , \tag{2.3.7}$$

in the vicinity of the insertion point x, where r is the radial coordinate. The BPS condition, the condition relating F and ϕ_3, is given by

$$F = - \star \mathrm{d}\phi_3 \ , \tag{2.3.8}$$

which follows from setting to zero the supersymmetry variations of the gauginos in the theory, see [29, 31] for details.

These monopole operators can also be dressed by a polynomial in the complex scalars φ_a. The symmetric polynomials in φ_a and $u_a^{\pm}$ are thus gauge-invariant dressed monopole operators. Hence, the quantum corrected Coulomb branch is parameterised by the VEVs of the Coulomb branch operators, certain BPS gauge-invariant

combinations of the vector multiplets scalars and dressed monopole operators.

Importantly, the monopole operators satisfy some non-trivial quantum relations, which are the algebraic relations defining the Coulomb branch as a complex algebraic variety. For the case of $U(N)$ SQCD with N_f massless hypermultiplets, these relations, which modify the classical relations (2.3.4), take the form

$$u_a^+ u_a^- \prod_{b\neq a} (\varphi_b - \varphi_a)^2 = \varphi_a^{N_f} \ , \tag{2.3.9}$$

for all $a = 1, \ldots, N$ [32].

In [33, 34, 35, 36, 37] the monopole formula for the Coulomb branch was developed and studied. This crucially relied on the Hilbert series, the generating function that counts bosonic gauge-invariant chiral operators in the theory, graded according to their dimension and quantum numbers under global symmetries.[5] For a review see [40].

Additionally, [32] applied the abelianization approach to construct the quantum corrected Coulomb branch and its deformation quantization, which is known as the quantized Coulomb branch and is physically achieved by placing the 3d theory in an Omega background. The moduli space of 3d $\mathcal{N} = 4$ $U(N)$ SQCD theories were further studied in [41],[6] where good, bad, and ugly theories were examined, according to the classification of [43] based on the R charges of the monopole operators.

Finally, there has also been significant progress in the mathematics literature. A rigorous mathematical construction of the Coulomb branch for 3d $\mathcal{N} = 4$ theories was developed in [44, 45, 46].[7]

[5] See also [38, 39] for the monopole formula for the Hilbert series of 3d $\mathcal{N} = 2$ gauge theories.
[6] For theories with the gauge group $USp(2N)$ see [42].
[7] For introductory lectures see [47, 48].

	0	1	2	3	4	5	6	7	8	9
D3	X	X	X	X						
D5	X	X	X		X	X	X			
NS5'	X	X	X					X	X	X
D1				X				X		
D3'					X	X	X	X		
NS5				X	X	X	X		X	X

Table 2.2: Brane array for 3d $\mathcal{N} = 4$ theories.

2.3.5 Brane Construction and Realisation of Monopole Operators

A three-dimensional gauge theory can be realised as the low-energy theory of D3 branes stretched between NS5' and D5 branes in type IIB string theory [6]. The orientations of these objects are given in the first set of entries in the brane array Table 2.2, where X denote the worldvolume directions. A Dp brane is localised to live in a $(p+1)$-dimensional hypersurface with Neumann boundary conditions in $(p+1)$ directions and Dirichlet boundary conditions in the remaining $(10-1)-(p+1) = 8-p$ directions.[8] The D3, NS5', and D5 branes share 3 common directions, 012, and preserve 8 supercharges, a 1/4 of the 32 type IIB supercharges. Under S-duality, D5 and NS5 branes are interchanged whilst D3s are invariant.

A 3d $U(N)$ gauge theory is realised by a brane construction with N D3 branes stretched between two NS5' branes. k D5 branes intersecting these D3s realises k fundamental hypermultiplets. This is illustrated in Figure 2.2. The fundamental hypermultiplets are the light modes of D5-D3 open strings. The light modes of D3-D3 open strings stretched across NS5' branes are bifundamental hypermultiplets.

The brane realisation of monopole operators in abelian 3d $\mathcal{N} = 4$ gauge theories

[8]Recall, for the string parameterised by the spatial coordinate $\sigma \in [0, \pi]$, we have boundary conditions to tells us how the end points move. Neumann boundary conditions satisfy $\partial_\sigma X^\mu = 0$ at $\sigma = 0, \pi$, which allow the ends of the string to move freely (at the speed of light). Dirichlet boundary conditions impose $\delta X^\mu = 0$ at $\sigma = 0, \pi$, so the end points of the string are fixed in space, $X^\mu =$ constant.

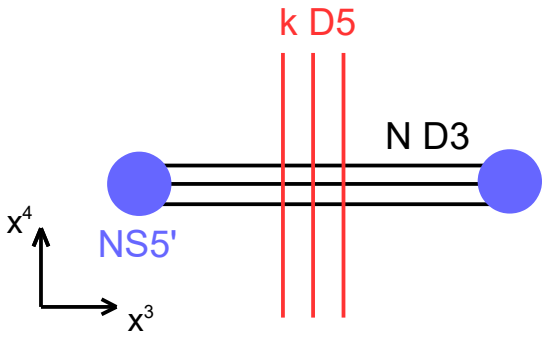

Figure 2.2: Brane configuration associated to a 3d $U(N)$ gauge theory.

was introduced and studied in [49].[9] To realise the inclusion of monopole operators in the theory, we introduce D1, D3', and NS5 branes, whose orientations are given in the second set of entries in Table 2.2. A monopole operator is then realised by adding a pair of NS5 branes and stretching a D1 between a D3 and one of the NS5s in the pair. The D3' branes will play no role in this thesis as we do not discuss the brane realisation of Casimir and dressed monopole operators, see section 5 of [4] for details.

In a given brane configuration, the D3 branes are taken separated, indicating that we consider a Coulomb branch configuration where the gauge group is broken to a maximal torus. We label the D3 branes by D3_a, where $a = 1, \ldots, N$. An NS5 pair refers to the pair of NS5 branes (NS5_+, NS5_-), where NS5_+ (NS5_-) indicates an NS5 brane placed to the right (left) of all the D3 and D5 branes in the x^7 direction.

In Figure 2.3 we illustrate the brane set-up associated to the realisation of the abelian operator u_{e_1}. We depict the brane set-up in both the x^{37} and x^{78} plane. In the rest of this thesis, we will only draw the brane diagrams in the x^{78} plane, where the NS5' branes span the whole space so we do not draw them. The NS5 branes in Figure 2.3 come in a pair, denoted by a $+$ on the right and a $-$ on the left, and we have the D3s and D5s located in the interval between them. A single D1 is stretched between the first D3 brane D3_1, and the NS5_+. The remaining $N-1$ D3 branes are

[9] See also [50] for the analogue in $\mathcal{N} = 3$ Chern-Simons-Matter theories.

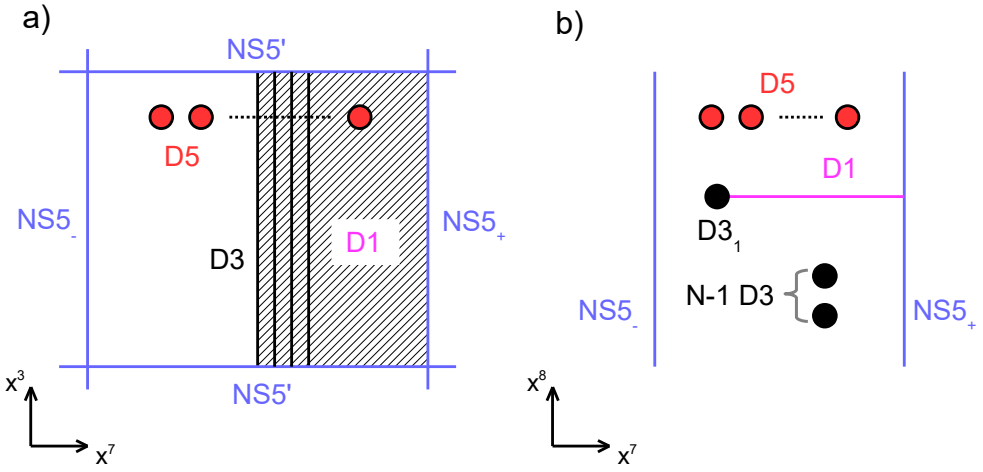

Figure 2.3: Brane set-up realising the insertion of the abelian monopole u_{e_1}. We depict the set-up in the x^{37} plane and in the x^{78} plane.

unconnected.

2.3.6 Hanany-Witten Transition

An important property of the brane set-up is that the triple (NS5, D3, D1) form a Hanany-Witten triple. Studying the brane array Table 2.2, the combination of the NS5 and D3 branes completely fill the whole 10 dimensional spacetime, apart from the single x^7 direction. When a D3 crosses an NS5, a brane is created that must span the x^7 direction. This created brane also spans all of the common worldvolume directions of the NS5 and D3 branes, i.e only x^3. Hence, this created brane is a D1. Consequently, there is a D1 creation/annihilation effect when a D3 crosses an NS5, which we illustrate in Figure 2.4.

This effect was justified in [6] using the conservation of magnetic charge. The total magnetic charge measured on a D3 brane is given by its linking number ℓ, which is defined by

$$\ell = \frac{1}{2}\left[n(\mathrm{NS5}_L) - n(\mathrm{NS5}_R)\right] + n(\mathrm{D1}_R) - n(\mathrm{D1}_L)\ , \tag{2.3.10}$$

where $n(\mathrm{NS5}_L)$, $n(\mathrm{NS5}_R)$ is the number of NS5s to the left, right of the D3 brane along the x^7 direction. Likewise, $n(\mathrm{D1}_L)$, $n(\mathrm{D1}_R)$ is the number of D1 strings ending on the D3 brane from the left, right along x^7. We can also define a linking number

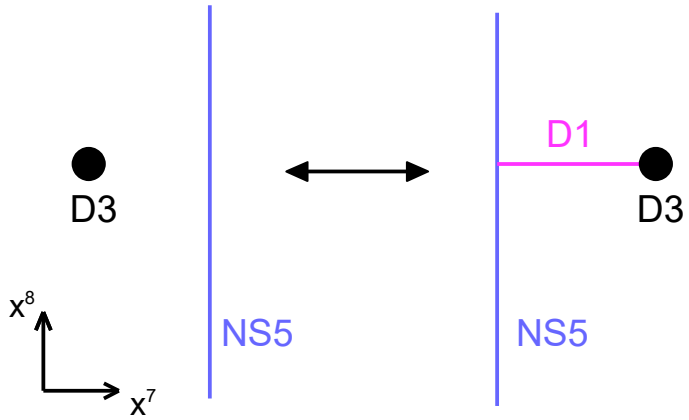

Figure 2.4: This figure illustrates a Hanany-Witten transition. A D1 string is created/annihilated as a D3 crosses an NS5.

h for an NS5 brane,

$$h = \frac{1}{2}\left[\widehat{n}(\mathrm{D3}_R) - \widehat{n}(\mathrm{D3}_L)\right] + \widehat{n}(\mathrm{D1}_L) - \widehat{n}(\mathrm{D1}_R) \ , \tag{2.3.11}$$

where the $\widehat{n}$'s are defined similar to the n's in the D3 brane linking number ℓ. These quantities satisfy the relation $\sum_b h_b = \sum_a \ell_a$ and must be preserved under any transition of branes.

For the set-up on the left hand side of Figure 2.4, we have $\ell = h = -\frac{1}{2}$. After performing the Hanany-Witten transition we obtain the set-up on the right hand side, with $\ell = h = \frac{1}{2} - 1 = -\frac{1}{2}$. These linking numbers match. We observe that without the presence of the D1 string on the right hand side, there would be a violation of the preservation of the linking numbers. The Hanany-Witten transition has another consequence. There is also an s-rule: at most one D1 string can be stretched between an NS5 and a D3 [6].

Chapter 3

Supersymmetric Localization and The Jeffrey-Kirwan Residue

In this chapter we present the localization argument for supersymmetric quantum field theories. We then review the Jeffrey-Kirwan residue operation [51], which first appeared in the physics literature in the computation of the elliptic genera of two-dimensional $\mathcal{N} = (2, 2)$ gauge theories using supersymmetric localization [52].

3.1 Supersymmetric Localization

Inspired by the mathematical works[1] [54, 55, 56], the technique of supersymmetric localization was first developed by Witten in the context of topological quantum field theories [12, 13]. Subsequently, a range of exact results have been successfully obtained for supersymmetric theories in curved backgrounds of various dimensions. In this context, the localization procedure was first applied to four-dimensional $\mathcal{N} = 2$ gauge theories in the Omega background [57], and, in particular, has been successfully applied to the calculation of partition functions for four-dimensional $\mathcal{N} = 2$ gauge theories on the 4-sphere S^4 [58], $\mathcal{N} = 2$ theories on S^3 [59, 60, 61],

[1]For a dictionary between the mathematical world of equivariant localization formulae for finite-dimensional integrals and supersymmetric localization see Table 1 in [53].

and 2d $\mathcal{N} = (2,2)$ theories on S^2 [62, 63, 64].[2] The aim of this section is to provide an introduction to the topic of supersymmetric localization. For more details see [53, 67], as well as the collection of articles in [68].

3.1.1 Intuitive Example

To begin this discussion of supersymmetric localization, let us consider a simple but illustrative example that shares a key idea with localization, which appears in [69, 53]. Consider the unit two-sphere S^2, with metric

$$\mathrm{d}s^2 = \mathrm{d}\theta^2 + \sin^2\theta \mathrm{d}\phi^2 \ , \tag{3.1.1}$$

in spherical coordinates $(0 \leq \theta \leq \pi, 0 \leq \phi < 2\pi)$, and compute the integral

$$I = \int_0^{2\pi} \mathrm{d}\phi \int_0^{\pi} \mathrm{d}\theta \sin\theta e^{it\cos\theta} \ , \tag{3.1.2}$$

where t is a constant parameter. This integral is easily evaluated and we find

$$\begin{aligned} I &= 2\pi \int_{-1}^{1} \mathrm{d}(\cos\theta) e^{it\cos\theta} \\ &= \frac{2\pi}{t}\left[-ie^{it} + ie^{-it}\right] = \frac{4\pi\sin t}{t} \ . \end{aligned} \tag{3.1.3}$$

This is an exact result. Now we can ask the question: can this integral be computed using another method?

The answer is yes. We can consider the large t scenario and apply the stationary phase approximation. For an integral of the form

$$\int \mathrm{d}^n x e^{itf(x)} \ , \tag{3.1.4}$$

where $f(x)$ is a real smooth function, the stationary phase approximation tells us that the leading contributions to the integral at large t are given by the stationary points x_k of $f(x)$. Taylor expanding $f(x)$ about each x_k, assuming that the stationary points are non-degenerate, and performing the resulting Gaussian integrals, (3.1.4)

[2] For a review of supersymmetric localization in 2d $\mathcal{N} = (2,2)$ gauge theories see [65, 66].

is given by

$$\left(\frac{2\pi}{t}\right)^{\frac{n}{2}} \sum_{x_k} e^{itf(x_k)} \frac{e^{i\sigma_k \frac{\pi}{4}}}{|\mathrm{det}H\left(f(x_k)\right)|^{\frac{1}{2}}} \ , \tag{3.1.5}$$

where we sum over all the stationary points x_k, $H\left(f(x_k)\right)$ is the Hessian matrix of $f(x)$ at x_k, and $\sigma_k = \sigma_k^+ - \sigma_k^-$, where σ_k^+ and σ_k^- are the number of positive and negative eigenvalues of the matrix $H\left(f(x_k)\right)$, respectively.

In this case, the leading contributions to the integral (3.1.2) arise from the stationary points of $\cos\theta$. There are two stationary points, the North and South poles of S^2. Rewriting the integral in terms of Cartesian coordinates, where the unit two-sphere S^2 is defined by the equation $x^2 + y^2 + z^2 = 1$, (3.1.2) becomes

$$I = \int_{S^2} \mathrm{d}A e^{itz} \ , \tag{3.1.6}$$

and $\mathrm{d}A$ is the area element with the normalisation $\int_{S^2} \mathrm{d}A = 4\pi$. We Taylor expand about each stationary point, where

$$z_N = 1 - \frac{1}{2}(x^2 + y^2) \ , \tag{3.1.7}$$

for the North pole, and

$$z_S = -1 + \frac{1}{2}(x^2 + y^2) \ , \tag{3.1.8}$$

for the South pole. Hence, for the North pole we find

$$H(z_N) = \begin{pmatrix} -1 & 0 \\ 0 & -1 \end{pmatrix} \ , \tag{3.1.9}$$

and so $\mathrm{det}H(z_N) = 1$ and $\sigma_N = -2$. Likewise, for the South pole we find

$$H(z_S) = \begin{pmatrix} 1 & 0 \\ 0 & 1 \end{pmatrix} \ , \tag{3.1.10}$$

and so $\mathrm{det}H(z_S) = 1$ and $\sigma_S = -2$. Consequently, using (3.1.5) and adding the contributions from the two stationary points together gives

$$I \approx \frac{2\pi}{t}\left[e^{it}e^{-i\frac{\pi}{2}} + e^{-it}e^{i\frac{\pi}{2}}\right] = \frac{2\pi}{t}\left[-ie^{it} + ie^{-it}\right] = \frac{4\pi \sin t}{t} \ , \tag{3.1.11}$$

which matches the previous exact computation. There is no reason for these methods to be equal. This is an example of a scenario where the stationary phase approximation gives the exact result. This is a localization result, since the integral localizes to the stationary points of $\cos\theta$, i.e. it picks up a contribution from the North and South poles of S^2. Hence, localization formulae can be viewed as instances when the stationary phase approximation (or semi-classical expansion) is exact.

3.1.2 The Localization Technique

The object that we wish to study is the path integral of a supersymmetric QFT. The Euclidean partition function of a theory is defined by[3]

$$Z = \int_{\mathcal{M}} [\mathcal{D}X]\, e^{-S[X]} \,, \tag{3.1.12}$$

where $\mathcal{M}$ is a compact curved manifold. Field theories on compact manifolds are free of infrared divergences and so their path integrals are well defined. $S[X]$ denotes the action, where X is used to collectively represent the set of all bosonic and fermionic fields comprising the theory. This object is often extremely difficult to compute, the tools of perturbation theory work well at weak coupling but break down at strong coupling. Hence, we require non-perturbative techniques to obtain an exact result. Supersymmetric localization relies on supersymmetry to prove that the path integral only receives contributions from the fixed points of the supersymmetry and quadratic fluctuations around these. This reduces the infinite-dimensional integral to a lower finite-dimensional integral, which can be solved exactly in favourable situations.

Supersymmetric localization is crucially dependent on the construction of supersymmetry in curved space. Commonly, a manifold does not admit covariantly constant spinors. There are two approaches to defining a supersymmetric field theory in curved space:

1. Trial and error. Introduce a curvature length scale r and add curvature de-

[3]We set $\hbar = 1$.

pendent corrections to the flat space supersymmetry transformations $\delta^{(0)}$ and supersymmetric Lagrangian $\mathcal{L}^{(0)}$:

$$\begin{aligned} \delta &= \delta^{(0)} \,|_{\eta\to g,\partial\to\nabla} + \sum_{n\geq 1} \frac{1}{r^n}\delta^{(n)} \ , \\ \mathcal{L} &= \mathcal{L}^{(0)} \,|_{\eta\to g,\partial\to\nabla} + \sum_{n\geq 1} \frac{1}{r^n}\mathcal{L}^{(n)} \ , \end{aligned} \tag{3.1.13}$$

replacing the flat metric η by the curved metric g and the ordinary derivatives ∂ by covariant derivatives ∇, until the supersymmetry algebra closes and the supersymmetric variation of the Lagrangian is at most a total derivative $\delta\mathcal{L} = \nabla_\mu(\ldots)^\mu$. However, this method can be time consuming and is not guaranteed to work.

2. Follow the generic model independent method proposed by Festuccia and Seiberg [70]: 1) Non-linearly couple the flat space theory to off-shell supergravity background fields; 2) Solve the generalised Killing spinor equations that are obtained by setting the gravitinos and their variation to zero.

The technique of localization concerns supersymmetric field theories consisting of conserved supercharges Q, which obey the relation

$$Q^2 = B \ , \tag{3.1.14}$$

where B is a bosonic symmetry (or zero). The action $S[X]$ is invariant under supersymmetry

$$QS[X] = 0 \ , \tag{3.1.15}$$

where again X collectively denotes the set of all fields. This condition tells us that $S[X]$ is Q-closed. The supersymmetric transformations schematically take the form

$$Q(bosons) = (fermions) \quad , \quad Q(fermions) = (bosons) \ . \tag{3.1.16}$$

The expectation value of a gauge-invariant Q-exact BPS operator $\mathcal{A}$ is given by

$$\langle \mathcal{A} \rangle = \int_{\mathcal{M}} [\mathcal{D}X]\, \mathcal{A} e^{-S[X]} \ , \tag{3.1.17}$$

up to an overall normalisation factor, which we ignore to ease notation. Since it is Q-exact, the operator $\mathcal{A}$ can be written as Q acting on another operator $\mathcal{O}$. Hence, by substituting $\mathcal{A} = Q\mathcal{O}$ into (3.1.17), we can show that the expectation value for a Q-exact operator vanishes,

$$\langle Q\mathcal{O}\rangle = \int_{\mathcal{M}} [\mathcal{D}X]\,(Q\mathcal{O})\,e^{-S[X]} = \int_{\mathcal{M}} [\mathcal{D}X]\,Q\left(\mathcal{O}e^{-S[X]}\right) = 0\ . \tag{3.1.18}$$

This is true provided that the integrand decays fast enough, i.e. $e^{-S[X]} \to 0$ as $|X| \to \infty$, so that no boundary terms exist, and $S[X]$ satisfies (3.1.15). One way to see this is that in superspace formalism, the supercharge Q is a derivative, see (2.1.7), which obeys Leibniz rules. Hence, Q is the generator of shifts along a fermionic direction and we end up with an integral of a total derivative, which vanishes due to an analogue of Stokes' theorem.

Alternatively, we can consider this using operator formalism, where the expectation value is given by

$$\langle 0|\,\{Q,\mathcal{O}]\,|0\rangle\ , \tag{3.1.19}$$

for a supersymmetric vacuum state $|0\rangle$. The notation $\{Q,\mathcal{O}]$ denotes the commutator $[Q,\mathcal{O}]$ if $\mathcal{O}$ is bosonic and the anti-commutator $\{Q,\mathcal{O}\}$ if $\mathcal{O}$ is fermionic. The vacuum state $|0\rangle$ is annihilated by Q and $\langle 0|\,Q = 0$, so the expectation value of a Q-exact operator must vanish.

Consequently, a freedom exists to deform the path integral by a Q-exact term,

$$Z = \int_{\mathcal{M}} [\mathcal{D}X]\,e^{-S[X]-tS_{loc}[X]}\ , \tag{3.1.20}$$

where t is a deformation parameter. The Q-exact deformation term is written as the localizing action

$$S_{loc}[X] = QV[X]\ , \tag{3.1.21}$$

where $V[X]$ is a fermionic functional, which is invariant under Q^2. Significantly, using a similar logic to the vanishing of the expectation value of a Q-exact operator,

it is possible to show that Z is independent of t,

$$\frac{\mathrm{d}Z}{\mathrm{d}t} = -\int_{\mathcal{M}} [\mathcal{D}X]\, S_{loc}[X] e^{-S[X]-tS_{loc}[X]} = -\int_{\mathcal{M}} [\mathcal{D}X]\, Q\left(V[X] e^{-S[X]-tS_{loc}[X]}\right) = 0 \ , \tag{3.1.22}$$

since the integral of a total derivative vanishes.

Consequently, upon taking the limit $t \to \infty$, the partition function (3.1.12) is equally described by

$$Z = \lim_{t\to\infty} \int_{\mathcal{M}} [\mathcal{D}X]\, e^{-S[X]-tS_{loc}[X]} \ . \tag{3.1.23}$$

In the limit $t \to \infty$, the semi-classical approximation in $\frac{1}{t}$ is exact, and the integrand is dominated by the saddle points of $S_{loc}[X]$.

A natural question to ask is what is the localizing action $S_{loc}[X]$? This term is any Q-exact expression that takes the form (3.1.21), but a suitable choice can make the computation more manageable. For example, if the kinetic terms associated to the chiral multiplets in the theory are Q-exact, then it is convenient to use these Q-exact pieces as the localizing action.

The canonical choice for the localizing action contains a sum over all the fermionic fields ψ in the theory and is given by

$$V[X] = \sum_{\psi} \left[(Q\psi)^\dagger \psi + \psi^\dagger \left(Q\psi^\dagger\right)^\dagger \right] \ , \tag{3.1.24}$$

so that the bosonic piece of S_{loc} is a positive semi-definite sum of squares.

The saddle point configurations, to which the path integral localises, are obtained by setting

$$\begin{aligned} \psi = \psi^\dagger = 0 \quad &\Rightarrow \quad fermions = 0 \ , \\ Q\psi = Q\psi^\dagger = 0 \quad &\Rightarrow \quad Q(fermions) = 0 \ , \end{aligned} \tag{3.1.25}$$

which are the fixed points of the action of the supercharge Q. The deformed path integral (3.1.23) is evaluated by expanding the fields X about the saddle points X_0 of $S_{loc}[X]$,

$$X = X_0 + \frac{1}{\sqrt{t}} \delta X \ , \tag{3.1.26}$$

where $\sqrt{t}$ has been added to ensure canonical normalisation. This means that

$$S[X] + tS_{loc}[X] \to S[X_0] + \frac{1}{2}\int \left.\frac{\delta^2 S_{loc}[X]}{\delta X^2}\right|_{X=X_0} (\delta X)^2 \ , \tag{3.1.27}$$

where the localizing action evaluated at the saddle points is zero, and taking the limit $t \to \infty$, the higher order terms vanish. Consequently, the localization formula for the path integral is

$$Z = \int_{\mathcal{M}_Q} [\mathcal{D}X_0]\, Z_{classical} Z_{1-loop} \ , \tag{3.1.28}$$

which we arrive at by integrating out the transverse quadratic fluctuations $(\delta X)^2$ and performing a Gaussian integral to obtain the one-loop term. This formula describes the path integral localized to a subspace, the BPS locus of Q-invariant configurations, which is given by

$$\mathcal{M}_Q = \{[X] \in \mathcal{M} |\ fermions = 0,\ Q(fermions) = 0\} \ . \tag{3.1.29}$$

The classical piece is

$$Z_{classical} = e^{-S[X_0]} \ , \tag{3.1.30}$$

and the one-loop determinant is given by

$$Z_{1-loop} = \mathrm{SDet}\left[\frac{\delta^2 S_{loc}[X_0]}{\delta X_0^2}\right] = \frac{\mathrm{Det}\Delta_{fermion}}{\mathrm{Det}\Delta_{boson}} \ , \tag{3.1.31}$$

where $\Delta_{fermion}$ and Δ_{boson} are the kinetic operators for the fermionic and bosonic fluctuations, respectively. Evaluating the one-loop determinant is often the most difficult part of a localization calculation. Strategies to compute Z_{1-loop} include field decomposition into spherical harmonics, eigenmode pairing, and index theorems.

To conclude, using supersymmetric localization, the path integral has been reduced to an integral over the saddle point configurations of the localizing action, which can be solved to give an exact result for the partition function of the theory. A supersymmetry preserving operator can be inserted into the formula (3.1.28) to compute its expectation value. The main point is summarised by emphasising that when the path integral is deformed by a localizing action term, the semi-

classical approximation in $\frac{1}{t}$ is exact, and the path integral is localized to the fixed points of the Q-invariant field configurations given by solving $fermions = 0$ and $Q\,(fermions) = 0$.

It is important to point out that different choices for the localizing action can lead to results that appear to be different but it will be possible to show that they are equivalent. For example, concerning two-dimensional $\mathcal{N} = (2,2)$ theories on S^2 [62], Coulomb branch localization writes the partition function as an integral over the vector multiplet configurations. On the other hand, an alternative (dual) description is obtained via Higgs branch localization, where the partition function reduces to a discrete sum over the product of vortex and anti-vortex excitations at the poles of S^2. These two descriptions are identical since the localization argument ensures that the final result is independent of the choice of the deformation.

3.1.3 Localization Example

We now demonstrate how the localization procedure can be applied to compute the exact two-sphere S^2 partition function of $\mathcal{N} = (2,2)$ Landau-Ginzburg (LG) models with an arbitrary gauge-invariant twisted superpotential $\widetilde{W}$. This reproduces a result from [64], although we use the notation of [71] in this presentation.

This theory comprises the twisted chiral multiplet $\Omega = \left(\omega, \eta_-, \overline{\eta}_+, G\right)$ - where ω is a complex scalar, $\eta_-, \overline{\eta}_+$ are complex Dirac fermions, and G is a complex auxiliary scalar - and the twisted anti-chiral multiplet $\overline{\Omega} = \left(\overline{\omega}, \overline{\eta}_-, \eta_+, \overline{G}\right)$. In flat space, the twisted chiral multiplet satisfies $D_-\Omega = \overline{D}_+\Omega = 0$, whereas the twisted anti-chiral multiplet obeys $D_+\overline{\Omega} = \overline{D}_-\overline{\Omega} = 0$. The supersymmetry transformations of the

components in these multiplets are[4]

$$\begin{aligned}
&\delta\omega = \sqrt{2}\left(\overline{\zeta}_+\eta_- - \zeta_-\overline{\eta}_+\right) , && \delta\overline{\omega} = -\sqrt{2}\left(\zeta_+\overline{\eta}_- - \overline{\zeta}_-\eta_+\right) ,\\
&\delta\eta_- = \sqrt{2}\zeta_- G + 2\sqrt{2}i\zeta_+ D_1\omega , && \delta\overline{\eta}_- = \sqrt{2}\overline{\zeta}_- \overline{G} - 2\sqrt{2}i\overline{\zeta}_+ D_1\overline{\omega} ,\\
&\delta\overline{\eta}_+ = \sqrt{2}\overline{\zeta}_+ G + 2\sqrt{2}i\overline{\zeta}_- D_{\overline{1}}\omega , && \delta\eta_+ = \sqrt{2}\zeta_+ \overline{G} - 2\sqrt{2}i\zeta_- D_{\overline{1}}\overline{\omega} ,\\
&\delta G = 2\sqrt{2}i\left(\zeta_+ D_1\overline{\eta}_+ - \overline{\zeta}_- D_{\overline{1}}\eta_-\right) , && \delta\overline{G} = 2\sqrt{2}i\left(\overline{\zeta}_+ D_1\eta_+ - \zeta_- D_{\overline{1}}\overline{\eta}_-\right) ,
\end{aligned} \tag{3.1.32}$$

where 1 and $\overline{1}$ are holomorphic and anti-holomorphic frame indices, respectively. The Killing spinors $\zeta_\pm$ and $\overline{\zeta}_\pm$ are the supersymmetric parameters corresponding to the four preserved supercharges in the theory. On S^2, these spinors satisfy the Killing spinor equations

$$D_\mu\zeta_\pm = \frac{i}{2r}\gamma_\mu\zeta_\pm \quad , \quad D_\mu\overline{\zeta}_\pm = \frac{i}{2r}\gamma_\mu\overline{\zeta}_\pm , \tag{3.1.33}$$

where r is the radius of the sphere and the two-dimensional gamma matrices γ_μ are the Pauli matrices.

The action in the path integral contains a kinetic term $\mathcal{L}_{\overline{\Omega}\Omega}$, a holomorphic twisted superpotential term $\mathcal{L}_{\widetilde{W}}$, and an anti-holomorphic twisted superpotential term $\mathcal{L}_{\overline{\widetilde{W}}}$. The kinetic term is described by the Lagrangian

$$\begin{aligned}
\mathcal{L}_{\overline{\Omega}\Omega} &= 2D_{\overline{1}}\overline{\omega}D_1\omega + 2D_1\overline{\omega}D_{\overline{1}}\omega - \overline{G}G + 2i\eta_+D_1\overline{\eta}_+ - 2i\overline{\eta}_-D_{\overline{1}}\eta_-\\
&= -4\overline{\omega}D_1D_{\overline{1}}\omega - \overline{G}G + 2i\eta_+D_1\overline{\eta}_+ - 2i\overline{\eta}_-D_{\overline{1}}\eta_- ,
\end{aligned} \tag{3.1.34}$$

upon integration by parts. Combining the holomorphic and anti-holomorphic twisted superpotential terms gives the twisted superpotential couplings

$$\mathcal{L}_{\widetilde{W}+\overline{\widetilde{W}}} = G^i\partial_i\widetilde{W} + \eta_-^i\overline{\eta}_+^j\partial_i\partial_j\widetilde{W} + \frac{i}{r}\widetilde{W} + \overline{G}^i\partial_i\overline{\widetilde{W}} - \overline{\eta}_-^i\eta_+^j\partial_i\partial_j\overline{\widetilde{W}} + \frac{i}{r}\overline{\widetilde{W}} . \tag{3.1.35}$$

It is possible to show that (3.1.34) and (3.1.35) are invariant under the supersymmetry transformations (3.1.32).

We now follow the localization argument to compute the S^2 partition function using

[4]We follow the convention to abuse notation slightly. Here δ on the left hand side of these expressions represents $\delta + \overline{\delta}$, where the δ and $\overline{\delta}$ pieces are associated to the terms with $\zeta_\pm$ and $\overline{\zeta}_\pm$ on the right hand side of these supersymmetry transformation, respectively.

(3.1.28). It is possible to show that the twisted chiral kinetic term $\mathcal{L}_{\overline{\Omega}\Omega}$ can be written in the form[5]

$$\mathcal{L}_{\overline{\Omega}\Omega} = \delta\overline{\delta}\left(-\frac{1}{2}\overline{\omega}G\right) \ . \tag{3.1.36}$$

Therefore, this term is Q-exact and so is a good choice for the deformation term $S_{loc}[X]$. The saddle (fixed) points are the Q-exact BPS configurations obtained by solving the constraints (3.1.25). Hence, we must solve

$$\eta_- = 0 \ \ , \ \ \overline{\eta}_+ = 0 \ \ , \ \ \delta\eta_- = 0 \ \ , \ \ \delta\overline{\eta}_+ = 0 \ , \tag{3.1.37}$$

for the twisted chiral multiplet Ω. Using (3.1.32), we find $\delta\eta_- = 0$ and $\delta\overline{\eta}_+ = 0$ are satisfied by

$$G = 0 \ , \ D_j\omega = 0 \ \Rightarrow \ \omega = \text{constant} = x + iy \ , \tag{3.1.38}$$

where $j = 1, \overline{1}$ and x, y are real constants. Therefore, the saddle point configurations are

$$\begin{aligned} &\eta_- = 0 \ \ , \ \ \overline{\eta}_+ = 0 \ \ , \ \ G = 0 \ \ , \ \ \omega = x + iy \ , \\ &\eta_+ = 0 \ \ , \ \ \overline{\eta}_- = 0 \ \ , \ \ \overline{G} = 0 \ \ , \ \ \overline{\omega} = x - iy \ , \end{aligned} \tag{3.1.39}$$

where the second line is obtained by repeating the argument for the twisted anti-chiral multiplet $\overline{\Omega}$.

Consequently, the localized partition function is given by

$$Z_{S^2} = \int [DX_0]\, e^{-S[X_0]} Z_{1-loop} \ . \tag{3.1.40}$$

Substituting the saddle point solutions (3.1.39) into (3.1.40) gives

$$[DX_0] = [D\omega][D\overline{\omega}] \ , \tag{3.1.41}$$

and

$$\exp\left(-S[X_0]\right) = \exp\left(-\left(\frac{i}{r}\widetilde{W} + \frac{i}{r}\overline{\widetilde{W}}\right)4\pi r^2\right) \ , \tag{3.1.42}$$

where the $4\pi r^2$ term arises from the volume of the two-sphere. The one-loop determinant term is given by the ratio of the determinants of the fermionic and bosonic

[5] Also, $\mathcal{L}_{\overline{\Omega}\Omega} = \overline{\delta}\delta\left(\frac{1}{2}\overline{\omega}G\right)$.

operators (3.1.31). Rewriting the localizing action (3.1.34) in the form

$$\mathcal{L}_{\overline{\Omega}\Omega} = \overline{\omega}\Delta_b\omega - \overline{G}G + (\eta_+, \overline{\eta}_-)\Delta_f \begin{pmatrix} \eta_- \\ \\ \overline{\eta}_+ \end{pmatrix} \ , \tag{3.1.43}$$

where the operators are given by

$$\Delta_b = -4D_1 D_{\overline{1}} \ \ , \ \ \Delta_f = 2i \begin{pmatrix} 0 & D_1 \\ \\ -D_{\overline{1}} & 0 \end{pmatrix}. \tag{3.1.44}$$

There is no kinetic operator for the fields $G, \overline{G}$ because these are auxiliary fields. The kinetic operators (3.1.44) satisfy the relation

$$(\Delta_f)^2 = -\Delta_b \mathbb{1}_2, \tag{3.1.45}$$

where $\mathbb{1}_2$ is the 2×2 identity matrix. Therefore, all of the fermionic and bosonic eigenstates are paired by supersymmetry, and so the fermionic and bosonic contributions to the one-loop determinant cancel out, and we have

$$Z_{1-\text{loop}} = 1 \ . \tag{3.1.46}$$

Consequently, combining these results the localized S^2 partition function is given by

$$\begin{aligned} Z_{S^2} &= \int [D\omega]\,[D\overline{\omega}] \exp\left(-4\pi i r \widetilde{W}(\omega) - 4\pi i r \overline{\widetilde{W}}(\overline{\omega})\right) \\ &= \int \mathrm{d}x\mathrm{d}y \exp\left(-4\pi i r \widetilde{W}(x+iy) - 4\pi i r \overline{\widetilde{W}}(x-iy)\right) \ , \end{aligned} \tag{3.1.47}$$

which depends on the twisted superpotential $\widetilde{W}$.

3.2 The Jeffrey-Kirwan Residue

The Jeffrey-Kirwan (JK) residue operation was introduced in [51]. The work of Jeffrey and Kirwan was motivated by a physical discussion in [72], where Witten re-examined the non-abelian localization of Duistermaat and Heckman [54] in the context of two-dimensional Yang-Mills theory. The JK residue has become a useful

tool in the study of exact results from supersymmetric localization for the partition functions and correlations functions of gauge theories in various examples, see for example [52, 73, 74]. Recently, the JK residue has also been used to strengthen the relation between scattering amplitudes and geometry by linking it to the amplituhedron [75]. The review of the JK residue operation in this section follows closely [52, 76], for more details concerning the constructive definition see [77].

3.2.1 Defining Properties

Let G be a rank r gauge group with Lie algebra $\mathfrak{g}$ and Cartan subalgebra $\mathfrak{h} \subset \mathfrak{g}$, with dual $\mathfrak{h}^*$.

To define the JK residue we need to consider n hyperplanes meeting at $\mathbf{u} = \mathbf{u}_* = 0 \in \mathbb{C}^r$:

$$H_i = \{\mathbf{u} \in \mathbb{C}^r \mid Q_i(\mathbf{u}) = 0\} \ , \tag{3.2.1}$$

where $i = 1, \ldots, n$ and $Q_i \in (\mathbb{R}^r)^*$. The set of charges $Q_* \equiv Q(\mathbf{u}_*) = \{Q_i\}$ meeting at $\mathbf{u}_*$ define the hyperplanes H_i and give them an orientation.

In all of our cases of interest, the arrangement of hyperplanes will satisfy a projective arrangement: $Q_* \subset Q$ lies within an open half-space of $\mathfrak{h}^*$ and the associated intersection point $\mathbf{u} = \mathbf{u}_* = \mathbf{0}$ is called the projective point. We will first assume that the arrangement of hyperplanes is non-degenerate, i.e. the number of hyperplanes meeting at $\mathbf{u}_*$ obeys $n = r$. The degenerate scenario, $n > r$, will be discussed further below.

Consider the integrand

$$\frac{du_1 \wedge \ldots \wedge du_r}{Q_1(\mathbf{u}) \ldots Q_r(\mathbf{u})} \ , \tag{3.2.2}$$

where the set of charges $Q_* = \{Q_1, \ldots, Q_r\}$ define the r hyperplanes that intersect at the projective point $\mathbf{u}_* = 0$, realising a codimension-r pole. The generic scenario with a non-zero $\mathbf{u}_*$ is obtained by an appropriate coordinate shift. The JK residue

JK-Res$_{\mathbf{u}=\mathbf{u}_*}[Q_*,\eta]$ is given by

$$\underset{\mathbf{u}=0}{\text{JK-Res}}\,[Q_*,\eta]\,\frac{du_1\wedge\ldots\wedge du_r}{Q_1(\mathbf{u})\ldots Q_r(\mathbf{u})}=\begin{cases}\frac{1}{|\det(Q_1,\ldots,Q_r)|} & \text{if } \eta\in\text{Cone}\,(Q_1,\ldots,Q_r)\ ,\\ 0 & \text{if } \eta\notin\text{Cone}\,(Q_1,\ldots,Q_r)\ ,\end{cases} \tag{3.2.3}$$

where Cone $(Q_1,\ldots,Q_r)$ is the closed cone spanned by $Q_1,\ldots,Q_r$ and $\eta\in(\mathbb{R}^r)^*$ is the JK parameter. The role of the JK parameter will become more clear when we consider some examples in section 3.2.3.

For the simple case $r=1$, with a single term in the denominator of the integrand, (3.2.3) reduces to

$$\underset{\mathbf{u}=0}{\text{JK-Res}}\,[q,\eta]\,\frac{du}{qu}=\begin{cases}\frac{\text{sign}(q)}{q} & \text{if } \eta q>0\ ,\\ 0 & \text{if } \eta q<0\ ,\end{cases} \tag{3.2.4}$$

with charge q. This tells us that if η and q share the same sign, then the condition $\eta\in\text{Cone}(q)$ is satisfied and we obtain a non-zero result. On the other hand, if η is positive and q is negative, or vice versa, we obtain 0 as the condition $\eta\in\text{Cone}(q)$ is not satisfied.

3.2.2 Constructive Definition

An equivalent formulation of the JK residue is given by the constructive definition, which is expressed in terms of a sum of iterated residues. To write down this definition we first need to introduce some more objects.

Let Cone$_{sing}(Q_*)$ be the union of the cones generated by all subsets of the set of charges Q_* with $r-1$ elements. This divides the space $\mathfrak{h}^*$ into chambers, where a chamber is defined to be a connected component of $\mathfrak{h}^*\setminus\text{Cone}_{sing}(Q_*)$. ΣQ_* is the set of elements of $\mathfrak{h}^*$ obtained by the partial sums of the elements of $Q_*=\{Q_1,\ldots Q_n\}$:

$$\Sigma Q_*=\left\{\sum_{i\in\pi}Q_i\mid\pi\subset\{1,\ldots,n\}\right\}\ , \tag{3.2.5}$$

where $n \geq r$. For example,

$$\begin{aligned} Q_* = \{Q_1, Q_2\} &\Rightarrow \Sigma Q_* = \{Q_1, Q_2, Q_1 + Q_2\} \ , \\ Q_* = \{Q_1, Q_2, Q_3\} &\Rightarrow \Sigma Q_* = \left\{Q_1, Q_2, Q_3, Q_1 + Q_2, Q_1 + Q_3, Q_2 + Q_3, \sum_{i=1}^{3} Q_i\right\} \ . \end{aligned} \tag{3.2.6}$$

The chambers are divided into sub-chambers by $\text{Cone}_{sing}(\Sigma Q_*)$. We impose that the JK parameter η obeys the strong regularity condition $\eta \notin \text{Cone}_{sing}(\Sigma Q_*)$, which automatically guarantees $\eta \notin \text{Cone}_{sing}(Q_*)$. This tells us that the possible values of η are restricted; η must lie within the interior of a chamber, and not along the (sub-)chamber walls.

In addition, let $\mathcal{FL}(Q_*)$ be the finite set of flags

$$F = [F_0 = \{0\} \subset F_1 \subset \ldots \subset F_r = \mathfrak{h}^*] \ , \ \text{dim} F_j = j \ , \tag{3.2.7}$$

such that Q_* contains a basis for each of the flags F_j, where $j = 1, \ldots, r$. The first j elements in the ordered set $B(F) = (Q_{j_1}, \ldots, Q_{j_r})$ give a basis of F_j.

For the ordered basis $B(F)$ of each $F \in \mathcal{FL}(Q_*)$, the iterated residue $\operatorname*{Res}_F$ of $w = w_{1,\ldots,r}\ dQ_{j_1}(\mathbf{u}) \wedge \ldots \wedge dQ_{j_r}(\mathbf{u})$ is defined by

$$\operatorname*{Res}_F w = \operatorname*{Res}_{Q_{j_r}(\mathbf{u})=0} \ldots \operatorname*{Res}_{Q_{j_1}(\mathbf{u})=0} w_{1,\ldots,r} \ , \tag{3.2.8}$$

where in each step of the residue operations on the right hand side, the other variables remain to be free. The iterated residue only depends on the flag F, and not on the choice of the ordered basis. However, for each flag, it is important to stress that the order of the residue operations in (3.2.8) is crucial.

Furthermore, for each flag F, the vectors κ_j^F are defined to be the sums of the elements of Q_*,

$$\kappa_j^F = \sum_{Q_i \in F_j} Q_i \ , \tag{3.2.9}$$

where $j = 1, \ldots, r$. The number $\nu(F)$ is given by

$$\nu(F) = \text{sign det} \left(\kappa_1^F \ldots \kappa_r^F\right) \ , \tag{3.2.10}$$

where $\nu(F) = 1$ (-1) if κ_j^F are linearly independent and the ordered basis $\kappa^F = (\kappa_1^F, \ldots, \kappa_r^F) \in \mathfrak{h}^*$ is positively (negatively) oriented, and $\nu(F) = 0$ if κ_j^F are linearly dependent.

Finally, the closed cone for a flag $F \in \mathcal{FL}(Q_*)$ is given by

$$\mathfrak{s}^+(F, Q_*) = \sum_{j=1}^{r} \mathbb{R}_{\geq 0} \kappa_j^F \ , \tag{3.2.11}$$

and $\mathcal{FL}^+(Q_*, \eta)$ represents the set of flags such that η is contained in the cone $\mathfrak{s}^+(F, Q_*)$. The strong regularity condition ensures that $\nu(F) = \pm 1$ for every $F \in \mathcal{FL}^+(Q_*, \eta)$.

We can now write down the constructive definition of the JK residue. For a JK parameter η satisfying the strong regularity condition, the JK residue at a projective point $\mathbf{u} = \mathbf{u}_* = 0$ is defined by

$$\underset{\mathbf{u}=0}{\text{JK-Res}}\,[Q_*, \eta] = \sum_{F \in \mathcal{FL}^+(Q_*, \eta)} \nu(F) \operatorname*{Res}_F w \ , \tag{3.2.12}$$

which is written in terms of the iterated residue (3.2.8) and $\nu(F)$ is defined in (3.2.10). It is important to emphasise that the result of the JK residue is independent of the choice of η. Both (3.2.3) and (3.2.12) provide equivalent formulations of the JK residue. In this thesis, the constructive definition will be applied to compute JK integrals for non-degenerate cases, $n = r$, as well as degenerate cases, $n > r$.

So far we have assumed that the arrangement of hyperplanes is non-degenerate, $n = r$ hyperplanes meet at a point. What happens if we have a degenerate scenario, where $n > r$ hyperplanes meet at a point? To deal with degenerate cases, we can introduce a mass regulator to the terms in the denominator of the integrand, which separates the hyperplanes and ensures that the situation becomes non-degenerate.[6] This allows us to follow the prescription to compute the JK integral using (3.2.12) and then the result is obtained by taking the limit of vanishing regulator. After taking the limit, the individual residues that originated from non-degenerate arrangements of

[6] This is the technique implemented in section 4.3 of [52].

hyperplanes may depend on the regulator but the full JK residue, which is the sum of all the iterated residues, is independent of the choice of the regulator.

3.2.3 Jeffrey-Kirwan Residue Examples

To illustrate how to apply the formula (3.2.12) to compute JK integrals we now present some examples. The aim of these examples, in particular the second one, is to provide explicit details of the objects defined in the constructive definition of section 3.2.2. The JK prescription is implemented to determine the poles that contribute to the integral in a specific chamber. The examples discussed are solely non-degenerate, more computations of JK integrals, including degenerate cases, appear in chapters 4 and 5.

One-dimensional JK Integral

Firstly, we can study an $r = 1$ example by considering the following integral

$$I_1 = \oint_{\text{JK}} \frac{dz}{2\pi i} \frac{(2\epsilon)}{[\pm(z-\varphi_1)+\epsilon]\,[\pm(z-\varphi_2)+\epsilon]} \,, \tag{3.2.13}$$

where $\pm(z-\varphi_a) = (z-\varphi_a)(-z+\varphi_a)$. There are 4 charge covectors,

$$Q_1 = (1) \quad , \quad Q_2 = (-1) \quad , \quad Q_3 = (1) \quad , \quad Q_4 = (-1) \,, \tag{3.2.14}$$

which are read off from the coefficient of the integration variable z for each of the terms in the denominator of the integrand.

The integral can be computed in two chambers, depending on whether the sign of the JK parameter η is positive or negative. For $\eta > 0$, we determine the poles that contribute in this chamber by establishing if we can solve $\eta = aQ_i$ for some $a > 0$ for each Q_i, where $i = 1, \ldots, 4$. Hence, we find that the poles corresponding to the terms associated to the charge covectors Q_1 and Q_3 will contribute in this chamber. This tells us that the poles contributing to the JK residue in the positive chamber are $z = \varphi_j - \epsilon$, where $j = 1, 2$. Repeating the exercise for the $\eta < 0$ case, we determine

	X_1	Y_1	X_2	Y_2	X_3	Y_3	FI
$U(1)_1$	-1	1	1	-1	0	0	ξ_1
$U(1)_2$	0	0	-1	1	1	-1	ξ_2

Table 3.1: Gauge charges for the chiral multiplets and FI parameters in the two-dimensional JK integral example.

that the poles contributing in the negative chamber are $z = \varphi_j + \epsilon$, which come from the terms associated to Q_2 and Q_4 in the integrand.

Evaluating the integral in both cases, we find the chamber independent result

$$I_1 = -\frac{1}{\varphi_{12}\left(\varphi_{12} - 2\epsilon\right)} - \frac{1}{\varphi_{12}\left(\varphi_{12} + 2\epsilon\right)} = \frac{2}{\left(\pm\varphi_{12} + 2\epsilon\right)} \ , \tag{3.2.15}$$

with the shorthand notation $\varphi_{12} = \varphi_1 - \varphi_2$.

Two-dimensional JK integral

We can consider a two-parameter model with two $U(1)$ gauge fields and 6 chiral multiplets, whose charges are given in Table 3.1. We would like to use the JK prescription to compute the integral

$$I_2 = \oint_{\text{JK}} dz_1 dz_2 \frac{(2\epsilon)^2}{\left[\pm(z_1 - z_0) + \epsilon\right]\left[\pm(z_2 - z_3) + \epsilon\right]\left[\pm(z_1 - z_2) + \epsilon\right]} \ . \tag{3.2.16}$$

This model has 6 phases as the FI parameters are varied, which are illustrated in Figure 3.1. The blue lines in a) represent the charge covectors $Q_i \in \mathfrak{h}^*$ associated to each chiral multiplet, which divide the FI space into the 6 chambers. In b) we draw a slice of the hyperplanes, which demonstrates that this example is non-degenerate because at most two hyperplanes intersect at a point. These hyperplanes, which arise from each of the terms in the denominator of the integrand in I_2, are defined by

$$\begin{aligned} &H_{X_1} : 0 = z_0 - z_1 + \epsilon \ \ , \ \ H_{Y_1} : \ \ 0 = z_1 - z_0 + \epsilon \ , \\ &H_{X_2} : 0 = z_1 - z_2 + \epsilon \ \ , \ \ H_{Y_2} : \ \ 0 = z_2 - z_1 + \epsilon \ , \\ &H_{X_3} : 0 = z_2 - z_3 + \epsilon \ \ , \ \ H_{Y_3} : \ \ 0 = z_3 - z_2 + \epsilon \ . \end{aligned} \tag{3.2.17}$$

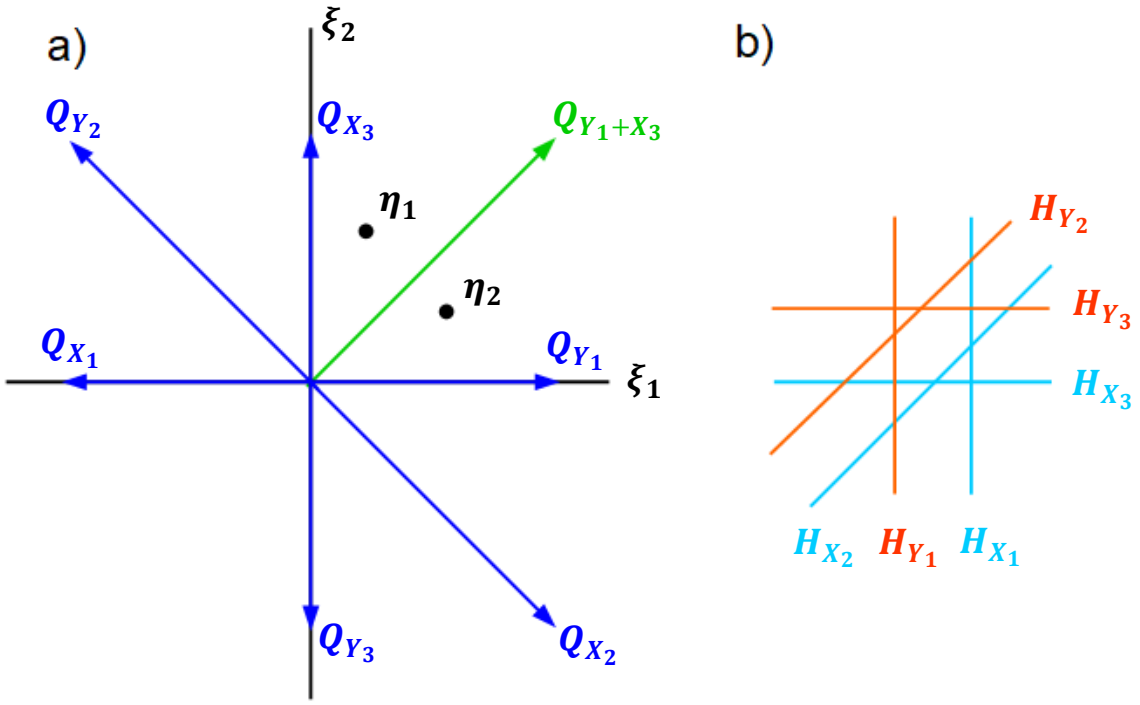

Figure 3.1: a) FI parameter space for the two-parameter model, with the charge covectors in blue, which separate the space into chambers. The chamber $\text{Cone}(Q_{Y_1}, Q_{X_3})$ is divided into the sub-chambers $\text{Cone}(Q_{Y_1}, Q_{Y_1+X_3})$ and $\text{Cone}(Q_{Y_1+X_3}, Q_{X_3})$ by the sum of the charges defining the chamber walls, which is represented by the green arrow. Similarly, the other chambers are also divided into sub-chambers but for ease of presentation this is not illustrated in the figure. η_1 and η_2 denote the JK parameters used to evaluate the integral in the chamber $\xi_1 > 0, \xi_2 > 0$. b) slice of the hyperplanes, which are normal to the charge covectors. We see that this example is non-degenerate as at most two hyperplanes meet at a point.

In this example we discuss the explicit computation of the integral in the chamber $\xi_1 > 0, \xi_2 > 0$, the upper-right quadrant of the graph in Figure 3.1-a). A similar exercise can be repeated for the other chambers.

The chamber $\xi_1 > 0, \xi_2 > 0$ is defined by the region enclosed by $\text{Cone}(Q_{Y_1}, Q_{X_3})$ and the JK residue receives contributions from

1. $H_{Y_1} \cap H_{X_3}$,
2. $H_{Y_1} \cap H_{Y_2}$,
3. $H_{X_2} \cap H_{X_3}$.

For $H_{Y_1} \cap H_{X_3}$ the set of relevant charges is $Q_* = \{Q_{Y_1}, Q_{X_3}\}$. The set of flags F,

with their respective vectors κ_j^F, is

$$\begin{aligned} F_1^1 &= \left\{Y_1, \mathbb{R}^2\right\} \qquad \kappa_1^1 = \{Y_1, Y_1 + X_3\} = \left\{\begin{pmatrix}1\\0\end{pmatrix}, \begin{pmatrix}1\\1\end{pmatrix}\right\} \quad \nu(F_1^1) = 1 \ , \\ F_2^1 &= \left\{X_3, \mathbb{R}^2\right\} \qquad \kappa_2^1 = \{X_3, Y_1 + X_3\} = \left\{\begin{pmatrix}0\\1\end{pmatrix}, \begin{pmatrix}1\\1\end{pmatrix}\right\} \quad \nu(F_2^1) = -1 \ . \end{aligned} \tag{3.2.18}$$

For $H_{Y_1} \cap H_{Y_2}$ the set of relevant charges is $Q_* = \{Q_{Y_1}, Q_{Y_2}\}$. The set of flags with their respective vectors κ_j^F is

$$\begin{aligned} F_1^2 &= \left\{Y_1, \mathbb{R}^2\right\} \qquad \kappa_1^2 = \{Y_1, Y_1 + Y_2\} = \left\{\begin{pmatrix}1\\0\end{pmatrix}, \begin{pmatrix}0\\1\end{pmatrix}\right\} \quad \nu(F_1^2) = 1 \ , \\ F_2^2 &= \left\{Y_2, \mathbb{R}^2\right\} \qquad \kappa_2^2 = \{Y_2, Y_1 + Y_2\} = \left\{\begin{pmatrix}-1\\1\end{pmatrix}, \begin{pmatrix}0\\1\end{pmatrix}\right\} \quad \nu(F_2^1) = -1 \ . \end{aligned} \tag{3.2.19}$$

For $H_{X_2} \cap H_{X_3}$ the set of relevant charges is $Q_* = \{Q_{X_2}, Q_{X_3}\}$. The set of flags with their respective vectors κ_j^F is

$$\begin{aligned} F_1^3 &= \left\{X_2, \mathbb{R}^2\right\} \qquad \kappa_1^3 = \{X_2, X_2 + X_3\} = \left\{\begin{pmatrix}1\\-1\end{pmatrix}, \begin{pmatrix}1\\0\end{pmatrix}\right\} \quad \nu(F_1^1) = 1 \ , \\ F_2^3 &= \left\{X_3, \mathbb{R}^2\right\} \qquad \kappa_2^3 = \{X_3, X_2 + X_3\} = \left\{\begin{pmatrix}0\\1\end{pmatrix}, \begin{pmatrix}1\\0\end{pmatrix}\right\} \quad \nu(F_2^1) = -1 \ . \end{aligned} \tag{3.2.20}$$

To compute the JK integral in this chamber we choose a JK parameter that obeys the strong regularity condition, i.e. it must lie within the interior of $\text{Cone}(Q_{Y_1}, Q_{X_3})$ (not on the chamber walls) and it cannot take a value along $Q_{Y_1+X_3}$, the line in green on Figure 3.1-a), which divides this chamber into two sub-chambers. This gives two choices, η_1 and η_2 in Figure 3.1-a), where η_1 is a JK parameter that lies within the interior of $\text{Cone}(Q_{X_3}, Q_{Y_1+X_3})$, for example $\eta_1 = (1, 2)$. Whilst, η_2 is a JK parameter

that lies within the interior of $\text{Cone}(Q_{Y_1+X_3}, Q_{Y_1})$, for example $\eta_1 = (2, 1)$.

Consequently, we pick either of these JK parameters and follow the prescription to determine the flags F for each set of the relevant charges Q_* that we must select to ensure that the JK parameter is contained in the positive cone $\mathfrak{s}^+(F, Q_*)$, and then perform the sum of the iterated residue in (3.2.12). We will now show that both choices for the JK parameter give the same result.

Firstly, consider η_1 and determine the flags to select for each of the contributions to the JK residue. For $H_{Y_1} \cap H_{X_3}$ we need to establish whether η_1 is located in the positive $\text{Cone}(Q_{Y_1}, Q_{Y_1+X_3})$ or $\text{Cone}(Q_{X_3}, Q_{Y_1+X_3})$. Since we are dealing with polyhedral cones with as many generators as the dimension, it is possible to determine this by expressing η_1 in the basis of the generators of the cone and checking whether the coefficients are strictly positive. Hence, it is possible to see that we cannot write $\eta_1 = \alpha Q_{Y_1} + \beta Q_{Y_1+X_3}$ with $\alpha, \beta > 0$ but we can write $\eta_1 = \alpha Q_{X_3} + \beta Q_{Y_1+X_3}$ with $\alpha, \beta > 0$. Therefore, η_1 is in the positive $\text{Cone}(Q_{X_3}, Q_{Y_1+X_3})$ and the flag F_2^1 must be selected to compute this contribution to the integral. This could have been simply deduced from the graph in Figure 3.1-a), but this method is advantageous as it can be generalised to cases of higher dimensions, where it is not possible to draw the graph. This method can also be used to implement the JK prescription using Mathematica, see further details below. Repeating the exercise for the other two contributions, $H_{Y_1} \cap H_{Y_2}$ and $H_{X_2} \cap H_{X_3}$, we see that η_1 is in the positive $\text{Cone}(Q_{Y_1}, Q_{Y_1+Y_2})$ and $\text{Cone}(Q_{X_3}, Q_{X_2+X_3})$, respectively. Consequently, for η_1 the relevant flags are F_2^1, F_1^2, F_2^3.

Finally, to compute the JK integral in this chamber using η_1, we choose $B(F_2^1) = \{Q_{X_3}, Q_{Y_1}\}$, $B(F_1^2) = \{Q_{Y_1}, Q_{Y_2}\}$, and $B(F_2^3) = \{Q_{X_3}, Q_{X_2}\}$ for the ordered basis of the flag from each of the contributions. The constructive definition (3.2.12) tells us the I_2 is given by

$$I_2 = \nu(F_2^1) \operatorname*{Res}_{F_2^1} + \nu(F_1^2) \operatorname*{Res}_{F_1^2} + \nu(F_2^3) \operatorname*{Res}_{F_2^3} , \tag{3.2.21}$$

where the iterated residues are

$$\begin{aligned}
\operatorname*{Res}_{F_2^1} &= \operatorname*{Res}_{z_1=z_0-\epsilon} \operatorname*{Res}_{z_2=z_3-\epsilon} I_2(z_1,z_2)\ \mathrm{d}z_2\wedge dz_1\ ,\\
\operatorname*{Res}_{F_1^2} &= \operatorname*{Res}_{z_2=z_1-\epsilon=z_0-2\epsilon} \operatorname*{Res}_{z_1=z_0-\epsilon} I_2(z_1,z_2)\ \mathrm{d}z_1\wedge dz_2\ ,\\
\operatorname*{Res}_{F_2^3} &= \operatorname*{Res}_{z_1=z_2-\epsilon=z_3-2\epsilon} \operatorname*{Res}_{z_2=z_3-\epsilon} I_2(z_1,z_2)\ \mathrm{d}z_2\wedge dz_1\ ,
\end{aligned} \tag{3.2.22}$$

and $I_2(z_1,z_2)$ is the integrand in (3.2.16). Substituting the values of $\nu(F)$ into (3.2.21) and using the anti-symmetric property of the wedge product, $-\mathrm{d}z_2\wedge dz_1=\mathrm{d}z_1\wedge dz_2$, we obtain

$$I_2=\frac{1}{(\pm z_{03}+\epsilon)}-\frac{1}{(z_{03}+\epsilon)\,(z_{03}+3\epsilon)}-\frac{1}{(z_{03}-\epsilon)\,(z_{03}-3\epsilon)}=\frac{3}{(\pm z_{03}+3\epsilon)}\ . \tag{3.2.23}$$

The same procedure can be implemented to compute the integral using the JK parameter η_2. In this case, the relevant flags are F_1^1,F_1^2,F_2^3, and I_2 is given by

$$I_2=\nu(F_1^1)\operatorname*{Res}_{F_1^1}+\nu(F_1^2)\operatorname*{Res}_{F_1^2}+\nu(F_2^3)\operatorname*{Res}_{F_2^3}\ . \tag{3.2.24}$$

The second and third term in this sum are identical to the second and third term in (3.2.21) from the computation using η_1. The only difference is in the first term, where the iterated residue $\mathrm{Res}_{F_1^1}$ is[7]

$$\operatorname*{Res}_{F_1^1} = \operatorname*{Res}_{z_2=z_3-\epsilon} \operatorname*{Res}_{z_1=z_0-\epsilon} I_2(z_1,z_2)\ \mathrm{d}z_1\wedge dz_2\ , \tag{3.2.25}$$

where the order of the residues has been switched compared to $\mathrm{Res}_{F_2^1}$ in (3.2.22). Evaluating (3.2.24) we obtain the same result as the η_1 case, given in (3.2.23), which is expected because both of these JK parameters are located in the same chamber. Hence, the JK prescription produces two expressions, (3.2.21) and (3.2.24), for this integral in the chamber $\xi_1>0,\xi_2>0$. These expressions depend on the sub-chamber that the JK parameter lies in but are equivalent upon evaluation.

This analysis can be repeated to compute the JK integral in the other chambers. Although the multi-dimensional poles contributing in each chamber differ, it is

[7]Using the ordered basis $B(F_1^1)=\{Q_{Y_1},Q_{X_3}\}$.

Chamber of FI space	Sign of $\nu(F)$	Multi-dimensional Pole
$\xi_1 > 0$	$+$	$(z_2 = z_3 - \epsilon, z_1 = z_0 - \epsilon)$
$\xi_2 > 0$	$+$	$(z_1 = z_0 - \epsilon, z_2 = z_0 - 2\epsilon)$
$\xi_1 + \xi_2 > 0$	$+$	$(z_2 = z_3 - \epsilon, z_1 = z_3 - 2\epsilon)$
$\xi_1 > 0$	$-$	$(z_1 = z_0 - \epsilon, z_2 = z_3 + \epsilon)$
$\xi_2 < 0$	$-$	$(z_1 = z_0 - \epsilon, z_2 = z_0)$
$\xi_1 + \xi_2 > 0$	$+$	$(z_1 = z_2 - \epsilon, z_2 = z_3 - \epsilon)$
$\xi_1 > 0$	$+$	$(z_2 = z_1 + \epsilon, z_1 = z_0 + \epsilon)$
$\xi_2 < 0$	$-$	$(z_2 = z_3 + \epsilon, z_1 = z_0 - \epsilon)$
$\xi_1 + \xi_2 < 0$	$-$	$(z_1 = z_2 - \epsilon, z_2 = z_3 + \epsilon)$
$\xi_1 < 0$	$+$	$(z_2 = z_3 + \epsilon, z_1 = z_0 + \epsilon)$
$\xi_2 < 0$	$+$	$(z_1 = z_0 + \epsilon, z_2 = z_0 + 2\epsilon)$
$\xi_1 + \xi_2 < 0$	$+$	$(z_2 = z_3 + \epsilon, z_1 = z_3 + 2\epsilon)$
$\xi_1 < 0$	$-$	$(z_1 = z_0 + \epsilon, z_2 = z_3 - \epsilon)$
$\xi_2 > 0$	$-$	$(z_1 = z_0 + \epsilon, z_2 = z_0)$
$\xi_1 + \xi_2 < 0$	$+$	$(z_1 = z_2 + \epsilon, z_2 = z_3 + \epsilon)$
$\xi_1 < 0$	$+$	$(z_2 = z_1 - \epsilon, z_1 = z_0 - \epsilon)$
$\xi_2 > 0$	$-$	$(z_2 = z_3 - \epsilon, z_1 = z_0 + \epsilon)$
$\xi_1 + \xi_2 > 0$	$-$	$(z_1 = z_2 + \epsilon, z_2 = z_3 - \epsilon)$

Table 3.2: Multi-dimensional poles contributing to the JK integral I_2 (3.2.16) in each of the 6 chambers.

possible to show that the overall result for this integral, from the sum of the iterated residues, is the same, as stated in (3.2.23). In Table 3.2 we summarise the multi-dimensional poles contributing in each chamber, where each pole comes with its sign $\nu(F)$ appearing in the sum of the iterated residues and the residue operations are performed from left to right.

Performing the JK integral in each chamber can be a labour intensive task. As a result, this procedure can be implemented using Mathematica to determine the poles that contribute in each chamber and to compute the sum of the iterated residues. For the Mathematica code used to evaluate this JK integral in each chamber, see appendix A.

Chapter 4

Correlators of 2d $\mathcal{N} = (2, 2)$ Gauged Linear Sigma Models

In this chapter we examine two-dimensional $\mathcal{N} = (2, 2)$ Gauged Linear Sigma Models (GLSMs) on the Omega-deformed two-sphere background S^2_Ω. Firstly, we begin by summarising the main result of [74]. This is then used to investigate a model for a GLSM describing a non-compact geometry, which was originally studied in [19, 20] and again in [74].

4.1 Summary of the Localization Result on the Omega-deformed Two-sphere

Correlation functions of two-dimensional $\mathcal{N} = (2, 2)$ GLSMs on the Omega-deformed sphere were studied in [74] (see also [73]). The technique of supersymmetric localization was employed to obtain an exact formula, written in terms of a Jeffrey-Kirwan (JK) residue on the Coulomb branch. This result was derived by performing a careful analysis of the contour of integration for the auxiliary field D, following the approach of [52, 78].

The supersymmetry background is obtained using the method of Festuccia and

Seiberg [70] outlined in section 3.1.2. The 2d $\mathcal{N}=(2,2)$ flat space theory is coupled to the off-shell supergravity background $\left(\Sigma, g_{\mu\nu}, A_\mu^{(R)}, C_\mu, \widetilde{C}_\mu\right)$, which contains a metric $g_{\mu\nu}$ on a closed orientable Riemann surface Σ, a background R symmetry gauge field $A_\mu^{(R)}$, and the graviphoton vector fields $C_\mu, \widetilde{C}_\mu$ that couple to the conserved currents associated to the central charges of the supersymmetry algebra.[1]

The Omega-deformed two-sphere S^2_Ω is described, using the canonical complex frame $e^1 = e^1_z \mathrm{d}z = g^{\frac{1}{4}}\mathrm{d}z, e^{\overline{1}} = e^{\overline{1}}_{\overline{z}}\mathrm{d}\overline{z} = g^{\frac{1}{4}}\mathrm{d}\overline{z}$, by $\Sigma = \mathbb{CP}^1$ with metric

$$\mathrm{d}s^2 = 2g_{z\overline{z}}(|z|^2)\mathrm{d}z\mathrm{d}\overline{z} = \sqrt{g}\mathrm{d}z\mathrm{d}\overline{z} = e^1 e^{\overline{1}} \ , \tag{4.1.1}$$

and a $U(1)$ isometry generated by the real Killing Vector V,

$$V = iz\partial_z - i\overline{z}\partial_{\overline{z}} \ , \tag{4.1.2}$$

whose fixed points are located at the North and South poles, $z=0$ and $z=\infty$, respectively. The supersymmetric background contains the global R symmetry gauge field

$$A_\mu^{(R)} = \frac{1}{2}\omega_\mu \ , \tag{4.1.3}$$

where ω_μ is the spin connection,[2] and the graviphoton dual field strengths

$$\mathcal{H} = -i\epsilon^{\mu\nu}\partial_\mu C_\nu = \frac{\epsilon_\Omega}{2}\epsilon^{\mu\nu}\partial_\mu V_\nu \quad , \quad \widetilde{\mathcal{H}} = -i\epsilon^{\mu\nu}\partial_\mu \widetilde{C}_\nu = 0 \ , \tag{4.1.4}$$

where ϵ_Ω is the Omega deformation complex parameter [57], a constant of mass dimension 1. The Killing spinor solutions for this background are given by

$$\zeta = \begin{pmatrix} \zeta_- \\ \\ \zeta_+ \end{pmatrix} = \begin{pmatrix} i\epsilon_\Omega V_1 \\ \\ 1 \end{pmatrix} \quad , \quad \overline{\zeta} = \begin{pmatrix} \overline{\zeta}_- \\ \\ \overline{\zeta}_+ \end{pmatrix} = \begin{pmatrix} 1 \\ \\ -i\epsilon_\Omega V_{\overline{1}} \end{pmatrix} \ . \tag{4.1.5}$$

The Omega-deformed two-sphere background preserves two out of the four supercharges and corresponds to a one-parameter deformation of the A-twisted sphere,

[1] For more details of two-dimensional $\mathcal{N}=(2,2)$ supersymmetric backgrounds see [71].

[2] The spin connection is given by $\omega_z = -\frac{i}{4}\partial_z \log g$, $\omega_{\overline{z}} = \frac{i}{4}\partial_{\overline{z}} \log g$, which are obtained by using the torsion vanishing condition $\mathrm{d}e^a + \omega^a{}_b \wedge e^b = 0$, raising and lowering frame indices with $\delta^{1\overline{1}} = 2$, $\delta_{1\overline{1}} = \frac{1}{2}$, imposing the anti-symmetry condition $\omega^{ab} = -\omega^{ba}$, and applying the definition $\omega_\mu = -2i(\omega_{1\overline{1}})_\mu$.

which is recovered by setting $\epsilon_\Omega = 0$.

The correlation functions of gauge-invariant polynomials in σ, the complex scalar in the vector multiplet, are given by

$$\left\langle \mathcal{O}^{(N)}(\sigma)\mathcal{O}^{(S)}(\sigma)\right\rangle = \frac{(-1)^{N_*}}{|\mathcal{W}|}\sum_k q^k \widetilde{Z}_k\left(\mathcal{O}\right) \ , \tag{4.1.6}$$

where $\mathcal{O}^{(N)}(\sigma)$ and $\mathcal{O}^{(S)}(\sigma)$ denote the operators inserted at the North and South poles of S^2_Ω, respectively. We now discuss the terms that appear on the right hand side of (4.1.6).

Firstly, the factor $(-1)^{N_*}$ appears due to a R charge dependent sign ambiguity associated to the chiral multiplets. The ambiguity is resolved by the prescription to assign R charge 0 (2) to chiral multiplets of charge $+1$ (-1). N_* denotes the number of field components of R charge 2 in the GLSM. For a gauge group G, $|\mathcal{W}|$ is the order of the Weyl group. We sum over the topological sectors labelled by k, the magnetic fluxes belonging to the weight lattice of the GNO (or Langlands) dual group $G^\vee$ of G [79, 80, 81]. The instanton factor q is given by

$$q_I = e^{2\pi i \tau_I} \ , \tag{4.1.7}$$

for each $U(1)$ factor in G, where τ_I is the complexified FI coupling

$$\tau_I = \frac{\theta_I}{2\pi} + i\xi_I \ , \tag{4.1.8}$$

for $I = 1, \ldots, n$, where $n \leq \text{rank}(G)$. The contribution q^k in (4.1.6) is the classical action component from the localization computation, which occurs due to the presence of the linear twisted superpotential

$$\widetilde{W}(\sigma) = \tau^I \text{tr}_I(\sigma) \ . \tag{4.1.9}$$

On the right hand side of (4.1.6) we also have

$$\widetilde{Z}_k\left(\mathcal{O}\right) = \oint_{\text{JK}(\xi^{\text{UV}}_{\text{eff}})} \left(\prod_{a=1}^{\text{rank}(G)} \frac{\mathrm{d}\widehat{\sigma}_a}{2\pi i}\right) Z_k^{1-\text{loop}}(\widehat{\sigma};\epsilon_\Omega)\mathcal{O}^{(N)}\left(\widehat{\sigma} - \epsilon_\Omega\frac{k}{2}\right)\mathcal{O}^{(S)}\left(\widehat{\sigma} + \epsilon_\Omega\frac{k}{2}\right) \ , \tag{4.1.10}$$

where the contour integral is a JK integral, which gives a sum of the residues of the codimension-rank(G) poles in the integrand. This depends on the effective FI parameter in the UV $\xi_{\text{eff}}^{\text{UV}}$, which is needed to ensure that the series in q in (4.1.6) converges. The localization locus is the classical Coulomb branch, which is spanned by the vacuum expectation values

$$\sigma = \text{diag}(\sigma_a) \quad , \quad \overline{\sigma} = \text{diag}(\overline{\sigma}_a) \ , \tag{4.1.11}$$

where $a = 1, \ldots, \text{rank}(G)$. The integral is over the constant mode $\widehat{\sigma}$, which is defined as the average $\widehat{\sigma} = \frac{1}{2}(\sigma_N + \sigma_S)$, where the values of σ at the poles are

$$(\sigma_a)_N = \widehat{\sigma}_a - \epsilon_\Omega \frac{k_a}{2} \quad , \quad (\sigma_a)_S = \widehat{\sigma}_a + \epsilon_\Omega \frac{k_a}{2} \ . \tag{4.1.12}$$

Finally, the one-loop term $Z_k^{1-\text{loop}}(\widehat{\sigma}; \epsilon_\Omega)$ takes the form

$$Z_k^{1-\text{loop}}(\widehat{\sigma}; \epsilon_\Omega) = Z_k^{\text{vector}}(\widehat{\sigma}; \epsilon_\Omega) \prod_i Z_k^{\Phi_i}(\widehat{\sigma}; \epsilon_\Omega) \ . \tag{4.1.13}$$

The vector multiplet contribution is given by

$$Z_k^{\text{vector}}(\widehat{\sigma}; \epsilon_\Omega) = (-1)^{\sum_{\alpha>0}(\alpha(k)+1)} \Delta\left(\widehat{\sigma} + \frac{k}{2}\epsilon_\Omega\right) \Delta\left(\widehat{\sigma} - \frac{k}{2}\epsilon_\Omega\right) \ , \tag{4.1.14}$$

where $\alpha > 0$ denotes the positive roots of the gauge group G, and

$$\Delta(x) = \prod_{\alpha>0} \alpha(x) \ , \tag{4.1.15}$$

is the Vandermonde determinant of G. The contribution from each chiral multiplet Φ_i, which transforms in a representation $\mathcal{R}_i$ of G and carries R charge r_i, is

$$Z_k^{\Phi_i}(\widehat{\sigma}; \epsilon_\Omega) = \prod_{\rho_i \in \mathcal{R}_i} \left(\epsilon_\Omega^{\, r_i - \rho_i(k) - 1} \frac{\Gamma\left(\frac{\rho_i(\widehat{\sigma})}{\epsilon_\Omega} + \frac{r_i - \rho_i(k)}{2}\right)}{\Gamma\left(\frac{\rho_i(\widehat{\sigma})}{\epsilon_\Omega} - \frac{r_i - \rho_i(k)}{2} + 1\right)} \right) \ , \tag{4.1.16}$$

where ρ_i denote the weights of $\mathcal{R}_i$. This expression can be conveniently written as

$$Z_k^{\Phi_i}(\widehat{\sigma}; \epsilon_\Omega) = \prod_{\rho_i \in \mathcal{R}_i} Z^{(r_i - \rho_i(k))}(\widehat{\sigma}; \epsilon_\Omega) \ , \tag{4.1.17}$$

where

$$Z^{\mathbf{r}}\left(\widehat{\sigma};\epsilon_\Omega\right)=\begin{cases}\prod\limits_{m=-\frac{\mathbf{r}}{2}+1}^{\frac{\mathbf{r}}{2}-1}\left(\rho_i(\widehat{\sigma})+\epsilon_\Omega m\right) & \text{if } \mathbf{r}>1\ ,\\ 1 & \text{if } \mathbf{r}=1\ ,\\ \prod\limits_{m=-\frac{|\mathbf{r}|}{2}}^{\frac{|\mathbf{r}|}{2}}\left(\rho_i(\widehat{\sigma})+\epsilon_\Omega m\right)^{-1} & \text{if } \mathbf{r}<1\ ,\end{cases} \tag{4.1.18}$$

and $\mathbf{r}=r_i-\rho_i(k)$.

The only modification in the presence of a flavour symmetry F, a non-R continuous global symmetry, acting on the chiral multiplets Φ_i is to turn on the twisted masses m_i^F and send $\rho_i(\widehat{\sigma})\to\rho_i(\widehat{\sigma})+m_i^F$ in the chiral multiplet one-loop contribution (4.1.16). In general, the correlation function (4.1.6) depends holomorphically on the parameters ϵ_Ω, q, and any twisted masses m_i^F that are turned on.

The formula for the A-model correlators is obtained by sending $\epsilon_\Omega\to 0$, which gives

$$\langle\mathcal{O}(\sigma)\rangle=\frac{(-1)^{N_*}}{|\mathcal{W}|}\sum_k q^k\oint_{\mathrm{JK}(\xi_{\mathrm{eff}}^{\mathrm{UV}})}\left(\prod_{a=1}^{\mathrm{rank}(G)}\frac{\mathrm{d}\widehat{\sigma}_a}{2\pi i}\right)Z_k^{1-\mathrm{loop}}(\widehat{\sigma})\mathcal{O}(\widehat{\sigma})\ , \tag{4.1.19}$$

where the insertion point of the operator $\mathcal{O}(\sigma)$ is now no longer specified since a gauge-invariant operator can be inserted anywhere on the A-twisted two-sphere due to the topological nature of the theory.

To end this section we state the recursion relations that the ϵ_Ω-dependent correlation functions obey in the case of abelian theories. These relations are useful as they can be applied to efficiently compute higher-point correlators from lower-point correlators and can be used as a consistency check to verify results. For each $U(1)_a$ gauge group factor, the correlators satisfy

$$\begin{aligned}&\left\langle\mathcal{O}^{(N)}(\sigma_N)\prod_{i,Q_i^a>0}\prod_{l=0}^{Q_i^a-1}\left[Q_i(\sigma_N)+m_i^F+\epsilon_\Omega\left(\frac{r_i}{2}+l\right)\right]\right\rangle\\&=q_a\cdot\left\langle\mathcal{O}^{(N)}\left(\sigma_N-\epsilon_\Omega\delta(a)\right)\prod_{i,Q_i^a<0}\prod_{l=0}^{|Q_i^a|-1}\left[Q_i(\sigma_N)+m_i^F+\epsilon_\Omega\left(\frac{r_i}{2}+l\right)\right]\right\rangle\ ,\end{aligned} \tag{4.1.20}$$

for the case where all of the operators are inserted at the North pole. A relation for the operators inserted at the South pole is obtained by applying $N\to S,\epsilon_\Omega\to-\epsilon_\Omega$

	X_1	X_2	Y	Z	W	FI
$U(1)_1$	1	1	1	$-N$	-1	ξ_1
$U(1)_2$	0	0	1	1	-2	ξ_2

Table 4.1: Gauge charges for the chiral multiplets and FI parameters in the GLSM for the non-compact orbifold $\mathbb{C}^3/\mathbb{Z}_{(2N+1)(2,2,1)}$.

to this expression. In the limit $\epsilon_\Omega \to 0$, (4.1.20) reduces to the quantum chiral ring relations (quantum cohomology relations) of the A-twisted theory.

4.2 Investigation of $\mathbb{C}^3/\mathbb{Z}_{(2N+1)(2,2,1)}$

In this section, we use (4.1.19) to re-investigate the computation of the correlators of an A-twisted GLSM for a non-compact orbifold, a model examined originally in [19, 20] and subsequently in [74]. We find that the result for the three-point correlators is ambiguous; it depends on the twisted masses that are used to make the JK integral non-degenerate. We turn on the Omega deformation and compute the correlators using (4.1.6) to see if this resolves the ambiguity. The results for these correlators are tested using the recursion relations (4.1.20) and explicitly compared with the evaluation of these correlators in [20].

4.2.1 A-twisted Correlators

Consider the GLSM for the non-compact orbifold $\mathbb{C}^3/\mathbb{Z}_{(2N+1)(2,2,1)}$, which has a $U(1)^2$ gauge group and 5 chiral multiplets of R charge zero and the gauge charges given in Table 4.1. We observe that the sum of the $U(1)_2$ gauge charges vanishes, whereas the sum of the $U(1)_1$ charges depends on the value of N, $\sum Q_{U(1)_1} = -N + 2$. We consider the scenario $N > 2$, so that this sum is negative, and the axial R symmetry has a mixed anomaly with the $U(1)_1$ gauge group.

We are interested in computing the correlators for this GLSM in the geometric phase, where the effective FI parameters in the UV are $\xi_{\text{eff}}^{\text{UV}} = (-\infty, \xi_2)$. The geometric phase is the region satisfying $-Nk_1 + k_2 \geq 0$ and $-k_1 - 2k_2 \geq 0$, which is related to

k_1	0	-1	-2	-3	...	$-l$	...
k_2	0	$-N,\ldots,0$	$-2N,\ldots,1$	$-3N,\ldots,1$	...	$-lN,\ldots,\lvert\lfloor\frac{l}{2}\rfloor\rvert$	...

Table 4.2: The allowed values of the integers k_1 and k_2 in the geometric phase for the GLSM. These appear in the sum over the topological sectors in the formula for the correlator $F_{a,b}$. Values of $k_1 > 0$ are not possible in the region satisfying $-Nk_1 + k_2 \geq 0$ and $-k_1 - 2k_2 \geq 0$. $\lfloor a \rfloor$ denotes the greatest integer less than or equal to a.

the region $-2\xi_1 + \xi_2 > 0, -\xi_1 - N\xi_2 > 0$ in FI space. In Table 4.2 we illustrate the allowed values of k_1 and k_2 in this region.

The correlators for this GLSM are given by

$$F_{a,b} = \left\langle \sigma_1^a \sigma_2^b \right\rangle \ , \tag{4.2.1}$$

where $a, b \in \mathbb{Z}_{\geq 0}$, and σ_1 and σ_2 are the complex scalars in the vector multiplets for $U(1)_1$ and $U(1)_2$, respectively. These correlators obey a selection rule due to axial and gravitational anomalies. The gravitational anomaly for this GLSM is $d_{\text{grav}} = -2 - (-5) = 3$, and since the sum of the $U(1)_1$ charges is non-zero, this tells us that the non-vanishing correlators must satisfy the constraint

$$a + b = 3 + (2 - N)k_1 \ , \tag{4.2.2}$$

where k_1 is the flux of the $U(1)_1$ gauge group.

The correlators $F_{a,b}$ can be evaluated in the UV geometric phase using (4.1.19). The JK residue prescription informs us that we must select the multi-dimensional pole that arises from the intersection of the hyperplanes associated to the fields Z and W. The prescription also specifies the order in which the residue operations should be carried out. The geometric phase is divided into two sub-chambers, $\text{Cone}(Q_W, Q_{W+Z})$ and $\text{Cone}(Q_Z, Q_{W+Z})$. Taking the JK parameter η to lie within the interior of the sub-chamber $\text{Cone}(Q_W, Q_{W+Z})$, it is possible to find a solution to $\eta = \alpha Q_W + \beta Q_{W+Z}$ for constants $\alpha, \beta > 0$, where Q_W is the vector comprised of the gauge charges of the field W. On the other hand, it is not possible to solve $\eta = \alpha Q_Z + \beta Q_{W+Z}$ for $\alpha, \beta > 0$. Therefore, the residue of the pole from W must come before the residue of

the pole from Z in the iterated residue for this sub-chamber. Taking η to lie within the interior of the other sub-chamber, $\text{Cone}(Q_Z, Q_{W+Z})$, reverses the order in the iterated residue but does not change the final result, as expected from the discussion in section 3.2.3.

This computation is also an example of a degenerate JK integral. This is because more than two hyperplanes intersect at the point $\sigma_1 = \sigma_2 = 0$. To overcome this issue we make the integral non-degenerate by turning on a generic twisted mass m_i for each term in the denominator of the integrand. Consequently, the twisted masses act as a regulator allowing us to compute the integral then take the limit of vanishing twisted masses, as discussed at the end of section 3.2.2. It is important to stress that in this work we select a general choice for the twisted mass regulation compared to the one used in [74], where a single common twisted mass term is turned on for each term in the denominator of the integrand.

Hence, with generic masses turned on, the correlators (4.2.1) are given by

$$F_{a,b} = \sum_{k_1,k_2} q_1^{k_1} q_2^{k_2} \operatorname*{Res}_{\widehat{\sigma}_1=\frac{m_5+2m_4}{1+2N}} \operatorname*{Res}_{\widehat{\sigma}_2=\frac{-\widehat{\sigma}_1+m_5}{2}} \widehat{\sigma_1}^a \widehat{\sigma}_2^b Z_k^{X_1} Z_k^{X_2} Z_k^Y Z_k^Z Z_k^W \ , \tag{4.2.3}$$

where we sum over all the allowed values of k_1 and k_2 in the geometric phase, and we have

$$\begin{aligned} Z_k^{X_i} &= (\widehat{\sigma}_1 + m_i)^{-(k_1+1)} & Z_k^Y &= (\widehat{\sigma}_1 + \widehat{\sigma}_2 + m_3)^{-(k_1+k_2+1)} \\ Z_k^Z &= (-N\widehat{\sigma}_1 + \widehat{\sigma}_2 + m_4)^{-(-Nk_1+k_2+1)} & Z_k^W &= (-\widehat{\sigma}_1 - 2\widehat{\sigma}_2 + m_5)^{-(-k_1-2k_2+1)} \end{aligned} \ , \tag{4.2.4}$$

for $i = 1, 2$.

All that remains is to compute the sum of the iterated residues and take the limit of vanishing twisted masses. We will focus on the result for the three-point correlators, $a + b = 3$, where the selection rule (4.2.2) tells us that $k_1 = 0$, which implies $k_2 = 0$. Consequently, the poles in (4.2.3) are simple, and we obtain

$$F_{3-b,b} = \frac{(2m_4 + m_5)^{(3-b)}(-m_4 + Nm_5)^b}{(1+2N)\Delta} \ , \tag{4.2.5}$$

where $b = 0, \ldots, 3$, and

$$\begin{aligned}\Delta = &[(1+2N)m_1 + 2m_4 + m_5]\,[(1+2N)m_2 + 2m_4 + m_5] \\ &\times [(1+2N)m_3 + m_4 + (1+N)m_5] \ .\end{aligned} \tag{4.2.6}$$

Taking the limit of vanishing twisted mass we find that the result is ambiguous since it depends on the order in which the limits are taken. Performing $\lim_{m_4\to 0}\lim_{m_5\to 0}$ or $\lim_{m_5\to 0}\lim_{m_4\to 0}$ directly on (4.2.5) we obtain 0. On the other hand, we obtain a non-zero result by performing the following limits

$$\lim_{m_5\to 0}\lim_{m_4\to 0}\lim_{m_3\to 0}\lim_{m_2\to 0}\lim_{m_1\to 0} F_{3-b,b} = \frac{N^b}{(2N^2+3N+1)} \ , \tag{4.2.7}$$

$$\lim_{m_4\to 0}\lim_{m_5\to 0}\lim_{m_3\to 0}\lim_{m_2\to 0}\lim_{m_1\to 0} F_{3-b,b} = \frac{(-1)^b 2^{(1-b)}}{(1+2N)} \ . \tag{4.2.8}$$

We find that the limits of m_1, m_2, and m_3 commute with each other, but exchanging m_4 and m_5 we obtain a different answer. Thus, the result is ambiguous. We continue our study of these three-point correlators in the next section by turning on the Omega deformation to see if this resolves the ambiguity. It is hoped that the introduction of the Omega deformation will regulate the JK integral by separating the coincident hyperplanes so that at most two hyperplanes intersect at a point.

4.2.2 Turning on the Omega Deformation

The evaluation of the correlators $F_{a,b}$ in the geometric phase can be repeated with the Omega deformation parameter turned on. We consider the case where all of the operators are inserted at the North pole and the twisted masses are turned off since we are using ϵ_Ω as a regulator.

Correlator expression

Inserting twisted chiral operators at the North pole, using the formula (4.1.6), and

applying the shift $\widehat{\sigma} \to \widehat{\sigma} + \frac{k}{2}\epsilon_\Omega$, the correlator $F_{a,b}$ is given by

$$F_{a,b} = \left\langle \sigma_1^a \sigma_2^b \right\rangle_N = \sum_{k_1,k_2} \sum_{p_z=0}^{-Nk_1+k_2} \sum_{p_w=0}^{-k_1-2k_2} q_1^{k_1} q_2^{k_2} \operatorname*{Res}_{\widehat{\sigma}_1=\frac{(p_w+2p_z)\epsilon_\Omega}{(2N+1)}} \operatorname*{Res}_{\widehat{\sigma}_2=\frac{1}{2}(-\widehat{\sigma}_1+\epsilon_\Omega p_w)} \widehat{\sigma}_1^a \widehat{\sigma}_2^b I \ , \tag{4.2.9}$$

where the poles and the order of the residue operations result from the JK residue prescription, as in (4.2.3), and we again sum over all the allowed values of k_1 and k_2, see Table 4.2. The term I in the integrand is given by

$$\begin{aligned} I = & \prod_{p_z=0}^{-Nk_1+k_2} (-N\widehat{\sigma}_1 + \widehat{\sigma}_2 + \epsilon_\Omega p_z)^{-1} \prod_{p_w=0}^{-k_1-2k_2} (-\widehat{\sigma}_1 - 2\widehat{\sigma}_2 + \epsilon_\Omega p_w)^{-1} \\ & \times \left(\begin{cases} \prod_{p_x=0}^{k_1} (\widehat{\sigma}_1 + \epsilon_\Omega p_x)^{-1} & \text{if } k_1 \geq 0 \\ 1 & \text{if } k_1 = -1 \\ \prod_{p_x=0}^{-k_1-2} (\widehat{\sigma}_1 + \epsilon_\Omega (p_x + k_1 + 1)) & \text{if } k_1 \leq -2 \end{cases} \right)^2 \\ & \times \begin{cases} \prod_{p_y=0}^{k_1+k_2} (\widehat{\sigma}_1 + \widehat{\sigma}_2 + \epsilon_\Omega p_y)^{-1} & \text{if } k_1+k_2 \geq 0 \\ 1 & \text{if } k_1+k_2 = -1 \\ \prod_{p_y=0}^{-k_1-k_2-2} (\widehat{\sigma}_1 + \widehat{\sigma}_2 + \epsilon_\Omega (p_y + k_1 + k_2 + 1)) & \text{if } k_1+k_2 \leq -2 \end{cases} , \end{aligned} \tag{4.2.10}$$

from the chiral multiplet one-loop determinant (4.1.17).

The selection rule (4.2.2) is modified for $F_{a,b}$ with the Omega deformation turned on. The correlator (4.2.9) obeys

$$a + b = 3 + (2 - N)k_1 + j \ , \tag{4.2.11}$$

where the new term $j \in \mathbb{Z}$, compared to (4.2.2), denotes the power of the ϵ_Ω parameter. This modification is required as the R charge of ϵ_Ω is 2.

Results

Computing (4.2.9) we obtain the following results

- Lower-point correlators

$$F_{a,b} = 0 \quad \text{when} \quad a + b \leq 2 \ . \tag{4.2.12}$$

The terms contributing to the sum over k_1 and k_2 contain negative powers of ϵ_Ω and sum to zero.

- Three-point correlators

$$F_{3-b,b} = \left\langle \sigma_1^{3-b} \sigma_2^b \right\rangle_N = \frac{(-1)^b 2^{(1-b)}}{(1+2N)} \ , \tag{4.2.13}$$

which explicitly gives

$$\begin{aligned} F_{3,0} &= \frac{2}{(1+2N)} \qquad & F_{2,1} &= -\frac{1}{(1+2N)} \\ F_{1,2} &= \frac{1}{2(1+2N)} \qquad & F_{0,3} &= -\frac{1}{4(1+2N)} \end{aligned} \quad . \tag{4.2.14}$$

The only term that does not cancel in the k_1, k_2 sum is the one associated with $k_1 = k_2 = 0$. Hence, these results are q_1, q_2, and ϵ_Ω independent. It is interesting to observe that these results match (4.2.8).

- For four-point correlators we state the results for the cases $N = 3$ and $N = 4$.

  - $N = 3$

$$\begin{aligned} F_{4,0} &= \frac{32}{16807 q_1} - \frac{64}{5764801 q_1 q_2^3} + \frac{136}{823543 q_1 q_2^2} - \frac{104}{117649 q_1 q_2} \ , \\ F_{3,1} &= \frac{12}{16807 q_1} - \frac{192}{5764801 q_1 q_2^3} + \frac{296}{823543 q_1 q_2^2} - \frac{137}{117649 q_1 q_2} \ , \\ F_{2,2} &= -\frac{20}{16807 q_1} - \frac{576}{5764801 q_1 q_2^3} + \frac{552}{823543 q_1 q_2^2} - \frac{82}{117649 q_1 q_2} \ , \\ F_{1,3} &= \frac{17}{16807 q_1} - \frac{1728}{5764801 q_1 q_2^3} + \frac{648}{823543 q_1 q_2^2} + \frac{153}{117649 q_1 q_2} \ , \\ F_{0,4} &= -\frac{12}{16807 q_1} - \frac{5184}{5764801 q_1 q_2^3} - \frac{1080}{823543 q_1 q_2^2} - \frac{108}{117649 q_1 q_2} \ . \end{aligned} \tag{4.2.15}$$

  - $N = 4$

$$F_{4,0} = F_{3,1} = F_{2,2} = F_{1,3} = F_{0,4} = 0 \ . \tag{4.2.16}$$

For the case $N = 3$, only the $k_1 = -1$ terms give a non-cancelling contribution to the result and there is no ϵ_Ω dependence, from the selection rule (4.2.11). For $N = 4$, these correlators vanish as the sum contains terms with only negative powers of ϵ_Ω, which sum to zero.

- The first correlators with a positive ϵ_Ω dependence appear at $a+b=5$, where again the terms with negative powers of ϵ_Ω cancel in the sum over k_1 and k_2.

Testing using recursion relations

These results can be verified using the recursion relations (4.1.20). For $U(1)_1$ we have

$$\begin{aligned}&\left\langle \sigma_1^{l_1}\sigma_2^{l_2}\sigma_1^2\left(\sigma_1+\sigma_2\right)\right\rangle_N = \\ &q_1\cdot\left\langle \left(\sigma_1-\epsilon_\Omega\right)^{l_1}\sigma_2^{l_2}\left(-\sigma_1-2\sigma_2\right)\prod_{l=0}^{N-1}\left(-N\sigma_1+\sigma_2+\epsilon_\Omega l\right)\right\rangle_N ,\end{aligned} \tag{4.2.17}$$

and for $U(1)_2$ we have

$$\begin{aligned}&\left\langle \sigma_1^{l_1}\sigma_2^{l_2}\left(\sigma_1+\sigma_2\right)\left(-N\sigma_1+\sigma_2\right)\right\rangle_N = \\ &q_2\cdot\left\langle \sigma_1^{l_1}\left(\sigma_2-\epsilon_\Omega\right)^{l_2}\left(-\sigma_1-2\sigma_2\right)\left(-\sigma_1-2\sigma_2+\epsilon_\Omega\right)\right\rangle_N ,\end{aligned} \tag{4.2.18}$$

where $l_1, l_2 \in \mathbb{Z}_{\geq 0}$. Both of these recursion relations match the quantum cohomology relations in [19] when $\epsilon_\Omega = 0$, as expected.

We have explicitly verified, using Mathematica, that the results for the correlators (4.2.9) obey the q_1 relation (4.2.17) for low values of l_1 and l_2. We also find that, in general, these results obey the q_2 relation (4.2.18), except in two cases:

- For $l_1 = 1, l_2 = 0$ we find

$$\begin{aligned}&\left\langle \sigma_1\left(\sigma_1+\sigma_2\right)\left(-N\sigma_1+\sigma_2\right)\right\rangle_N \\ &-q_2\cdot\left\langle \sigma_1\left(-\sigma_1-2\sigma_2\right)\left(-\sigma_1-2\sigma_2+\epsilon_\Omega\right)\right\rangle_N = -\frac{1}{2} .\end{aligned} \tag{4.2.19}$$

- For $l_1 = 0, l_2 = 1$ we find

$$\begin{aligned}&\left\langle \sigma_2\left(\sigma_1+\sigma_2\right)\left(-N\sigma_1+\sigma_2\right)\right\rangle_N \\ &-q_2\cdot\left\langle \left(\sigma_2-\epsilon_\Omega\right)\left(-\sigma_1-2\sigma_2\right)\left(-\sigma_1-2\sigma_2+\epsilon_\Omega\right)\right\rangle_N = \frac{1}{4} .\end{aligned} \tag{4.2.20}$$

Hence, there is a mild violation of the ϵ_Ω-dependent recursion relation (4.2.18), which is caused by the three-point correlators. In [20] the authors argue that the quantum cohomology relations are violated for $F_{a,b}$ when $a+b=3$, and we observe that the

violation is still present when ϵ_Ω is non-zero. This also agrees with the statement in [74] that the correlators $F_{3-b,b}$ are quantum cohomology violating constants.

Comparison with [20]

We can now study how the results from the evaluation of the correlators with the Omega deformation turned on compare with the computation of these correlators in [20], where the correlators $F_{a,b}$ were found to be given by the contour integral

$$F_{a,b} = q_1^{k_1} \sum_{\hat{w}=w_+,w_-} \oint_{C(\hat{w})} \frac{dw}{2\pi i} \frac{w^b s(w)^{k_1}}{(1+2w)P(w)} \ , \tag{4.2.21}$$

where $C(\hat{w})$ is a small contour about $w = \hat{w}$, and $w_\pm$ are the roots of $P(w)$, with

$$\begin{aligned} P(w) &= (1+w)(-N+w) - q_2(1+2w)^2 \ , \\ s(w) &= \frac{(-1-2w)(-N+w)^N}{(1+w)} \ . \end{aligned} \tag{4.2.22}$$

w is related to the vector multiplet scalars σ_1, σ_2 through $\sigma_2 = w\sigma_1$.

Evaluating (4.2.21) at the roots of $P(w)$ and comparing with the results obtained for the correlators (4.2.9) we find:

- For $a + b \leq 2$, the lower-point correlators vanish, which matches (4.2.12).
- The results for the higher-point correlators, $a + b \geq 4$, determined from (4.2.9) agree with the results from (4.2.21) in the limit $\epsilon_\Omega \to 0$.

We will be more explicit for the case of the three-point correlators. We require $k_1 = 0$ from the selection rule. The roots of $P(w)$ are

$$w_\pm = \frac{(1-N-4q_2) \pm \sqrt{1+2N+N^2-4q_2-8Nq_2}}{2(-1+4q_2)} \ . \tag{4.2.23}$$

In the limit $q_2 \to \infty$ both of these roots tend to $w = -\frac{1}{2}$. Computing the residue for each of these roots and summing the answers we find

$$\begin{aligned} F_{3,0} &= \frac{2}{(1+2N)} & F_{2,1} &= -\frac{1}{(1+2N)} \\ F_{1,2} &= \frac{2q_2-N-1}{(1+2N)(4q_2-1)} & F_{0,3} &= \frac{-4q_2^2+(5+6N)q_2+N^2-N-1}{(1+2N)(4q_2-1)^2} \end{aligned} \ , \tag{4.2.24}$$

which match the results from [19]. These results satisfy the q_2 recursion relation (4.2.18) (with $\epsilon_\Omega = 0$) for $l_1 = 1, l_2 = 0$, and $l_1 = 0, l_2 = 1$, and so satisfy the quantum cohomology relations. However, as discussed, the three-point correlators are quantum cohomology violating objects. Interestingly, the correlators $F_{3,0}$ and $F_{2,1}$ match those in (4.2.14) from the computation with the Omega deformation. However, the correlators $F_{1,2}$ and $F_{0,3}$ are q_2 dependent and there is no q_2 dependence in (4.2.14).

We can also evaluate (4.2.21) at the poles $w = -\frac{1}{2}$ and $w = \infty$ (from Cauchy's theorem) for each case, $b = 0, \ldots, 3$. Evaluating minus of the contribution from the pole at $w = -\frac{1}{2}$ we obtain

$$\begin{aligned} b=0 &: \frac{2}{(1+2N)} \qquad b=1 : -\frac{1}{(1+2N)} \\ b=2 &: \frac{1}{2\,(1+2N)} \qquad b=3 : -\frac{1}{4\,(1+2N)} \quad . \end{aligned} \tag{4.2.25}$$

Evaluating minus of the contribution from the pole at $w = \infty$ we obtain

$$\begin{aligned} b=0 &: 0 \qquad\qquad\qquad b=1 : 0 \\ b=2 &: \frac{1}{2\,(1-4q_2)} \qquad b=3 : -\frac{(3-2N-12q_2)}{4(1-4q_2)^2} \quad . \end{aligned} \tag{4.2.26}$$

Summing the contributions (4.2.25) and (4.2.26) we find agreement with the results (4.2.24), as expected. Significantly, we observe that the results from the evaluation of the residues at $w = -\frac{1}{2}$ agree with the results (4.2.14) from the Omega deformation computation.

In addition, since we observe that the residue of the pole at $w = -\frac{1}{2}$ matches the results from the Omega deformation computation, one can ask where does the contribution from the pole at $w = \infty$ arise in the Omega deformation case? As $\sigma_2 = w\sigma_1$, $w \to \infty$ corresponds to either $\sigma_2 \to \infty$ or $\sigma_1 \to 0$.

We observe that[3]

$$-\sum_{k_1,k_2} \sum_{p_z=0}^{-Nk_1+k_2} \sum_{p_w=0}^{-k_1-2k_2} q_1^{k_1} q_2^{k_2} \operatorname*{Res}_{\widehat{\sigma}_1=0} \operatorname*{Res}_{\widehat{\sigma}_2=0} \widehat{\sigma}_1^{3-b} \widehat{\sigma}_2^{b} I \ , \tag{4.2.27}$$

[3]Where I is the integrand in (4.2.10).

and

$$-\sum_{k_1,k_2}\sum_{p_z=0}^{-Nk_1+k_2}\sum_{p_w=0}^{-k_1-2k_2} q_1^{k_1}q_2^{k_2}\operatorname*{Res}_{\widehat{\sigma}_2=\infty}\operatorname*{Res}_{\widehat{\sigma}_1=\infty}\widehat{\sigma}_1^{3-b}\widehat{\sigma}_2^{b}I\ , \tag{4.2.28}$$

reproduce (4.2.26) in the limit $q_2 \to 0$. For each case, it appears that only the $k_1 = k_2 = 0$ term gives a non-vanishing contribution to the sum. However, we are unable to find a way to fully reproduce the expressions in (4.2.26) (for the non-zero cases $b = 2$ and $b = 3$).

Applying the substitution $\sigma_2 = w\sigma_1$ to the q_2 violating recursion relations and taking the limit $\epsilon_\Omega \to 0$, (4.2.19) and (4.2.20) become

$$\begin{aligned}\sigma_1^3 P(w) &= -\frac{1}{2}\quad ,\\ \sigma_1^3 w P(w) &= \ \ \frac{1}{4}\quad ,\end{aligned} \tag{4.2.29}$$

respectively. Solving for w we find $w = -\frac{1}{2}$. As discussed for the three-point correlators, evaluating the residue of the integral (4.2.21) at the pole $w = -\frac{1}{2}$ reproduces the results (4.2.14) from the Omega deformation computation, which precisely matches (4.2.8) from one of the specific orderings of vanishing twisted masses. No agreement is found with (4.2.7).

Turning on twisted masses

We can also turn on generic twisted masses, compute the correlators $F_{a,b}$, and verify that the recursion relations with both ϵ_Ω and twisted masses are satisfied. In the presence of generic twisted masses for each chiral multiplet, the recursion relations (4.2.17) and (4.2.18) become

$$\begin{aligned}&\left\langle \sigma_1^{l_1}\sigma_2^{l_2}(\sigma_1+m_1)(\sigma_1+m_2)\left(\sigma_1+\sigma_2+m_3\right)\right\rangle_N\\ &= q_1\cdot\left\langle (\sigma_1-\epsilon_\Omega)^{l_1}(\sigma_2)^{l_2}(-\sigma_1-2\sigma_2+m_5)\prod_{l=0}^{N-1}(-N\sigma_1+\sigma_2+m_4+\epsilon_\Omega l)\right\rangle_N\ ,\end{aligned} \tag{4.2.30}$$

and

$$\begin{aligned}&\left\langle \sigma_1^{l_1}\sigma_2^{l_2}\left(\sigma_1+\sigma_2+m_3\right)\left(-N\sigma_1+\sigma_2+m_4\right)\right\rangle_N\\ &= q_2\cdot\left\langle (\sigma_1)^{l_1}(\sigma_2-\epsilon_\Omega)^{l_2}(-\sigma_1-2\sigma_2+m_5)\left(-\sigma_1-2\sigma_2+m_5+\epsilon_\Omega\right)\right\rangle_N\ ,\end{aligned} \tag{4.2.31}$$

respectively. We find that these recursion relations are obeyed for the correlators computed with the Omega deformation and twisted masses turned on. This matches the statement in [74] that the quantum cohomology relations hold in the massive theory and there is a mild violation in the massless theory, as was observed earlier in this section.

The three-point correlators have zero axial R charge and behave differently compared to the higher-point (lower-point) correlators with positive (negative) axial R charge.[4] The three-point correlators $F_{3-b,b}$ are the only non-zero contributions when the limit of vanishing twisted masses is taken. The lower-point correlators are ill-defined due to their 1/mass behaviour and the higher-point correlators are zero when the limit is taken. The computation of the three-point correlators is complicated by the non-compactness of the geometry. The three-point correlators display 0/0 phenomena when the vanishing of twisted masses limit is performed, which leads to their ambiguous nature and the observed violation of the quantum cohomology relations.

Issue with ambiguity

Turning on the Omega deformation is unsuccessful at lifting the ambiguity in the three-point correlators. This is because the $k_1 = k_2 = 0$ contribution to the term (4.2.10) in the integrand contains no ϵ_Ω dependence and so would still require regulating due to the coincident hyperplanes at $\sigma_1 = \sigma_2 = 0$. The ambiguity in the three-point correlators is observed in the limit of vanishing regulating terms, as in section 4.2.1.

Due to the ambiguity one question that we can ask is how can we obtain different results from the contour integral (4.2.21)? In this analysis we have chosen to set $N = 3$ for convenience. Applying the substitution $m_4 = cm_5$ to the result (4.2.5) with generic twisted masses turned on and $\epsilon_\Omega = 0$, where c is a constant, and performing $\lim_{m_5\to 0}\lim_{m_3\to 0}\lim_{m_2\to 0}\lim_{m_1\to 0}$ we again find that all of the q_1 recursion relations

[4]The correlator $F_{a,b}$ has the axial R charge $2(a+b-3)$ [74].

are satisfied and all of the q_2 recursion relations are satisfied, except in two cases:

- For $l_1 = 1, l_2 = 0$ we find

$$\begin{aligned} &\langle \sigma_1 (\sigma_1 + \sigma_2)(-3\sigma_1 + \sigma_2) \rangle_N \\ &- q_2 \cdot \left\langle \sigma_1 (-\sigma_1 - 2\sigma_2)^2 \right\rangle_N = -\frac{c(4+c) + 7q_2}{4 + 9c + 2c^2} \ . \end{aligned} \tag{4.2.32}$$

- For $l_1 = 0, l_2 = 1$ we find

$$\begin{aligned} &\langle \sigma_2 (\sigma_1 + \sigma_2)(-3\sigma_1 + \sigma_2) \rangle_N \\ &- q_2 \cdot \left\langle \sigma_2 (-\sigma_1 - 2\sigma_2)^2 \right\rangle_N = \frac{(-3+c)(c(4+c) + 7q_2)}{(4+c)(1+2c)^2} \ . \end{aligned} \tag{4.2.33}$$

For both of these cases to be satisfied we require $c(4 + c) + 7q_2 = 0$, which solving for q_2 gives $q_2 = -\frac{c(4+c)}{7}$. Substituting this value of q_2 into the integral (4.2.21) and evaluating the residue of the pole at the w_+ root of $P(w)$, we find that the result matches the result from the generic twisted masses computation, up to an overall constant factor, which is given by

$$\frac{4+c}{2(2+c)} \ . \tag{4.2.34}$$

4.2.3 Summary

To summarise, in this chapter we have studied the computation of the correlators for the Gauged Linear Sigma Model describing the non-compact orbifold $\mathbb{C}^3/Z_{(2N+1)(2,2,1)}$, using the localization result from [74]. When the Omega deformation is turned off, we regulate the JK integral by turning on generic twisted masses, and we find that the result for the three-point correlators is ambiguous. The result depends on how the twisted masses are introduced and on the limit of vanishing twisted masses. Turning on the Omega deformation, we find that the result for the three-point correlators matches the previous computation provided that the limits of vanishing twisted masses are taken in an appropriate fashion. We do not have a physical explanation for why the limits should be taken in a specific order. In

[76] the authors propose a prescription for turning on twisted masses to compute degenerate JK integrals appearing in the formula for A-twisted correlators. It is unclear if their prescription could be applied in this case because the sum of the $U(1)_1$ charges is non-zero.

We observe that, in general, the correlators computed with the Omega deformation obey the recursion relations (4.1.20), except for a mild violation caused by the three-point correlators. These three-point correlators do not depend on ϵ_Ω so this violation is the violation of the quantum cohomology relations discussed in [20]. Finally, the results for the correlators $F_{a,b}$ with ϵ_Ω turned on have been compared with the evaluation of these correlators in [20]. In both cases, the lower-point correlators, $a + b \leq 2$, vanish. The results for the higher-point correlators, $a + b \geq 4$, match the results obtained from the contour integral (4.2.21) in the limit $\epsilon_\Omega \to 0$. The results for the three-point correlators (4.2.14) do not match the results found by evaluating (4.2.21) at the roots of $P(w)$. However, the results obtained from computing the residue of the pole at $w = -\frac{1}{2}$ match the results from the Omega deformation computation. It remains unclear if it is possible to determine the origin of the contribution from the pole at $w = \infty$ in (4.2.21) for the Omega deformation case. Overall, we find that the introduction of the Omega deformation is unable to resolve the ambiguities in the three-point correlators for this model.

Chapter 5

Correlators of Monopole Operators in 3d $\mathcal{N} = 4$ $U(N)$ Theories

In this chapter we collect results from [4] on the computation of correlators of monopole operators in three-dimensional $\mathcal{N} = 4$ $U(N)$ gauge theories on the Omega background.[1] We discuss how a result from supersymmetric localization can be used to extract an expression for the vacuum expectation value of a monopole operator and then an expression for correlators containing a product of positively and negatively charged monopoles. We show how the type IIB brane construction from section 2.3.5 can be applied to recover these expressions.

We present explicit examples of the computation of correlators involving the product of monopoles of minimal positive and negative charges in the case of $U(2)$ SQCD. These correlators are written in terms of the abelian monopole operators and the bubbling factors associated to gauged Super-Matrix-Models (SMMs), which we explicitly evaluate using the Jeffrey-Kirwan (JK) residue prescription. Finally, we study some examples for the general case of $U(N)$ SQCD and focus on their wall-crossing behaviour.

[1] See [82] for an independent related work.

In this chapter we will only discuss the case of bare (undressed) monopole operators, but the story generalises. See section 5 of [4] for the brane realisation of Casimir and dressed monopole operators in the $U(N)$ SQCD theory, and the evaluation of correlators involving them.

5.1 Set-up

The power of supersymmetric localization and brane constructions allows us in principle to compute any correlator of monopole operators on $\mathbb{R} \times \mathbb{R}^2_\epsilon$, where $\mathbb{R}^2_\epsilon$ is the Omega background [83] with deformation parameter ϵ. Mathematically, this amounts to working equivariantly with respect to rotations in the $\mathbb{R}^2_\epsilon$ plane, with equivariant parameter ϵ. $\mathcal{O} = \mathcal{O}(x_i^0)$ denotes an operator inserted at the position x_i^0 along the line $\mathbb{R}$, the Euclidean time direction, and at the origin of $\mathbb{R}^2_\epsilon$.

The 3d $\mathcal{N} = 4$ theory preserves 8 supercharges. The insertion of half-BPS Coulomb operators breaks supersymmetry by a half, and the Omega background on $\mathbb{R}^2_\epsilon$ by another half. Hence, the background with operators $\mathcal{O}_i$ inserted at the origin of $\mathbb{R}^2_\epsilon$, and at arbitrary but different positions x_i^0 preserves two supercharges.

For a single operator, the vacuum expectation value (VEV) is simply independent of the position,

$$\mathcal{O} = \left\langle \mathcal{O}(x^0) \right\rangle \ . \tag{5.1.1}$$

The correlators $\langle \mathcal{O}_1(x_1^0)\mathcal{O}_2(x_2^0)\cdots \rangle$ are topological in the sense that they do not depend on the actual positions of the operator insertions x_i^0, except (possibly) for their ordering along $\mathbb{R}$.

For the correlator containing two operators, $\mathcal{O}_1 = \mathcal{O}_1(x_1^0)$ and $\mathcal{O}_2 = \mathcal{O}_2(x_2^0)$, interchanging the order of these operators along $\mathbb{R}$ does not necessarily give the same result,

$$\langle \mathcal{O}_1\mathcal{O}_2 \rangle \neq \langle \mathcal{O}_2\mathcal{O}_1 \rangle \ . \tag{5.1.2}$$

Consequently, for two local operator insertions, the correlators define an associative but non-commutative product, with

$$\mathcal{O}_1 \star \mathcal{O}_2 := \Big\langle \mathcal{O}_1(x^0+\delta)\mathcal{O}_2(x^0-\delta)\Big\rangle \quad , \quad \delta > 0 \ . \tag{5.1.3}$$

The right hand side is independent of δ, as long as $\delta > 0$, and the limit $\delta \to 0^+$ yields the VEV of a local chiral operator. In the limit $\epsilon \to 0$, we obtain Coulomb operator insertions on flat $\mathbb{R}^3$, which are independent of the positions in $\mathbb{R}^3$. There is no longer any ordering and the star product becomes the usual commutative product between holomorphic functions.

An expression for the vacuum expectation value of a monopole operator in three dimensions can be obtained by taking the supersymmetric localization result from [84] for the VEV of 't Hooft lines of four-dimensional $\mathcal{N} = 2$ theories on $\mathbb{R} \times \mathbb{R}^2_\epsilon \times S^1$ and performing dimensional reduction along S^1.

For SQCD theories with gauge group $U(N)$ and N_f flavours of hypermultiplets in the fundamental representation, the VEV of a monopole of minimal charge is

$$V_{(\pm 1, 0^{N-1})} = \sum_{a=1}^{N} u_{\pm e_a} \ , \tag{5.1.4}$$

where $e_a = \left(0^{a-1}, 1, 0^{N-a}\right)$ and the notation 0^{N-a} means 0 repeated $N-a$ times. This VEV is written in terms of a sum of the abelian variables $u_{\pm e_a}$, where the subscript denotes the vector for the magnetic charge. These abelian variables are rational functions, which are given by

$$u_{\pm e_a} = e^{\pm \chi_a} \left(\frac{\prod\limits_{k=1}^{N_f} (\varphi_a - m_k)}{\prod\limits_{b \neq a} \left[\pm(\varphi_a - \varphi_b) + \epsilon\right]} \right)^{\frac{1}{2}} \quad , \tag{5.1.5}$$

where φ_a and χ_a are the complex scalars defined in section 2.3.4. The term in the brackets in (5.1.5) is the one-loop contribution. This comprises a product of the contributions from the vector multiplet (in the denominator) and the hypermultiplets (in the numerator), where m_k denotes the complex mass for the k-th hypermultiplet.

The form of the abelian variables in (5.1.5) is extracted from the 4d localization result by taking an appropriate limit. In the 4d case, the one-loop contribution is given by a product of the contributions from the vector multiplet and hypermultiplets, where

$$\begin{aligned} Z^{\text{vec}}_{1-\text{loop}}(v) &= \prod_{\substack{\alpha\in G\\ \alpha>0}} \prod_{j=0}^{|\alpha.v|-1} \text{sh}\Big[\pm(\alpha.a) + \Big(|\alpha.v| - 2j\Big)\epsilon\Big]^{-1/2} \,, \\ Z^{\text{hyp}}_{1-\text{loop}}(v) &= \prod_{w\in\mathcal{R}} \prod_{j=0}^{|w.v|-1} \text{sh}\Big[w.a - m + \Big(|w.v| - 1 - 2j\Big)\epsilon\Big]^{1/2} \,, \end{aligned} \tag{5.1.6}$$

with $\text{sh}(x) := 2\sinh(\frac{x}{2})$ and $f(x\pm y) := f(x+y)f(x-y)$. The magnetic charges $v \in \Lambda_{\text{cochar}}$ belong to the cocharacter lattice of the gauge group G, $\alpha \in G$ denotes the non-zero roots α of the gauge algebra, and $w \in \mathcal{R}$ denotes the weight w of the representation $\mathcal{R}$. The electric chemical potentials a_a, with $a = 1, \ldots, \text{rank}(G)$, are the VEVs of the real parts of the eigenvalues of the adjoint complex scalars in the 4d $\mathcal{N}=2$ vector multiplet, complexified by the holonomies of their photon superpartners. Similarly, the magnetic chemical potentials b_a are the VEVs of the imaginary parts of the eigenvalues of the adjoint complex scalars, complexified by the holonomies of the dual photons (which are gauge bosons in four dimensions). The masses m_k are analogues of a_a for flavour symmetries.

In (5.1.6), the S^1 radius R has been set to one. We can re-introduce it by rescaling the dimensionful parameters by R to build the dimensionless quantities: $a_a \to Ra_a, m_k \to Rm_k, \epsilon \to R\epsilon$. The 3d limit is then obtained by taking $R \to 0$, keeping a_a, m_k, ϵ, and b_a fixed, and renormalising the leading order term by an appropriate power of R that is fixed by dimensional analysis to obtain a finite result. In this limit, the complex scalars a_a and b_a can be identified with the 3d complex scalars φ_a and $\chi_a = \frac{1}{g^2}\sigma_a + i\gamma_a$, respectively. In addition, the one-loop contributions simplify from trigonometric to rational functions, so (5.1.6) becomes

$$\begin{aligned} Z^{\text{vec}}_{1-\text{loop}}(\varphi; v) &= \prod_{\substack{\alpha\in G\\ \alpha>0}} \prod_{j=0}^{|\alpha.v|-1} \Big[\pm(\alpha.\varphi) + \Big(|\alpha.v| - 2j\Big)\epsilon\Big]^{-1/2} \,, \\ Z^{\text{hyp}}_{1-\text{loop}}(\varphi; v) &= \prod_{w\in\mathcal{R}} \prod_{j=0}^{|w.v|-1} \Big[w.\varphi - m + \Big(|w.v| - 1 - 2j\Big)\epsilon\Big]^{1/2} \,, \end{aligned} \tag{5.1.7}$$

and we can immediately identify the abelian variables discussed in [32],

$$u_v = e^{v\cdot\chi} Z_{1-\text{loop}}(\varphi; v) = e^{v\cdot\chi} \left(\frac{\prod_{w\in\mathcal{R}} \prod_{j=0}^{|w.v|-1} [w.\varphi - m + (|w.v| - 1 - 2j)\epsilon]}{\prod_{\alpha\in G} \prod_{j=0}^{|\alpha.v|-1} [\alpha.\varphi + (|\alpha.v| - 2j)\epsilon]} \right)^{1/2} , \tag{5.1.8}$$

which reduce to (5.1.5) for the case of $U(N)$ theories with a monopole of minimal (positive or negative) charge.

Furthermore, an expression for correlators containing products of monopole operators can be written down. Schematically, the correlator of N monopole operators V_{h_a} (of positive or negative charge) is given by

$$\left\langle T\left(\prod_{a=1}^{N} (V_{h_a})^{n_a} \right) \right\rangle = \sum_{|v|\leq|B|} u_v Z_{\text{SMM}}\left(\varphi, m, \epsilon; v, B\right) , \tag{5.1.9}$$

where $n_a \in \mathbb{Z}_{\geq 0}$ and h_a denote the number of and the magnetic charge vector of the operator V_{h_a}, respectively. The symbol T stands for time ordering, i.e. the order of these operators inserted along the x^0 direction.[2] These correlators are topological in the sense that they can depend on the ordering of the operators along the x^0 direction, but not on their actual positions.

On the right hand side of (5.1.9) we have the magnetic charges v. We sum over all the weights that appear in the representation of highest weight B, which is given by the linear combination $B = \sum_{a=1}^{N} n_a h_a$. We again have the abelian variables u_v, as in (5.1.4). These objects are well understood and we will not worry about their explicit form when computing the correlators in sections 5.3 and 5.4.

The new piece compared to the VEV (5.1.4) is Z_{SMM}. This is the contribution from monopole bubbling, which is the non-perturbative phenomenon whereby the magnetic charge of the singular Dirac monopole defining the monopole operator is screened by the magnetic charge of a smooth 't Hooft-Polyakov monopole [85]. Each bubbling contribution is given by the partition function of a specific $\mathcal{N} = (0, 2)$ deformation of a 0d $\mathcal{N} = (0, 4)$ theory, where SMM stands for a Super-Matrix-Model,

[2] To ease notation we do not write the insertion positions x^0 explicitly.

which is a zero-dimensional supersymmetric gauge theory.[3] The SMM multiplets and Lagrangian (in the $\epsilon \to 0$ limit) can be viewed as the dimensional reduction of the 2d $\mathcal{N}=(0,4)$ multiplets and Lagrangian[4] down to zero dimensions. The Omega deformation further breaks (the dimensional reduction of) $\mathcal{N}=(0,4)$ supersymmetry down to (the dimensional reduction of) $\mathcal{N}=(0,2)$ supersymmetry. Crucially, we will see that any dependence on the ordering of the operators will be contained in the Z_{SMM} terms. The correlator (5.1.9) can be written in the form

$$\left\langle T\left(\prod_{a=1}^{N}(V_{h_a})^{n_a}\right)\right\rangle = \sum_{B} u_B + \sum_{|v|<|B|} u_v Z_{\text{SMM}}\left(\varphi, m, \epsilon; v, B\right) \ , \tag{5.1.10}$$

where the first terms on the right hand side have no bubbling since $Z_{\text{SMM}}=1$ for the magnetic charges associated to the highest weight B. The remaining terms have non-trivial bubbling contributions.

Similar expressions to (5.1.9) have been obtained in the case of the computation of supersymmetric 't Hooft loops in 4d $\mathcal{N}=2$ theories [87, 88], where the bubbling factors Z_{SMM} become the partition functions of a supersymmetric quantum mechanics (SQM) rather than a matrix model. The computation of the bubbling contributions is a difficult and subtle task, see [89, 90, 91, 92]. In this chapter we address the computation of the correlators of monopole operators using the type IIB brane set-up discussed in chapter 2. We show how the brane construction reproduces the right hand side of (5.1.9) and allows us to explicitly compute the bubbling factors Z_{SMM}.

5.2 Star Product and PT Symmetry

We now discuss the realisation of the non-commutative product (5.1.3) as a Moyal (star) product and the role of Parity-Time (PT) symmetry. Both of these will be useful tools in testing the validity of the results obtained for the correlators of

[3]The $\mathcal{N}=(0,2)$ deformation is constructed by selecting an $\mathcal{N}=(0,2)$ subalgebra of the $\mathcal{N}=(0,4)$ supersymmetry algebra and turning on a constant background proportional to ϵ for the Cartan generator of the R symmetry of the $\mathcal{N}=(0,4)$ supersymmetry algebra, which commutes with the selected $\mathcal{N}=(0,2)$ subalgebra.

[4]For more details see [86].

monopole operators in later sections of this chapter.

5.2.1 Star Product as a Moyal Product

Following the 4d analysis in [84], the explicit definition of the non-commutative star product as a Moyal product is

$$(f \star g)(\varphi, \chi) := e^{\epsilon \sum_a (\partial_{\chi'_a} \partial_{\varphi a} - \partial_{\varphi' a} \partial_{\chi a})} f(\varphi, \chi) g(\varphi', \chi') \Big|_{\varphi'=\varphi,\ \chi'=\chi} . \tag{5.2.1}$$

The star product between two VEVs can be computed via the following formula. With the VEV of a monopole operator V given by the expression

$$V = \sum_v e^{v.\chi} Z_V(\varphi; v) := \sum_v Z_{V,\text{tot}}(\varphi, \chi; v) \ , \tag{5.2.2}$$

we have

$$\begin{aligned} \langle V_1 V_2 \rangle := V_1 \star V_2 &= \sum_{v_1} \sum_{v_2} Z_{V_1,\text{tot}}\Big(\varphi + \epsilon v_2, \chi; v_1\Big) Z_{V_2,\text{tot}}\Big(\varphi - \epsilon v_1, \chi; v_2\Big) \\ &= \sum_{v_1} \sum_{v_2} e^{(v_1+v_2).\chi} Z_{V_1}\Big(\varphi + \epsilon v_2; v_1\Big) Z_{V_2}\Big(\varphi - \epsilon v_1; v_2\Big) \ . \end{aligned} \tag{5.2.3}$$

Computing the star product of two abelian monopole variables we find the general abelian relations

$$u_{v_1} \star u_{v_2} = u_{v_1+v_2} \frac{\prod_{w \in \mathcal{R}} \prod_{j_w=-\frac{h^-(w,v_1,v_2)-1}{2}}^{\frac{h^-(w,v_1,v_2)-1}{2}} \Big[w.\varphi - m - \text{sgn}(w.v_{12}) h^+(w, v_1, v_2)\epsilon + 2j_w\epsilon\Big]}{\prod_{\alpha \in G} \prod_{j_\alpha=-\frac{h^-(\alpha,v_1,v_2)-1}{2}}^{\frac{h^-(\alpha,v_1,v_2)-1}{2}} \Big[\alpha.\varphi - \text{sgn}(\alpha.v_{12}) h^+(\alpha, v_1, v_2)\epsilon + (2j_\alpha + 1)\epsilon\Big]} , \tag{5.2.4}$$

where $w \in \mathcal{R}$ denotes the weight w of the representation $\mathcal{R}$, $\alpha \in G$ denotes the non-zero roots α of the gauge algebra, and

$$h^\pm(\sigma, v_1, v_2) := \frac{1}{2}\Big(|\sigma.v_1| + |\sigma.v_2| \pm |\sigma.(v_1 + v_2)|\Big) \ . \tag{5.2.5}$$

More generally,

$$(u_{v_1} f_1(\varphi)) \star (u_{v_2} f_2(\varphi)) = (u_{v_1} \star u_{v_2}) f_1(\varphi + v_2\epsilon) f_2(\varphi - v_1\epsilon) \ , \tag{5.2.6}$$

and in particular,

$$u_v \star f(\varphi) = u_v \cdot f(\varphi - v\epsilon) \quad , \quad f(\varphi) \star u_v = u_v \cdot f(\varphi + v\epsilon) \ . \tag{5.2.7}$$

These are the quantized abelian relations, which reduce to the abelian relations conjectured in [32] in the commutative limit $\epsilon \to 0$.

The abelian monopole variables $u_{\pm e_a}$ in (5.1.5) obey the star product relations

$$\begin{aligned}
u_{e_a} \star u_{-e_a} &= (-1)^{N-1} \frac{\prod_{k=1}^{N_f} (\varphi_a - m_k - \epsilon)}{\prod_{b\neq a} \varphi_{ab}(\varphi_{ab} - 2\epsilon)} \ , \quad a = 1, \dots, N \ , \\
u_{-e_a} \star u_{e_a} &= (-1)^{N-1} \frac{\prod_{k=1}^{N_f} (\varphi_a - m_k + \epsilon)}{\prod_{b\neq a} \varphi_{ab}(\varphi_{ab} + 2\epsilon)} \ , \quad a = 1, \dots, N \ , \\
u_{e_a} \star u_{-e_b} &= u_{-e_b} \star u_{e_a} = u_{e_a - e_b} \ , \quad a \neq b \ , \\
u_{e_a} \star u_{e_b} &= -\frac{1}{\varphi_{ab}(\varphi_{ab} - 2\epsilon)} u_{e_a + e_b} \ , \\
u_{-e_a} \star u_{-e_b} &= -\frac{1}{\varphi_{ab}(\varphi_{ab} + 2\epsilon)} u_{-e_a - e_b} \ , \\
(u_{\pm e_a})^{\star n} &= u_{\pm n e_a} \ , \quad n > 0 \ ,
\end{aligned} \tag{5.2.8}$$

where we have explicitly

$$\begin{aligned}
u_{e_a+e_b} &= e^{\chi_a + \chi_b} \left(\frac{\prod_{k=1}^{N_f} (\varphi_a - m_k)(\varphi_b - m_k)}{\prod_{c\neq a,b} (\pm\varphi_{ac} + \epsilon)(\pm\varphi_{bc} + \epsilon)} \right)^{1/2} \quad , \\
u_{e_a-e_b} &= e^{\chi_{ab}} \left(\frac{\prod_{k=1}^{N_f} (\varphi_a - m_k)(\varphi_b - m_k)}{(\pm\varphi_{ab})(\pm\varphi_{ab} + 2\epsilon) \prod_{c\neq a,b} (\pm\varphi_{ac} + \epsilon)(\pm\varphi_{bc} + \epsilon)} \right)^{1/2} \quad , \\
u_{ne_a} &= e^{n\chi_a} \left(\frac{\prod_{k=1}^{N_f} \prod_{j=0}^{|n|-1} [\varphi_a - m_k + (|n| - 1 - 2j)\epsilon]}{\prod_{b\neq a} \prod_{j=0}^{|n|-1} [\pm\varphi_{ab} + (|n| - 2j)\epsilon]} \right)^{1/2} \quad , \qquad n \in \mathbb{Z} \ .
\end{aligned} \tag{5.2.9}$$

The star product can be used to generate monopole operators with higher magnetic charge from products of monopole operators with lower magnetic charges. However, to identify the precise operators that appear in a product, one first needs to know

the explicit expression for the monopole operators in terms of abelian variables. As such, for the results obtained in this analysis, the star product is a useful consistency test.

5.2.2 The Action of PT Symmetry

Another important consistency check of our results will be related to the action of the spacetime symmetry PT on monopole operators. PT is defined to act as a reflection on Euclidean time $x^0 \to -x^0$ and one coordinate $x^1 \to -x^1$. This is nothing but a rotation by π in the 01 plane. This rotation leaves invariant a monopole operator sitting at the origin (the reflection P or T alone would instead reverse the magnetic flux). On $\mathbb{R} \times \mathbb{R}^2_\epsilon$, the P symmetry can be implemented as the reversal of the Omega background parameter $\epsilon \to -\epsilon$, while the T action simply reverses the locations of the insertion points on the $\mathbb{R}$ axis.

For a single monopole operator of charge B sitting at the origin, this symmetry implies that the VEVs obey the property

$$V_B(\epsilon) = V_B(-\epsilon) \ . \tag{5.2.10}$$

For the insertion of two monopoles, that are brought to the origin, the T action reverses their ordering, and therefore we have the relation

$$V_{B_1} \star V_{B_2}(\epsilon) = V_{B_2} \star V_{B_1}(-\epsilon) \ . \tag{5.2.11}$$

Other identities in the same vein hold for higher-point functions.

5.3 $U(2)$ SQCD Theories

We now apply the brane construction from section 2.3.5 to reproduce the expression (5.1.4) for the VEV of a monopole operator and then compute the correlators (5.1.9) containing a product of monopole operators. We explicitly write down the

partition function for each monopole bubbling contribution and compute them using the Jeffrey-Kirwan residue prescription. Finally, we verify the evaluation of the correlators against the star product formula of section 5.2.1. We focus here on $U(2)$ SQCD theories with N_f flavours and study $U(N)$ theories in section 5.4.

We will use a convenient characterisation of a brane configuration in terms of two pairs of partitions (ρ^+, σ^+) and (ρ^-, σ^-).

The partitions $\rho^+ = (h_i^+)$ and $\rho^- = (h_i^-)$ collect different linking numbers for the NS5_+ and NS5_- branes, respectively. These are defined by

$$\begin{aligned} h^+ &= \widehat{n}(D3_R) + \widehat{n}(D1_L) - \widehat{n}(D1_R) \ \text{ for an } \text{NS5}_+ \ , \\ h^- &= \widehat{n}(D3_L) + \widehat{n}(D1_R) - \widehat{n}(D1_L) \ \text{ for an } \text{NS5}_- \ . \end{aligned} \tag{5.3.1}$$

These linking numbers $h^\pm$ are related but not equal to the linking numbers h defined in (2.3.11). The relation is $h_a = \pm(h_a^\pm - \frac{N}{2})$ for $\text{NS5}_\pm$ branes. $\text{NS5}_\pm$ branes with vanishing $h^\pm$ linking numbers are spectator branes (decoupled from the other branes) and we do not include them in $\rho^\pm$. We will always consider partitions $\rho^\pm$ ordered in a non-increasing fashion, namely $h_i^\pm \geq h_{i+1}^\pm$.

The partitions $\sigma^\pm$ are defined by the schematic split $\sigma = (\sigma^+, \vec{0}, -\sigma^-)$, where $\sigma^+ = p(\ell_a^+)$ collects the positive D3 linking numbers $\ell_a^+ = \ell_a > 0$, where ℓ is the D3 linking number defined in (2.3.10). Likewise, $\sigma^- = p(\ell_a^-)$ collects the negative D3 linking numbers $\ell_a^- = -\ell_a > 0$. Again, these partitions are ordered non-increasingly, where p represents the operation of ordering in a non-increasing fashion. For the $U(2)$ theory we have the linking numbers (ℓ_1, ℓ_2) for the two D3 branes.

These definitions are such that the four partitions $\rho^\pm, \sigma^\pm$ contain only strictly positive integers, ordered non-increasingly. The partitions are simply read from the pattern of the D1 strings stretched between the D3 and NS5_+ branes for (ρ^+, σ^+), and of the D1 strings stretched between the D3 and NS5_- branes for (ρ^-, σ^-). We remark that the partitions σ^+ and ρ^+ (and similarly σ^- and ρ^-) do not necessarily have the

same magnitude.[5] There is however a constraint

$$|\rho^-| - |\sigma^-| = |\rho^+| - |\sigma^+| \ , \tag{5.3.2}$$

which arises from requiring that all D1 strings end on NS5 or D3 branes on both sides.

A given brane configuration is then related to a specific abelian monopole VEV. For the D3 partition $\sigma = v$, we have

$$\text{Brane set-up } (\rho, \sigma) \quad \longleftrightarrow \quad u_\sigma Z_{\rho,\sigma} \ , \tag{5.3.3}$$

where u_σ is the abelian monopole VEV of charge $v = \sigma = (\sigma^+, \vec{0}, -\sigma^-)$, and $Z_{\rho,\sigma}$ is the matrix model that describes the low-energy theory living on the D1 strings. To read off the SMM living on the D1s, one has to move the D3s along the x^7 direction, taking into account the Hanany-Witten string creation/annihilation effects discussed in section 2.3.6, until there are no longer D3s connected to any D1s. This leads to configurations with D1 strings stretched between NS5 branes, supporting unitary gauge nodes of an $\mathcal{N} = (0,4)$ SMM.[6] D3 branes are the source of hypermultiplets in the SMM, while D5 branes are the source of Fermi multiplets.[7] If the configuration reached has no D1 strings left, we simply have $Z_{\rho,\sigma} = 1$. These are the non-bubbling sectors.

5.3.1 Vacuum Expectation Values

To obtain the VEV of a non-abelian monopole V_B, one has to sum over all the brane set-ups with fixed $\rho^\pm = \rho_B^\pm$. This means that we sum over all the patterns of the D1 strings attached to the NS5$_\pm$ in the specific arrangement given by the partition ρ_B, and ending on the D3 branes in any possible way, compatible with the s-rule.

[5] The magnitude of a partition μ is $|\mu| = \sum_k \mu_k$, where k is the length of the partition.

[6] Or rather an $\mathcal{N} = (0,2)$ deformation of an $\mathcal{N} = (0,4)$ in the presence of $\epsilon \neq 0$.

[7] A Fermi multiplet Λ contains a complex fermion λ and a complex auxiliary field G, which arises due to the property that in $\mathcal{N} = (0,2)$ theories the left-moving fermions are not necessarily accompanied by propagating, bosonic superpartners.

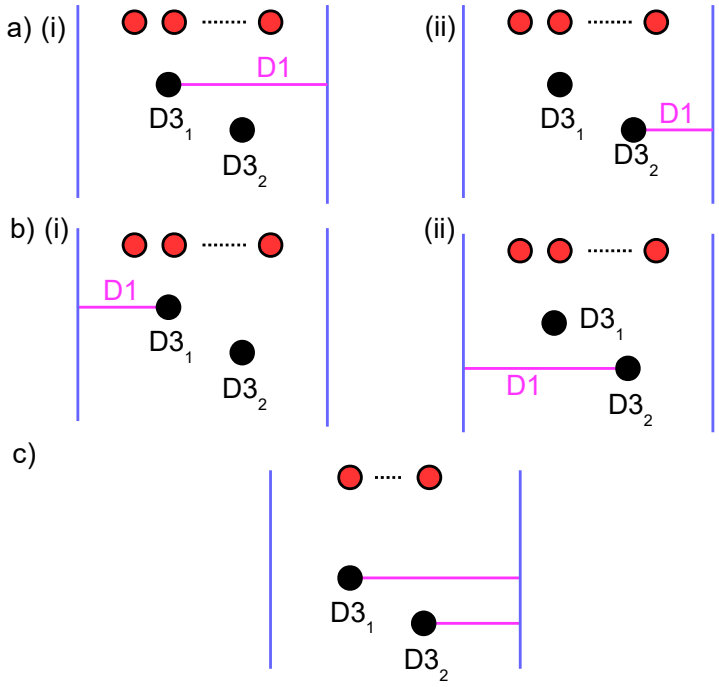

Figure 5.1: Brane set-ups realising the abelian contributions to a) $V_{(1,0)} = u_{e_1} + u_{e_2}$, b) $V_{(0,-1)} = u_{-e_1} + u_{-e_2}$, and c) $V_{(1,1)} = u_{e_1+e_2}$, depicted in the x^{78} plane.

We can consider the VEVs for the (non-abelian) monopoles of smallest magnetic charge in the $U(2)$ SQCD theory, which are $V_{(1,0)}$ and $V_{(-1,0)}$. To do this we require a set-up with two D3 branes, which we label D3_1 and D3_2, N_f D5 branes, and a pair of NS5 branes.

For $V_{(1,0)}$ we have $\rho^+ = (1)$ and $\rho^- = ()$ (empty). Hence, there is a single D1 string emanating from the NS5_+. This D1 string can end on either of the two D3s, leading to two possible abelian configurations, with $v = (1,0) = e_1$ or $v = (0,1) = e_2$, which we must sum together. Both configurations correspond to $\sigma^+ = (1)$ and $\sigma^- = ()$ (because the two v's are identical after reordering). These two configurations are depicted in Figure 5.1-a). After applying Hanany-Witten transitions, the D1 strings vanish, and so the bubbling contributions are trivial. Hence, the two configurations are associated to the abelian variables u_{e_1} and u_{e_2}. Consequently, $V_{(1,0)}$ is given by the sum

$$V_{(1,0)} = u_{e_1} + u_{e_2} \ , \tag{5.3.4}$$

which reproduces (5.1.4) for the case $N = 2$, the result for the VEV of a monopole

operator of minimal positive charge.

Similarly, for $V_{(0,-1)}$ we have $\rho^- = (1)$ and $\rho^+ = ()$. This set-up is identical to the previous case apart from the D1 connects to the NS5$_-$ rather than the NS5$_+$. Again, the D1 can end on either of the D3s, see Figure 5.1-b), which leads to the two abelian configurations u_{-e_1} and u_{-e_2}. Thus, we obtain

$$V_{(0,-1)} = u_{-e_1} + u_{-e_2} \ . \tag{5.3.5}$$

We can also consider the VEV for the monopole $V_{(1,1)}$. We have $\rho^+ = (2)$, $\rho^- = ()$, with two D1 strings ending on the NS5$_+$ of an NS5 pair. The two D1s must end on different D3s, due to the s-rule, which leads to a single configuration with the abelian charge $v = (1,1) = e_1 + e_2$, which we illustrate in Figure 5.1-c). Moving the D3s to the right, via Hanany-Witten transitions, we observe that both of the D1s disappear, resulting in a configuration without any D1s, and so the bubbling contribution is trivial. Hence, we obtain

$$V_{(1,1)} = u_{e_1+e_2} \ . \tag{5.3.6}$$

5.3.2 Monopole Correlators

The correlator of monopoles is given by a sum of the contributions associated to each allowed pattern of D1 strings in the brane configuration. The D1 strings emanating from the NS5 branes are not allowed to extend to $x^7 = \pm\infty$, so they must either end on other NS5 branes or on D3 branes, in a way consistent with the s-rule. We sum over all configurations with fixed linking numbers for the NS5 branes. The vector of linking numbers (ℓ_a) of the D3 branes, which encodes how the D1 strings end on the D3s, determines the magnetic charge $v = (\ell_a)$ of the abelian monopole operator u_v. To each pattern of D1s corresponds the given abelian monopole variable u_v and a bubbling factor Z_{SMM} equal to the partition function of the SMM theory living on the D1 strings. The resulting contribution to the correlator is $u_v Z_{\text{SMM}}$. This gives the structure of terms appearing in (5.1.9).

Contributions to the matrix model

Before presenting the computation of some correlators for $U(2)$ SQCD, we provide a discussion of the contributions to the matrix model $Z_{\rm SMM}$ in the case of $U(N)$ theories. To do this we introduce an alternative notation for the brane configurations.

In this alternative notation, we drop all spectator NS5 branes and label the brane configuration by the linking numbers of all D3 branes, the linking numbers of all (active) NS5 branes, and an extra integer L that specifies the NS5 brane interval in which the D5 branes lie. We choose not to move the D5 branes across the NS5 branes to avoid creating D3' branes, so the D5 branes still separate the NS5$_-$ from the NS5$_+$. Therefore, the N_f D5 branes lie in the interval between the L-th and $(L+1)$-th NS5 along x^7, where

$$L = \ell(\rho^-) \tag{5.3.7}$$

is the length (i.e. the number of non-zero entries) of ρ^-, namely the number of active NS5$_-$ branes. Analogously, $R = \ell(\rho^+)$ is the number of active NS5$_+$ branes.

The linking numbers for the D3 and NS5 branes can be re-defined asymmetrically as follows:

$$\begin{aligned} &\text{D3}: && \ell' := n(\text{NS5}_L) + n(\text{D1}_R) - n(\text{D1}_L) = \ell + L \ , \\ &\text{NS5}: && h' := \widehat{n}(\text{D3}_R) + \widehat{n}(\text{D1}_L) - \widehat{n}(\text{D1}_R) = h + N/2 \ , \end{aligned} \tag{5.3.8}$$

where ℓ and h were defined in (2.3.10) and (2.3.11), respectively. These linking numbers can be read off by moving all the D3 branes across all the NS5$_-$ branes, so that they lie to the left of all NS5 branes, and counting the net number of D1 strings ending on the D3 branes from the right and on the NS5 branes from the left. The D3 brane linking numbers are $v' = (\ell'_a) = v + L \equiv (\ell_a + L)$. The corresponding ordered partition is

$$\sigma' = p(v') = (\sigma^+ + L, L^{N-\ell(\sigma^+)-\ell(\sigma^-)}, -\sigma^- + L) \ , \tag{5.3.9}$$

where we use the shorthand notation $-\mu := (-\mu_\ell, \dots, -\mu_1)$ and $k + \mu := (k +$

$\mu_1, \ldots, k + \mu_\ell)$ for a partition $\mu = (\mu_1, \ldots, \mu_\ell)$ and an integer k.

Similarly, we label NS5 branes with increasing x^7 by an integer $I = 1, \ldots, L + R$ (so $x^7_{I+1} > x^7_I$) and we collect their linking numbers in an unordered partition[8]

$$\rho' = (\rho'_I) = (N - \rho^-, \rho^+) \ . \tag{5.3.10}$$

Using the constraint (5.3.2), we observe that σ' and ρ' are partitions of the same number n,

$$|\sigma'| = NL + |\sigma^+| - |\sigma^-| = NL + |\rho^+| - |\rho^-| = |\rho'| \equiv n \ . \tag{5.3.11}$$

In the rest of this section we will use this second notation to describe the brane configurations and we will omit the primes from the notation.

The gauged SMM

The prefactor that multiplies the abelian monopole variable u_v in the expansion of the topological correlation function is the partition function of an $\mathcal{N} = (0, 2)$ deformation of the gauged $\mathcal{N} = (0, 4)$ SMM, which describes the low-energy physics on the worlvolume of the D1 strings. The generic SMM is denoted by $T^\sigma_{\rho,L}[SU(N)]$, where σ and ρ are given by (5.3.9) and (5.3.10), respectively (with primes omitted). When no Fermi multiplets are present we can drop the L dependence.

The supersymmetric matrix model arises from the localization of the actions that descend from the 2d kinetic terms. Localizing the gauge multiplet first leads to a BPS locus parameterised by commuting σ and $\tilde{\sigma}$ (where all other fields vanish). They can therefore be diagonalised simultaneously by a complexified gauge transformation, reducing to an integral over a Cartan subalgebra of the gauge group, modulo the action of the Weyl group. Supersymmetry ensures that the dependence on $\tilde{\sigma}$ drops out [93, 52, 78, 94], so the partition function is computed by a holomorphic contour

[8]Note that NS5$_+$ branes with $h^+ = a$ and NS5$_-$ branes with $h^- = N - a$ have the same linking numbers $h' = a$ with D3 branes. They are however distinguished by their linking numbers with D5 branes (for the (NS5, D5, D3') Hanany-Witten triple), which differ by N_f.

integral in z_a, the eigenvalues of σ.

To read off the gauge group and matter content of the SMM, we move D3 branes along the x^7 direction, crossing NS5 branes until the D3s no longer have any D1 strings attached. We then count the number of:

- D1 strings - contributing vector multiplets from D1-D1 string modes,
- D3 branes - contributing fundamental hypermultiplets from D3-D1 string modes,
- D5 branes - contributing fundamental Fermi multiplets from D5-D1 string modes,

in each interval between two adjacent NS5 branes. The NS5 branes themselves contribute bifundamental hypermultiplets for adjacent gauge groups, from D1_i-D1_{i+1} strings modes.

The gauge and flavour nodes are labelled by a non-negative integer $I = 1, \ldots, L+R-1$, corresponding to the interval between the I-th and the $(I+1)$-th NS5 branes along x^7. The SMM quiver is then the same as for $T^\sigma_\rho[SU(N)]$ [43], reduced to zero dimensions and further decorated by N_f extra fundamental Fermi multiplets attached to the L-th gauge node. The number of flavours of fundamental hypermultiplets M_I, the ranks N_I, and the FI parameters ξ_I of the I-th gauge node ($I = 1, \ldots, L+R-1$) in the quiver for $T^\sigma_{\rho,L}[SU(N)]$ are given by

$$\begin{aligned} M_I &= \widehat{\sigma}_I - \widehat{\sigma}_{I+1} \ , \\ N_I &= \sum_{K>I} \rho_K - \sum_{K>I} \widehat{\sigma}_K \ , \\ \xi_I &= x^0_{I+1} - x^0_I \ , \end{aligned} \tag{5.3.12}$$

where x^0_I is the position of the I-th NS5 brane along x^0, and a hat denotes the dual (or transposed) partition. The FI parameters of the gauge nodes are related to the insertion points of the monopole operators along the line in the correlator (5.1.9).

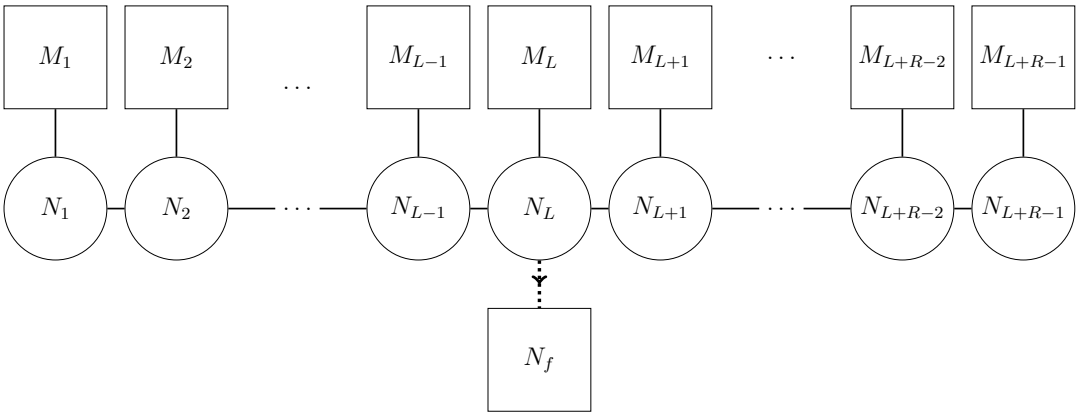

Figure 5.2: Quiver diagram for a generic gauged SMM from the brane construction.

We encode the field content of the gauged SMM in a quiver, as depicted in Figure 5.2, where gauge nodes are denoted by circles, flavour nodes are denoted by squares, and bifundamental hypermultiplets are denoted by the lines between two circles, or between a circle and a square. Equivalently, this quiver can be represented in the matrix notation by

$$\begin{bmatrix} M_1 & M_2 & \dots & M_{L-1} & M_L & M_{L+1} & \dots & M_{L+R-2} & M_{L+R-1} \\ N_1 & N_2 & \dots & N_{L-1} & \underline{N_L} & N_{L+1} & \dots & N_{L+R-2} & N_{L+R-1} \end{bmatrix} , \tag{5.3.13}$$

where the underline indicates the presence of N_f extra fundamental Fermi multiplets.

To avoid violating the s-rule and breaking supersymmetry [6], the NS5 brane partition ρ and the D3 brane partition σ must satisfy the inequalities[9]

$$\sum_{K>I} p(\rho)_K \geq \sum_{K>I} \widehat{\sigma}_K \quad \forall\ I\ , \qquad\qquad \ell(\sigma) \leq N\ , \tag{5.3.14}$$

otherwise the SMM partition function vanishes. The relevant D3 partitions σ, which appear for a given NS5 partition ρ, can be obtained by starting from the Young tableau associated to $\widehat{p(\rho)}$ and consecutively moving boxes in σ down to the next row or column. We refer to appendix B for details, where we show how to obtain the $T^{\sigma}_{\rho,L}[SU(N)]$ partition function with a non-trivial D3 brane partition σ by starting with the $T_{\rho,L}[SU(N)]$ partition function with the trivial partition $\sigma = (1^N)$ and

[9]Recall, $p(\rho)_K$ denotes the ordered partition associated to ρ_K.

applying a residue procedure.

The partition function of the SMM $T^{\sigma}_{\rho,L}[SU(N)]$

To conclude, the partition function of $T^{\sigma}_{\rho,L}[SU(N)]$ is a meromorphic function of the complex masses for the global symmetries:

- $m = \{m_\alpha\}_{\alpha=1}^{N_f}$ for the $U(N_f)$ flavour symmetry acting on the fundamental Fermi multiplets charged under the L-th gauge group.
- $\tilde{\varphi}_K = \{\tilde{\varphi}_{K,r}\}_{r=1}^{M_K}$ for the $U(M_K)$ flavour symmetry acting on the fundamental hypermultiplets of the K-th gauge group. We gather all the $\tilde{\varphi}_K$ in a vector $\tilde{\varphi} = (\tilde{\varphi}_K)$.
- ϵ for the R symmetry of the $\mathcal{N}=(0,4)$ superalgebra that commutes with the $\mathcal{N}=(0,2)$ subalgebra.

With this notation and conventions, the partition function of $T^{\sigma}_{\rho,L}[SU(N)]$ is computed by the integral

$$\begin{aligned} Z_{T^{\sigma}_{\rho,L}[SU(N)]}(\varphi, m, \epsilon;\, \xi) = \oint_{\mathrm{JK}(\xi)} \prod_K \left[\frac{d^{N_K} z_K}{(2\pi i)^{N_K} N_K!} (2\epsilon)^{N_K} \prod_{I\neq J}^{N_K} z_{K,IJ}(z_{K,IJ}+2\epsilon) \right] \\ \cdot \prod_K \frac{1}{\prod_{I=1}^{N_K} \left[\prod_{J=1}^{N_{K+1}} (\pm(z_{K,I}-z_{K+1,J})+\epsilon) \prod_{r=1}^{M_K} (\pm(z_{K,I}-\tilde{\varphi}_{K,r})+\epsilon) \right]} \\ \cdot \prod_{I=1}^{N_L} \prod_{\alpha=1}^{N_f} (z_{L,I}-m_\alpha)\ , \end{aligned} \tag{5.3.15}$$

where the products over the gauge groups in the first and second line run from $K=1$ to $K=L+R-1$, and the $\tilde{\varphi}$ variables are related to the φ variables as above. The three lines in the right hand side of (5.3.15) account for the contributions of 0d vector multiplets, hypermultiplets, and Fermi multiplets, respectively. We use the shorthand notation $z_{K,IJ} = z_{K,I} - z_{K,J}$ and $(\pm x + y) := (x+y)(-x+y)$.

The contour of integration JK(ξ) is given by the Jeffrey-Kirwan prescription with the JK parameter identified with the vector of FI parameters $\xi = (\xi_K)$. The multi-dimensional poles that are encircled by the JK integration cycle are in one-to-one correspondence with the Higgs vacua of the theory [87]. When the vector of FI parameters ξ is generic (that is, it lies in the interior of a chamber in FI space, where the Higgs vacua are isolated), the prescription is simple: the choice of contour only depends on the chamber that ξ belongs to. When ξ lies on a wall separating two different chambers, the JK integral is ill-defined and a 0d Coulomb branch opens up, as such the contour integral is much more subtle to determine. In this thesis, we focus on the cases where the FI parameters are non-vanishing, and the SMM can be readily evaluated from the Jeffrey-Kirwan prescription.

It is possible to derive a general result for the partition function of $T^{\sigma}_{\rho,L}[SU(N)]$, we refer to section 4 and appendix A of [4] for details. In the rest of this chapter we focus on the computation of correlators containing products of positively and negatively charged monopole operators. We explicitly evaluate the relevant matrix model partition functions by applying the JK residue prescription.

Computation of correlators

We can now consider the computation of correlators containing the minimal monopoles $V_{(1,0)}$, $V_{(0,-1)}$, $V_{(1,1)}$, and $V_{(-1,-1)}$ in the $U(2)$ SQCD theory. We will explicitly demonstrate the evaluation of some two- and three-point correlators.[10]

$\underline{\left\langle V^2_{(1,0)} \right\rangle}$:

We require a brane set-up with two pairs of NS5 branes, with one D1 emanating from each of the NS5$_+$, and the NS5$_-$ are spectators. The NS5$_+$ sit at different positions along the x^0 direction, since we have one NS5$_+$ for each operator, but the ordering will not matter as we are inserting the same monopole $V_{(1,0)}$ twice. The two D1s can end on the two D3s in three different patterns, which leads to three

[10] We will also assume that the monopole operators are time ordered.

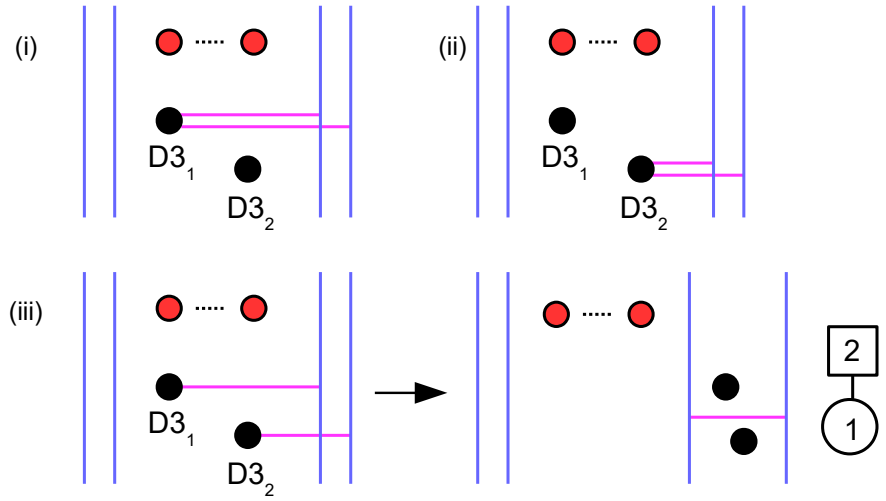

Figure 5.3: Set-up realising the three contributions to the correlator $\left\langle V^2_{(1,0)} \right\rangle = u_{2e_1} + u_{2e_2} + u_{e_1+e_2} Z_1$. The bubbling factor Z_1 is computed as the SMM described by the quiver in Figure (iii).

contributions to the correlator $\left\langle V^2_{(1,0)} \right\rangle$. These are illustrated in Figure 5.3. Both of the D1s can end on D3_1, or on D3_2, which gives the abelian variables u_{2e_1}, or u_{2e_2}, respectively. Both of these contributions have a trivial bubbling term as the D1 strings vanish after performing Hanany-Witten transitions, moving the D3_1, or D3_2, to the right so that D1s are no longer attached to the D3. The third possibility is to have one D1 ending on each D3, which realises $u_{e_1+e_2}$. In this third case, see Figure 5.3-(iii), we observe that after moving the D3s to the right, via Hanany-Witten transitions, there is a single D1 string remaining, which is stretched between the two NS5_+. This gives us a bubbling term associated to the SMM with a $U(1)$ gauge node and two hypermultiplets (from the D3-D1 modes) with masses φ_1 and φ_2 (the distance between the D1 and the D3s along the x^{8+i9} direction). Therefore, there is a non-trivial bubbling contribution $Z_{\text{SMM}} := Z_1$, which is described by the quiver diagram in Figure 5.3-(iii). Consequently, we obtain

$$\left\langle V^2_{(1,0)} \right\rangle = u_{2e_1} + u_{2e_2} + u_{e_1+e_2} Z_1(\varphi, \epsilon) \ . \tag{5.3.16}$$

The SMM for Z_1 is the $U(1)$ theory with two fundamental hypermultiplets of masses φ_1 and φ_2. This matrix model is given by the Jeffrey-Kirwan integral

$$Z_1(\varphi,\epsilon) = \oint_{\text{JK}} \frac{dz}{2\pi i} \frac{(2\epsilon)}{\prod_{a=1,2}[\pm(z-\varphi_a)+\epsilon]} \ . \tag{5.3.17}$$

To compute this integral we follow the JK prescription from section 3.2. We observe that (5.3.17) is the same as the JK integral that appeared in the one-dimensional JK integral example (3.2.13), so we simply state the poles and result again.

For the single $U(1)$ node there is an FI parameter ξ, which is given by the difference in the x^0 positions of the two NS5$_+$ branes. Hence, the JK prescription instructs us that we can compute the integral in one of two chambers, either the chamber in which the FI parameter is positive or negative. This then tells us the poles that contribute to the integral in each of these chambers. In this simple example, these poles are related by sending $\epsilon \to -\epsilon$. The JK prescription for the positive chamber $\xi > 0$ is to pick the residues at $z = \varphi_a - \epsilon$, for $a = 1, 2$, while for $\xi < 0$ we pick the residues at $z = \varphi_a + \epsilon$. Evaluating we obtain the chamber independent result

$$Z_1(\varphi,\epsilon) = \frac{2}{(\pm\varphi_{12}+2\epsilon)} \ , \tag{5.3.18}$$

where $\varphi_{12} = \varphi_1 - \varphi_2$. Hence, this result is the same in both chambers so the bubbling term is independent of ξ. This was to be expected since the operators in the correlator are identical and so commute. Consequently, the correlator is given by

$$\left\langle V^2_{(1,0)} \right\rangle = u_{2e_1} + u_{2e_2} + \frac{2}{(\pm\varphi_{12}+2\epsilon)} u_{e_1+e_2} \ . \tag{5.3.19}$$

If the FI parameter was zero, which would be the case where the two operators are on top of each other and so the NS5$_+$ branes share the same position in x^0, we would not be able to compute the integral (5.3.17) using the JK prescription. This would be an example of an on-the-wall partition function, whose computation remains to be a technical challenge. Although it may be tempting to conjecture that the result computed on-the-wall is the same as the result on both sides of the wall, we will not

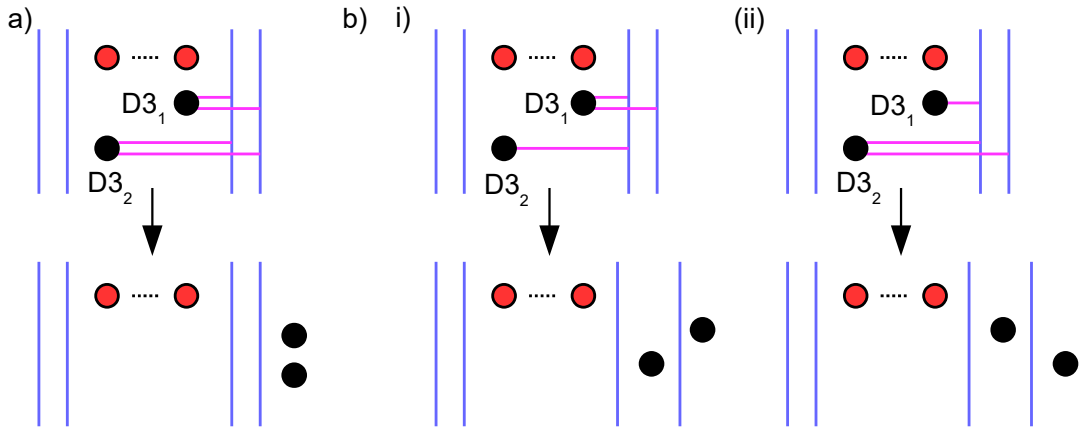

Figure 5.4: Brane patterns for two-point correlators in the $U(2)$ SQCD theory: a) $\left\langle V^2_{(1,1)} \right\rangle = u_{2e_1+2e_2}$ and b) $\left\langle V_{(1,0)} V_{(1,1)} \right\rangle = u_{2e_1+e_2} + u_{e_1+2e_2}$.

do so since we have no evidence for it. In fact, we suspect that the result computed at $\xi = 0$ is different.[11]

$\underline{\left\langle V^2_{(1,1)} \right\rangle}$:

The brane configuration consists of two NS5 pairs (one for each $V_{(1,1)}$ insertion) with two D1s emanating from each of the NS5$_+$. There is a single contribution to the correlator, which is given by each D3 having two D1s ending on it due to the s-rule, see Figure 5.4-a). The abelian variable is $u_{2e_1+2e_2}$ and the bubbling factor is trivial (since all the D1s disappear after moving the D3s to the right of the NS5$_+$s). Consequently, we obtain

$$\left\langle V^2_{(1,1)} \right\rangle = u_{2e_1+2e_2} \ . \tag{5.3.20}$$

$\underline{\left\langle V_{(1,0)} V_{(1,1)} \right\rangle}$:

The brane configuration comprises two NS5 pairs with two D1s attached to the left-most NS5$_+$ and one D1 attached to the right-most NS5$_+$ (the ordering of the NS5$_+$ along x^7 is non-increasing in linking numbers, as discussed). There are two possible D1 patterns: two D1s ends on D3$_1$ and one on D3$_2$, or vice versa, see Figure 5.4-b). These correspond to the abelian variables $u_{2e_1+e_2}$ and $u_{e_1+2e_2}$. After moving

[11] We thank Daniele Dorigoni for discussions on this point.

the D3 branes, we see that the bubbling factors are trivial, since there are no D1s remaining. We thus obtain

$$\left\langle V_{(1,0)}V_{(1,1)}\right\rangle = u_{2e_1+e_2} + u_{e_1+2e_2} \ . \tag{5.3.21}$$

Reversing the order of the insertions does not change the argument, so we conclude that the two operators commute

$$\left\langle V_{(1,1)}V_{(1,0)}\right\rangle = \left\langle V_{(1,0)}V_{(1,1)}\right\rangle \ . \tag{5.3.22}$$

$\underline{\left\langle V_{(1,0)}V_{(0,-1)}\right\rangle}$:

The brane configuration necessitates only a single NS5 pair,[12] with one D1 string attached to the NS5_+ and another D1 attached to the NS5_-. The D1s can either end on different D3s, leading to the abelian variables $u_{e_1-e_2}$ or $u_{-e_1+e_2}$, or alternatively they can reconnect with each other, leaving the D3s unconnected. For the latter case we have a single configuration with a D1 string stretched from the NS5_- to the NS5_+. There is no monopole charge, but we have a non-trivial bubbling contribution $Z_{\text{SMM}} := Z_2$. This is a $U(1)$ theory with two hypermultiplets, with mass $\varphi_{a=1,2}$ from the D1-D3 modes, and N_f Fermi multiplets, with mass $m_{k=1,\ldots,N_f}$ from the D1-D5 modes. We illustrate the contributions in Figure 5.5. There is a single FI parameter, which is given by $\xi = x_1 - x_{-1}$, where x_1/x_{-1} labels the x^0 position of the $\text{NS5}_+/\text{NS5}_-$.

Consequently, the correlator is given by

$$\left\langle V_{(1,0)}V_{(0,-1)}\right\rangle = u_{e_1-e_2} + u_{-e_1+e_2} + Z_2(\varphi, m, \epsilon; \xi > 0) \ , \tag{5.3.23}$$

where the matrix model Z_2 must be evaluated in the positive FI chamber.

Exchanging the order of the insertions corresponds to having $\xi < 0$ in the matrix

[12] To be consistent we should always introduce one pair of NS5 branes per minimal monopole inserted, with the two NS5 of a pair sitting at the same x^0 position. Among each pair, one NS5 is a spectator. In this case we have one NS5_+ spectator and one NS5_- spectator, which we suppress. Thus, the remaining NS5_+ and NS5_- sit at different positions in x^0.

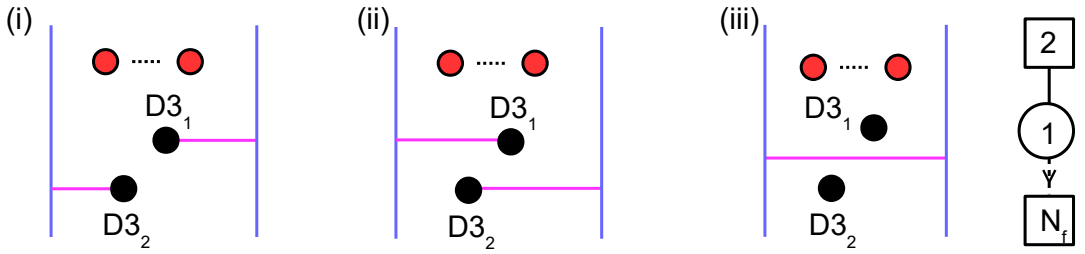

Figure 5.5: The three configurations contributing to $\left\langle V_{(1,0)}V_{(0,-1)}\right\rangle$: (i) $u_{e_1-e_2}$, (ii) $u_{-e_1+e_2}$, (iii) Z_2.

model, and we have

$$\left\langle V_{(0,-1)}V_{(1,0)}\right\rangle = u_{e_1-e_2} + u_{-e_1+e_2} + Z_2(\varphi, m, \epsilon; \xi < 0) \ . \tag{5.3.24}$$

What is the bubbling factor $Z_2(\xi \gtrless 0)$? Compared with the previous bubbling factor Z_1, the SMM for Z_2 has N_f extra Fermi multiplets with masses m_k. Thus, this matrix model is given by

$$Z_2(\varphi, m, \epsilon; \xi) = \oint_{\mathrm{JK}(\xi)} \frac{dz}{2\pi i} \frac{(2\epsilon)\prod_{k=1}^{N_f}(z-m_k)}{\prod_{a=1,2}[\pm(z-\varphi_a)+\epsilon]} \ , \tag{5.3.25}$$

where the extra term in the numerator comes from the Fermi multiplets. The JK prescription is the same as for the evaluation of (5.3.17). We now obtain two different results, depending on the sign of ξ,

$$Z_2(\varphi, m, \epsilon; \xi) = \begin{cases} -\frac{\prod_{k=1}^{N_f}(\varphi_1-m_k-\epsilon)}{\varphi_{12}(\varphi_{12}-2\epsilon)} + (\varphi_1 \leftrightarrow \varphi_2) & \xi > 0 \ , \\ -\frac{\prod_{k=1}^{N_f}(\varphi_1-m_k+\epsilon)}{\varphi_{12}(\varphi_{12}+2\epsilon)} + (\varphi_1 \leftrightarrow \varphi_2) & \xi < 0 \ . \end{cases} \tag{5.3.26}$$

Consequently, the correlators are given by

$$\begin{aligned} \left\langle V_{(1,0)}V_{(0,-1)}\right\rangle &= u_{e_1-e_2} + u_{-e_1+e_2} - \frac{\prod_{k=1}^{N_f}(\varphi_1-m_k-\epsilon)}{\varphi_{12}(\varphi_{12}-2\epsilon)} + (\varphi_1 \leftrightarrow \varphi_2) \ , \\ \left\langle V_{(0,-1)}V_{(1,0)}\right\rangle &= u_{e_1-e_2} + u_{-e_1+e_2} - \frac{\prod_{k=1}^{N_f}(\varphi_1-m_k+\epsilon)}{\varphi_{12}(\varphi_{12}+2\epsilon)} + (\varphi_1 \leftrightarrow \varphi_2) \ , \end{aligned} \tag{5.3.27}$$

which differ due to the non-trivial bubbling factor for each correlator.

We observe that in this case the two operators do not manifestly commute. A closer inspection, with the help of Mathematica, reveals that the two expressions are actually equal for $N_f = 0, 1, 2$, but begin to differ for $N_f \geq 3$, with the difference being a polynomial in φ_a and ϵ. This is a non-trivial result. For small values of N_f we have

- $N_f \in \{0, 1, 2\}$

$$\left\langle [V_{(1,0)}, V_{(0,-1)}] \right\rangle = 0 \ . \tag{5.3.28}$$

- $N_f = 3$

$$\left\langle [V_{(1,0)}, V_{(0,-1)}] \right\rangle = 2\epsilon \ . \tag{5.3.29}$$

- $N_f = 4$

$$\left\langle [V_{(1,0)}, V_{(0,-1)}] \right\rangle = -2\epsilon \left(\sum_{k=1}^{4} m_k - 2\varphi_1 - 2\varphi_2 \right) \ . \tag{5.3.30}$$

- $N_f = 5$

$$\left\langle [V_{(1,0)}, V_{(0,-1)}] \right\rangle = \epsilon \Big[4\epsilon^2 + \left(2\varphi_1^2 + 2\varphi_2^2 - \sum_k m_k^2 \right) + \left(2\varphi_1 + 2\varphi_2 - \sum_k m_k \right)^2 \Big] \ . \tag{5.3.31}$$

This is our first encounter with a wall-crossing phenomenon in SMM. As the FI parameter crosses the $\xi = 0$ wall, the SMM changes with contributions coming from residues at different poles. As a result, the two monopole operators do not commute.

$\underline{\left\langle V_{(1,1)} V_{(0,-1)} \right\rangle}$:

The brane configuration contains two NS5 pairs with two D1s emanating from the left-most NS5_+ and one D1 emanating from the right-most NS5_-. There are two D1 patterns, each with two D1s reconnecting and a single D1 ending on D3_1 or on D3_2 from the right, see Figure 5.6-a). Consequently, we obtain

$$\left\langle V_{(1,1)} V_{(0,-1)} \right\rangle = u_{e_1} Z_3(\varphi_2, m, \epsilon; \xi > 0) + u_{e_2} Z_3(\varphi_1, m, \epsilon; \xi > 0) \ , \tag{5.3.32}$$

where Z_3 is the non-trivial bubbling factor, which is a $U(1)$ theory with a hypermultiplet of mass $x = \varphi_2$ or $x = \varphi_1$, and N_f fundamental Fermi multiplets of masses

m_k. The matrix model is

$$Z_3(x,\varphi,m,\epsilon;\xi)=\oint_{\mathrm{JK}(\xi)}\frac{dz}{2\pi i}\frac{(2\epsilon)\prod_{k=1}^{N_f}(z-m_k)}{[\pm(z-x)+\epsilon]}\ . \tag{5.3.33}$$

In the positive FI chamber $\xi>0$, we pick the residue at $z=x-\epsilon$, which gives

$$Z_3(x,m,\epsilon;\xi>0)=\prod_{k=1}^{N_f}(x-m_k-\epsilon)\ . \tag{5.3.34}$$

Consequently, the correlator is given by

$$\left\langle V_{(1,1)}V_{(0,-1)}\right\rangle=u_{e_1}\prod_{k=1}^{N_f}(\varphi_2-m_k-\epsilon)+u_{e_2}\prod_{k=1}^{N_f}(\varphi_1-m_k-\epsilon)\ . \tag{5.3.35}$$

Permuting the order of the operator insertions changes the sign of the FI parameter in the SMM ($\xi<0$), which results in changing the poles to $z=x+\epsilon$. Consequently, the correlator is given by the same result with ϵ reversed,

$$\left\langle V_{(0,-1)}V_{(1,1)}\right\rangle=u_{e_1}\prod_{k=1}^{N_f}(\varphi_2-m_k+\epsilon)+u_{e_2}\prod_{k=1}^{N_f}(\varphi_1-m_k+\epsilon)\ , \tag{5.3.36}$$

as expected. As soon as $N_f\geq 1$, we observe a wall-crossing phenomenon, meaning that the commutator $\left\langle[V_{(1,1)},V_{(0,-1)}]\right\rangle$ does not vanish.

$\underline{\left\langle V_{(1,1)}V_{(-1,-1)}\right\rangle}$:

The brane configuration contains two NS5 pairs with two D1s emanating from the left-most NS5$_+$ and two D1s emanating from the right-most NS5$_-$. There is a single D1 pattern, where the D1s fully reconnect with each other and the abelian magnetic charge vanishes, see Figure 5.6-b). Consequently, we obtain

$$\left\langle V_{(1,1)}V_{(-1,-1)}\right\rangle=Z_4(\varphi,m,\epsilon;\xi>0)\ , \tag{5.3.37}$$

where the non-trivial bubbling factor Z_4 is the $U(2)$ theory with two hypermultiplets of masses φ_1,φ_2, and N_f fundamental Fermi multiplets of masses m_k. The matrix model is

$$Z_4(\varphi,m,\epsilon;\xi)=\oint_{\mathrm{JK}(\xi)}\frac{dz_1dz_2}{(2\pi i)^2}\frac{1}{2}\frac{(2\epsilon)^2(\pm z_{12})(\pm z_{12}+2\epsilon)\prod_{k=1}^{N_f}\prod_i(z_i-m_k)}{\prod_a\prod_i[\pm(z_i-\varphi_a)]+\epsilon)}\ . \tag{5.3.38}$$

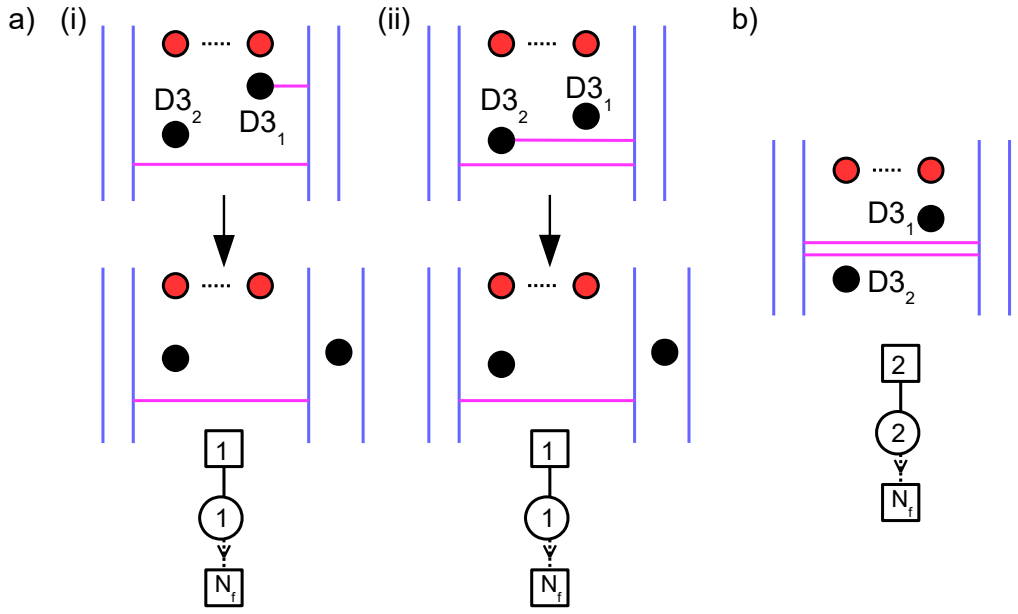

Figure 5.6: Brane patterns for two-point correlators in the $U(2)$ SQCD theory and associated SMMs: a) $\left\langle V_{(1,1)}V_{(0,-1)}\right\rangle = u_{e_1}Z_3(\varphi_2) + u_{e_2}Z_3(\varphi_1)$ and b) $\left\langle V_{(1,1)}V_{(-1,-1)}\right\rangle = Z_4$.

In the evaluation of Z_4 for $\xi > 0$, the only poles contributing are at $(z_1, z_2) = (\varphi_1 - \epsilon, \varphi_2 - \epsilon)$ and the permutation $z_1 \leftrightarrow z_2$. After simplification, we obtain

$$Z_4(\varphi, m, \epsilon; \xi > 0) = \prod_{a=1,2}\prod_{k=1}^{N_f}(\varphi_a - m_k - \epsilon) \ , \tag{5.3.39}$$

and so

$$\left\langle V_{(1,1)}V_{(-1,-1)}\right\rangle = \prod_{a=1,2}\prod_{k=1}^{N_f}(\varphi_a - m_k - \epsilon) \ . \tag{5.3.40}$$

For the commuted correlator, we compute $Z_4(\xi < 0)$, and find the same result with $\epsilon \to -\epsilon$, as expected,

$$\left\langle V_{(-1,-1)}V_{(1,1)}\right\rangle = \prod_{a=1,2}\prod_{k=1}^{N_f}(\varphi_a - m_k + \epsilon) \ . \tag{5.3.41}$$

Again, the two monopoles do not commute and we observe wall-crossing, as soon as $N_f \geq 1$.

$\underline{\left\langle V^2_{(1,0)}V_{(1,1)}\right\rangle}$:

The brane configuration has three NS5 pairs, one for each minimal monopole inserted,

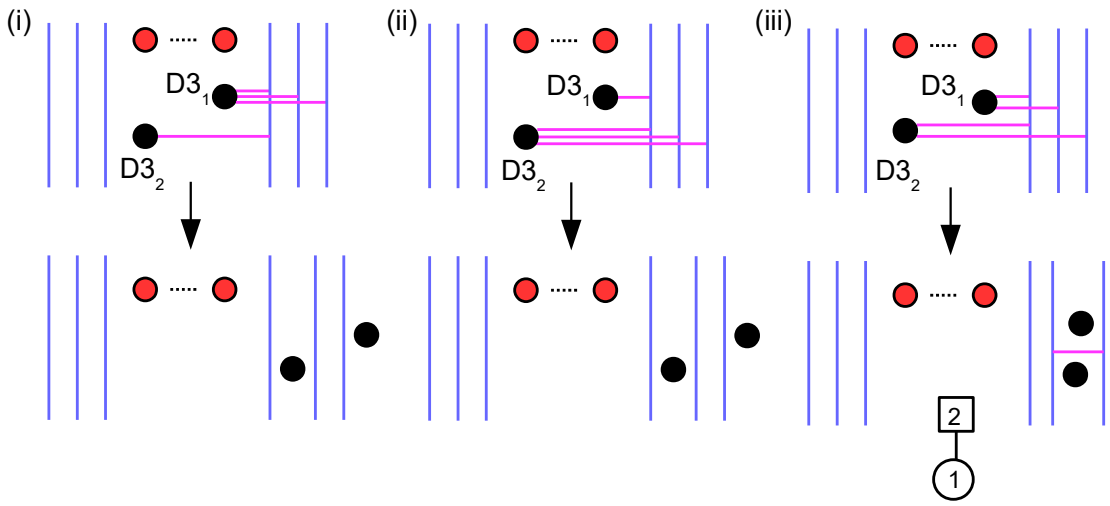

Figure 5.7: Brane patterns and associated SMM for the three-point correlator $\left\langle V^2_{(1,0)}V_{(1,1)}\right\rangle = u_{3e_1+e_2} + u_{e_1+3e_2} + u_{2e_1+2e_2}Z_1$.

with two D1s emanating from the left-most NS5$_+$ and one D1 emanating from the other two NS5$_+$. There are three D1 patterns, where the number of D1 strings ending on (D3$_1$,D3$_2$) are given by $(3,1),(2,2)$, and $(1,3)$, respectively, see Figure 5.7. Consequently, we obtain

$$\begin{aligned}\left\langle V^2_{(1,0)}V_{(1,1)}\right\rangle &= u_{3e_1+e_2} + u_{e_1+3e_2} + u_{2e_1+2e_2}Z_1(\varphi,\epsilon)\\ &= u_{3e_1+e_2} + u_{e_1+3e_2} + u_{2e_1+2e_2}\frac{2}{(\pm\varphi_{12}+2\epsilon)}\,,\end{aligned} \tag{5.3.42}$$

where Z_1 is the SMM with gauge group $U(1)$ and two hypermultiplets of mass φ_1,φ_2, which was already encountered in (5.3.16) for the evaluation of the correlator $\left\langle V^2_{(1,0)}\right\rangle$.

Changing the order of the insertions of the operators does not affect the final result. This is because, as found earlier, the operators $V_{(1,0)}$ and $V_{(1,1)}$ commute.

$\underline{\left\langle V_{(1,0)}V_{(1,1)}V_{(0,-1)}\right\rangle}$:

The brane realisation has three NS5 pairs, with two D1s emanating from the left-most NS5$_+$ and one D1 emanating from the middle NS5$_+$ and right-most NS5$_-$. The remaining NS5 branes (with no D1s attached) are spectators. In the language of partitions we have $\rho_+ = (2,1)$ and $\rho_- = (1)$. There are three patterns of D1s, with the D1 from the NS5$_-$ reconnecting with a D1 from an NS5$_+$ in all cases. The

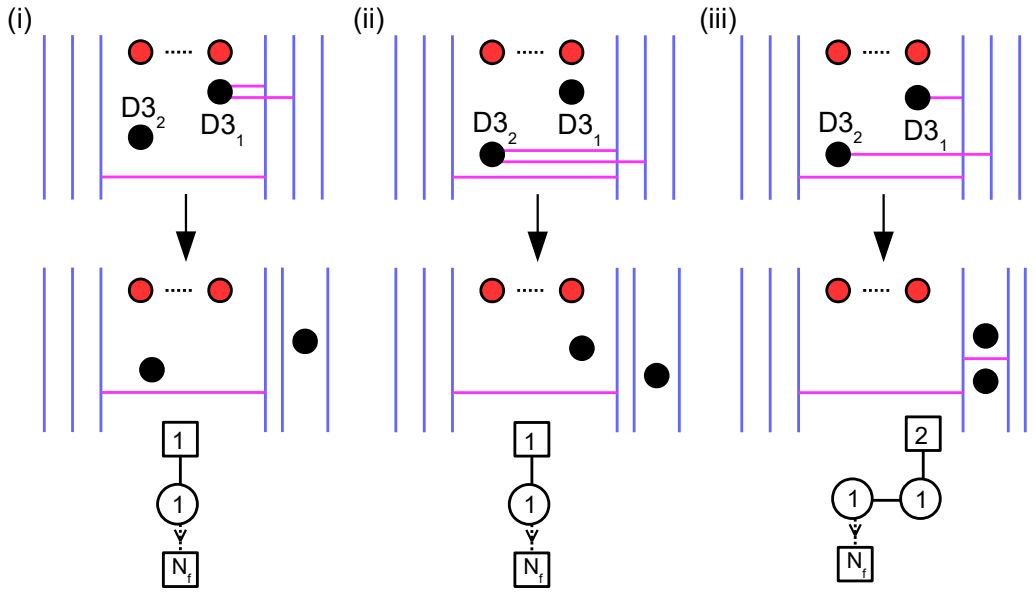

Figure 5.8: Brane patterns and associated SMM for the three-point correlator $\left\langle V_{(1,0)}V_{(1,1)}V_{(0,-1)}\right\rangle = u_{2e_1}Z_3(\varphi_2) + u_{2e_2}Z_3(\varphi_1) + u_{e_1+e_2}Z_5$.

remaining D1s end on the D3s, with either two D1s ending on a single D3 ($\sigma^+ = (2)$), or one D1 ending on each D3 ($\sigma^+ = (1,1)$), see Figure 5.8. The correlator is thus

$$\left\langle V_{(1,0)}V_{(1,1)}V_{(0,-1)}\right\rangle = u_{2e_1}Z_3(\varphi_2, \xi > 0) + u_{2e_2}Z_3(\varphi_1, \xi > 0) + u_{e_1+e_2}Z_5(\xi_{1,2} > 0) \ , \tag{5.3.43}$$

where Z_3 is the SMM that already appeared in the two-point correlator $\left\langle V_{(1,1)}V_{(0,-1)}\right\rangle$, see (5.3.32), and Z_5 is the bubbling factor described by the right-most quiver in Figure 5.8. The quiver SMM Z_5 is computed by

$$Z_5(\varphi, m, \epsilon; \xi) = \oint_{\mathrm{JK}(\xi)} \frac{dz}{2\pi i}\frac{d\hat{z}}{2\pi i}\frac{(2\epsilon)^2\prod_{k=1}^{N_f}(z-m_k)}{[\pm(z-\hat{z})+\epsilon]\prod_{a=1,2}[\pm(\hat{z}-\varphi_a)+\epsilon]} \ . \tag{5.3.44}$$

There are two FI parameters $\xi := (\xi_1, \xi_2)$, one for each $U(1)$ gauge node. In the case when they are both positive, we pick residues at $z = \hat{z} - \epsilon$ and $\hat{z} = \varphi_a - \epsilon$, for $a = 1, 2$. This gives

$$Z_5(\varphi, m, \epsilon; \xi_{1,2} > 0) = -\frac{\prod_{k=1}^{N_f}(\varphi_1 - m_k - 2\epsilon)}{\varphi_{12}(\varphi_{12} - 2\epsilon)} + (\varphi_1 \leftrightarrow \varphi_2) \ . \tag{5.3.45}$$

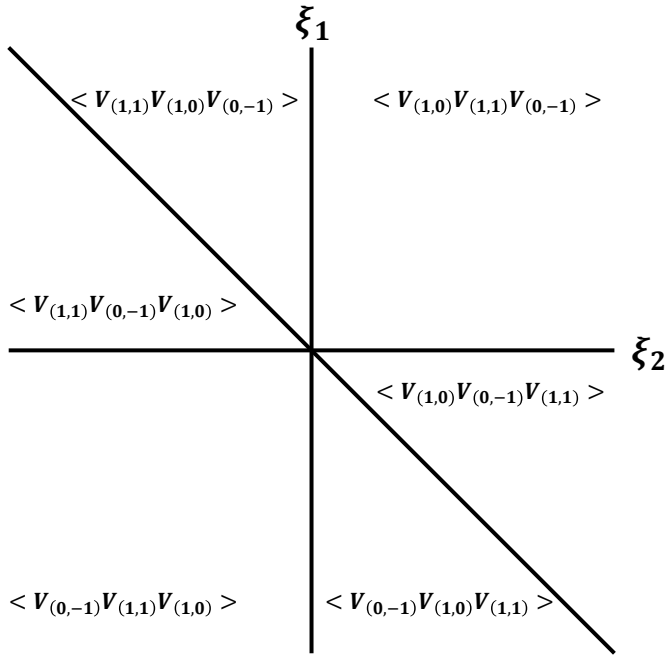

Figure 5.9: This figure illustrates the six distinct chambers in FI space. Each chamber corresponds to a specific ordering of the monopole operators $V_{(1,0)}, V_{(1,1)}$, and $V_{(0,-1)}$.

Thus, we have

$$\begin{aligned}\left\langle V_{(1,0)}V_{(1,1)}V_{(0,-1)}\right\rangle = u_{2e_1}P(\varphi_2-\epsilon) + u_{2e_2}P(\varphi_1-\epsilon) \\ - u_{e_1+e_2}\left[\frac{P(\varphi_1-2\epsilon)}{\varphi_{12}(\varphi_{12}-2\epsilon)} + (\varphi_1 \leftrightarrow \varphi_2)\right] ,\end{aligned} \tag{5.3.46}$$

with

$$P(x) := \prod_{k=1}^{N_f}(x-m_k) \ . \tag{5.3.47}$$

The other orderings of the operators in the correlator are given by the same computation but with the FI parameters in different chambers. There are six possible orderings of these monopole operators, which we illustrate in Figure 5.9. Here ξ_1 is both the single FI parameter of Z_3 and the left node FI parameter of Z_5, while ξ_2 is only the FI parameter of the right node in Z_5. Exchanging $V_{(1,0)}$ and $V_{(1,1)}$ corresponds to crossing the $\xi_1 = 0$ axis. In addition, exchanging $V_{(1,1)}$ and $V_{(0,-1)}$ corresponds to crossing the $\xi_2 = 0$ axis. Finally, exchanging $V_{(1,0)}$ and $V_{(0,-1)}$ corresponds to crossing the $\xi_1 + \xi_2 = 0$ line.

This is all worked out from the brane set-up. Each SMM node corresponds to D1 strings stretched between two NS5s. These two NS5s are associated to two monopole operator insertions and their positions along x^0 determine the FI parameter of the node $\xi = x^0_{\text{right}} - x^0_{\text{left}}$. By looking at the ordering in the operator insertions in the correlator, we can determine the chamber in FI space. To summarise, there is wall-crossing when $V_{(0,-1)}$ is commuted with either $V_{(1,0)}$ (wall at $\xi_1+\xi_2=0$) or $V_{(1,1)}$ (wall at $\xi_2=0$).

5.3.3 Comparison with Star Product

To conclude this section, we wish to show that the above results are compatible with the Moyal, or star, product structure from section 5.2.1. The explicit formula (5.2.3) allows us to compute the star product between any two monopole operators, and, by iteration, the star product of any number of operators. The star product is supposed to compute correlators (see (5.1.3)), therefore we can check whether it agrees with the computations presented in sections 5.3.1 and 5.3.2, based on the brane constructions. In order to apply the formula (5.2.3), one needs to first express the abelian monopoles u_v in terms of the abelian variables χ_a, φ_a, as in (5.1.5) and (5.2.9).

From the relations (5.2.8) with $N=2$, we find[13]

$$\begin{aligned}
V_{(1,0)} \star V_{(1,0)} &= u_{2e_1} + u_{2e_2} + u_{e_1+e_2}\frac{2}{(\pm\varphi_{12}+2\epsilon)} \;=\; \left\langle V^2_{(1,0)} \right\rangle \;, \\
V_{(1,0)} \star V_{(0,-1)} &= u_{e_1-e_2} + u_{-e_1+e_2} - \left[\frac{P(\varphi_1-\epsilon)}{\varphi_{12}(\varphi_{12}-2\epsilon)} + (\varphi_1 \leftrightarrow \varphi_2)\right] \;=\; \left\langle V_{(1,0)}V_{(0,-1)} \right\rangle \;, \\
V_{(0,-1)} \star V_{(1,0)} &= u_{e_1-e_2} + u_{-e_1+e_2} - \left[\frac{P(\varphi_1+\epsilon)}{\varphi_{12}(\varphi_{12}+2\epsilon)} + (\varphi_1 \leftrightarrow \varphi_2)\right] \;=\; \left\langle V_{(0,-1)}V_{(1,0)} \right\rangle \;,
\end{aligned} \tag{5.3.48}$$

which match in all cases. The third product is obtained from the second by reversing the sign of ϵ, in agreement with (5.2.11).

[13] Recall, we define $P(x) := \prod_{k=1}^{N_f}(x-m_k)$ in (5.3.47).

We can also consider some other examples:

$$\begin{aligned} V_{(1,0)} \star V_{(1,1)} &= \left[e^{\chi_1}\left(\frac{P(\varphi_1)}{(\pm\varphi_{12}+\epsilon)}\right)^{1/2} + (..._1 \leftrightarrow ..._2)\right] \star \left[e^{\chi_1+\chi_2}(P(\varphi_1)P(\varphi_2))^{1/2}\right] \\ &= e^{2\chi_1+\chi_2}\left(\frac{P(\varphi_1+\epsilon)P(\varphi_1-\epsilon)P(\varphi_2)}{(\pm\varphi_{12}+\epsilon)}\right)^{1/2} + (..._1 \leftrightarrow ..._2) \\ &= u_{2e_1+e_2} + u_{e_1+2e_2}\,. \end{aligned} \tag{5.3.49}$$

$$\begin{aligned} V_{(1,0)} \star V_{(1,1)} \star V_{(0,-1)} &= \left[e^{2\chi_1+\chi_2}\left(\frac{P(\varphi_1+\epsilon)P(\varphi_1-\epsilon)P(\varphi_2)}{(\pm\varphi_{12}+\epsilon)}\right)^{1/2} + (..._1 \leftrightarrow ..._2)\right] \\ &\star \left[e^{-\chi_1}\left(\frac{P(\varphi_1)}{(\pm\varphi_{12}+\epsilon)}\right)^{1/2} + (..._1 \leftrightarrow ..._2)\right] \\ &= e^{\chi_1+\chi_2}\left(\frac{P(\varphi_1)P(\varphi_1-2\epsilon)^2P(\varphi_2)}{\varphi_{12}^2(\varphi_{12}-2\epsilon)^2}\right)^{1/2} \\ &+ e^{2\chi_1}\left(\frac{P(\varphi_1+\epsilon)P(\varphi_1-\epsilon)P(\varphi_2-\epsilon)^2}{(\pm\varphi_{12}+2\epsilon)(\pm\varphi_{12})}\right)^{1/2} + (..._1 \leftrightarrow ..._2) \\ &= -u_{e_1+e_2}\left[\frac{P(\varphi_1-2\epsilon)}{\varphi_{12}(\varphi_{12}-2\epsilon)} + (\varphi_1 \leftrightarrow \varphi_2)\right] + u_{2e_1}P(\varphi_2-\epsilon) + u_{2e_2}P(\varphi_1-\epsilon)\,. \end{aligned} \tag{5.3.50}$$

Once again, this is in perfect agreement and is a strong consistency check of the computations based on branes.

5.4 $U(N)$ SQCD Theories

To conclude our analysis of topological correlation functions of monopole operators, we study a few correlators with a low number of monopoles of minimal positive and negative charge in $U(N)$ SQCD theories. The bubbling terms are determined by following the JK prescription to compute the partition functions for the relevant SMMs. We focus in particular on the relationship between the correlation functions containing a commutator of monopole operators, the non-zero contributions to the partition functions from poles at infinity, and wall-crossing phenomena.

5.4.1 One Positive and One Negative Minimal Monopole Operator

Firstly, we consider the correlator of the product of two minimal monopole operators of opposite charge, $U_1^+ \equiv V_{(1,0^{N-1})}$ and $U_1^- \equiv V_{(0^{N-1},-1)}$. Depending on the order of these operators, we obtain two different results. To compute these results we require a set-up containing an NS5_+ and an NS5_- brane, from each of which emanates a D1 string, that is $\rho^+ = \rho^- = (1)$. In total, there are $N(N-1)+1$ configurations contributing to the correlator. There are $N(N-1)$ configurations with the NS5_+ and the NS5_- connected to different D3 branes and the remaining $N-2$ D3 branes are unconnected ($\sigma^+ = \sigma^- = (1)$), which correspond to an abelian magnetic charge $e_a - e_b$, with $a \neq b$. There is a single configuration where the NS5 branes are connected by the D1 strings joining and the N D3 branes remain unconnected, with vanishing abelian magnetic charge ($\sigma^+ = \sigma^- = ()$). This tells us that

$$\begin{aligned} \langle U_1^+ U_1^- \rangle &= \sum_{a \neq b} u_{e_a - e_b} + Z^{+-}(\varphi, m, \epsilon) \ , \\ \langle U_1^- U_1^+ \rangle &= \sum_{a \neq b} u_{e_a - e_b} + Z^{-+}(\varphi, m, \epsilon) \ , \end{aligned} \tag{5.4.1}$$

where $e_a := (0^{a-1}, 1, 0^{N-a})$ and $a, b = 0, \ldots, N$.

As expected, the first term in each correlator has no bubbling factor. The bubbling factors $Z^{\pm\mp}(\varphi, m, \epsilon)$, arise from the configuration where the D1s are connected to each other. These are computed as the SMM described by the abelian quiver (in matrix notation)

$$\begin{bmatrix} N \\ \\ \underline{1} \end{bmatrix} \ , \tag{5.4.2}$$

whose partition function is given by

$$Z^{\pm\mp}(\varphi, m, \epsilon) = \oint_{\text{JK}(\pm\xi>0)} \frac{dz}{2\pi i} \frac{(2\epsilon) \prod_{k=1}^{N_f} [z - m_k]}{\prod_{a=1}^{N} [\pm(z - \varphi_a) + \epsilon]} \ , \tag{5.4.3}$$

where $\pm$ in $Z^{\pm\mp}$ corresponds to the FI chamber $\pm\xi > 0$ used in evaluating the

integral, which is directly linked to the order of the operators in the correlator. The FI parameter is given by the difference in the positions of the NS5 branes, $\xi = x_1 - x_{-1}$, where x_1/x_{-1} labels the $\text{NS5}_+/\text{NS5}_-$ position along x^0. This JK integral is ill-defined at the codimension-one wall corresponding to the FI parameter $\xi = 0$, which is the situation where the NS5_+ and NS5_- are at the same x^0 position and the operators $V_{(1,0^{N-1})}$ and $V_{(0^{N-1},-1)}$ collide.

The poles contributing in the FI chamber $\pm\xi > 0$ are at $z = \varphi_a \mp \epsilon$, where $a = 1, \ldots, N$, and the partition function evaluates to

$$Z^{\pm\mp}(\varphi, m, \epsilon) = (-1)^{N-1} \sum_{a=1}^{N} \frac{\prod_{k=1}^{N_f} [\varphi_a - m_k \mp \epsilon]}{\prod_{b\neq a} [\varphi_{ab} (\varphi_{ab} \mp 2\epsilon)]} \ . \tag{5.4.4}$$

As expected, the two results are related by sending $\epsilon \to -\epsilon$, see (5.2.11). Consequently, for the product of one minimal positive operator and one minimal negative operator we find

$$\begin{aligned} \langle U_1^+ U_1^- \rangle &= \sum_{a\neq b} u_{e_a - e_b} + (-1)^{N-1} \sum_{a=1}^{N} \frac{\prod_{k=1}^{N_f} [\varphi_a - m_k - \epsilon]}{\prod_{b\neq a} [\varphi_{ab} (\varphi_{ab} - 2\epsilon)]} \ , \\ \langle U_1^- U_1^+ \rangle &= \sum_{a\neq b} u_{e_a - e_b} + (-1)^{N-1} \sum_{a=1}^{N} \frac{\prod_{k=1}^{N_f} [\varphi_a - m_k + \epsilon]}{\prod_{b\neq a} [\varphi_{ab} (\varphi_{ab} + 2\epsilon)]} \ , \end{aligned} \tag{5.4.5}$$

which matches the result found using the star product from section 5.2.1. These results are our 3d analogue of the results obtained in section 3.2.2 of [88].

The vacuum expectation value of the commutator $\left[U_1^+, U_1^-\right]$, which is the difference between the results computed in the two chambers, is related to the non-zero contribution $Z^\infty(\varphi, m, \epsilon)$ from evaluating the residue of the integrand in (5.4.3) at $z = \infty$,

$$\left\langle \left[U_1^+, U_1^-\right] \right\rangle = Z^{+-}(\varphi, m, \epsilon) - Z^{-+}(\varphi, m, \epsilon) = -Z^\infty(\varphi, m, \epsilon) \ , \tag{5.4.6}$$

where

$$Z^{\infty}(\varphi, m, \epsilon) = \operatorname*{Res}_{z=\infty} \frac{(2\epsilon) \prod_{k=1}^{N_f} [z - m_k]}{\prod_{a=1}^{N} [\pm(z - \varphi_a) + \epsilon]} \ . \tag{5.4.7}$$

Therefore, to obtain the result for the partition function of the SMM in one chamber from the other chamber, we add or subtract the contribution from evaluating the residue of the pole at infinity. This corresponds to crossing the codimension-one wall where the FI parameter is zero, which is the location where the 0d Coulomb branch opens up. An identical observation could have been made for the $N = 2$ case with the correlators in (5.3.27).

For low values of N_f, there is no pole at infinity and the two monopole operators commute. The first non-zero contribution from the pole at infinity occurs at $N_f = 2N - 1$. This gives a polynomial of degree 1 in ϵ. In general, the contribution from evaluating the residue of the pole at infinity will be a polynomial in φ, m, and ϵ of total degree $N_f - 2N + 2$. The explicit contributions from the pole at infinity, which computes the monopole commutator in (5.4.6), for small values of N_f are

- $N_f = 0, 1, \ldots, 2N - 2$

$$Z^{\infty}(\varphi, m, \epsilon) = 0 \ . \tag{5.4.8}$$

- $N_f = 2N - 1$

$$Z^{\infty}(\varphi, m, \epsilon) = (-1)^{N-1}(2\epsilon) \ . \tag{5.4.9}$$

- $N_f = 2N$

$$Z^{\infty}(\varphi, m, \epsilon) = (-1)^{N-1}(2\epsilon) \left(2 \sum_{a=1}^{N} \varphi_a - \sum_{k=1}^{N_f} m_k \right) \ . \tag{5.4.10}$$

- $N_f = 2N + 1$

$$Z^{\infty}(\varphi, m, \epsilon) = (-1)^{N-1}\epsilon \left[2N\epsilon^2 + \left(2 \sum_a \varphi_a^2 - \sum_k m_k^2 \right) + \left(2 \sum_a \varphi_a - \sum_k m_k \right)^2 \right] . \tag{5.4.11}$$

5.4.2 Two Positive and One Negative Minimal Monopole Operators

We now expand our analysis by introducing a second minimal positive operator: we compute the correlator of the product of two minimal positive operators and one minimal negative operator. In this scenario we find three different results depending on the order of the operators. We require a set-up containing two NS5 pairs and we sum over configurations with three D1 strings, where a single string emanates from the two NS5_+, one string emanates from the inner-most NS5_-, and the remaining NS5_- is a spectator.

To read off the contributions to the correlator we sum over all of the configurations where the D1s connect to a D3 or a D1 from an NS5_- connects with a D1 from an NS5_+. The configurations contributing to the correlator are shown in Figure 5.10. There are $N(N-1)$ configurations with both the NS5_+ connected to the same D3 branes, D3_a, the NS5_- connected to a different D3, D3_b, and $N-2$ D3s remain unconnected. Additionally, there are N configurations where the NS5_- is connected to one of the NS5_+, the other NS5_+ is connected to a D3, D3_a, and the remaining $N-1$ D3 branes are unconnected. Finally, there are $\frac{N(N-1)(N-2)}{2}$ configurations where the NS5 branes are all connected to three different D3 branes and the remaining $N-3$ D3s are unconnected, where a and b are the D3s connected to the NS5_+s and c is the D3 connected to the NS5_-. This tells us that the correlator for the product of these monopole operators is given by

$$\left\langle T\left((U_1^+)^2 U_1^-\right)\right\rangle = \sum_{a\neq b} u_{2e_a-e_b} + \sum_a u_{e_a} Z_a(\varphi, m, \epsilon; \xi) + \sum_{\substack{a\neq b,c \\ b\neq c}} u_{e_a+e_b-e_c} Z_{ab}(\varphi, m, \epsilon)\ . \tag{5.4.12}$$

The first term on the right hand side in the correlator has no monopole bubbling contribution, the partition function of the associated SMM is trivial. The third term in the correlator comes from the cases where the NS5s are all connected to different D3s. The associated bubbling factor is computed as the SMM described by the

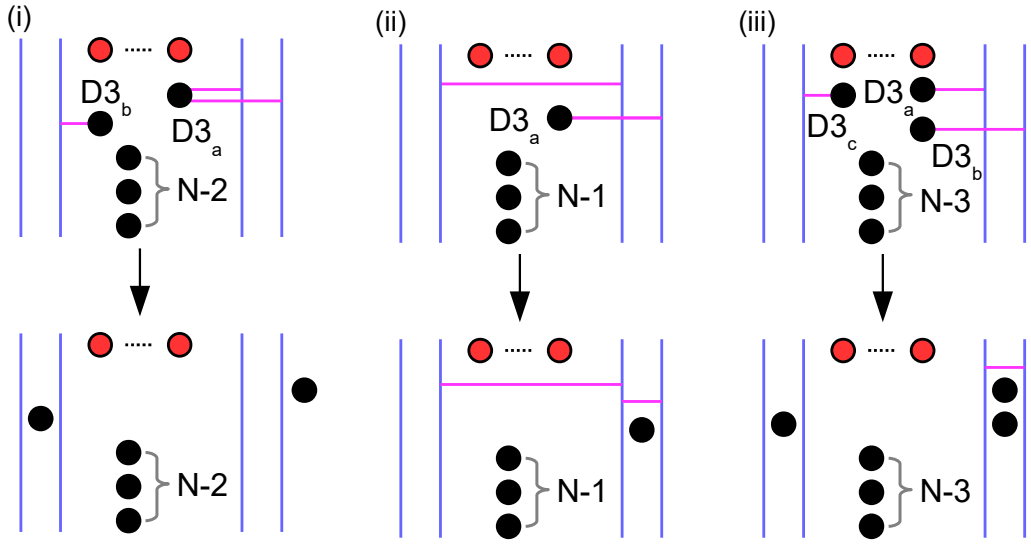

Figure 5.10: The brane set-up for the configurations contributing to the correlator of two minimal positive operators and one minimal negative operator. (i), (ii), and (iii) are an example of one of the diagrams contributing to each of the sums in the first, second, and third term on the right hand side of (5.4.12). The other terms contributing to these sums are given by permutations of the D3 branes.

matrix notation

$$\begin{bmatrix} 2 \\ 1 \end{bmatrix} , \tag{5.4.13}$$

so the SMM is the 0d SQED theory with two hypermultiplets of masses φ_a and φ_b. The partition function of this quiver was computed earlier in the evaluation of the correlator $\left\langle V^2_{(1,0)} \right\rangle$, see (5.3.16), and we simply state the result again,

$$Z_{ab}(\varphi, m, \epsilon) = \oint_{\text{JK}} \frac{dz}{2\pi i} \frac{(2\epsilon)}{[\pm(z-\varphi_a)+\epsilon]\,[\pm(z-\varphi_b)+\epsilon]} = \frac{2}{(\pm\varphi_{ab}+2\epsilon)} \ . \tag{5.4.14}$$

where a and b are the D3 branes that are connected to the two NS5_+ branes in the construction, see Figure 5.10-(iii). It is important to highlight that this result is the same regardless of the chamber in which we compute the JK integral.

The other bubbling factor in the correlator (5.4.12) is computed as the SMM de-

scribed by the quiver

$$\begin{bmatrix} N-1 & 1 \\ \underline{1} & 1 \end{bmatrix} , \tag{5.4.15}$$

where we underline the $U(1)$ gauge node attached to the Fermi multiplets. The partition function of this theory is given by

$$Z_a(\varphi, m, \epsilon; \xi) = \oint_{\mathrm{JK}(\xi)} \frac{dz_0 dz_1}{(2\pi i)^2} \frac{(2\epsilon)^2 \prod_{k=1}^{N_f} (z_0 - m_k)}{\prod_{b\neq a} \left[\pm(z_0-\varphi_b)+\epsilon\right]\left[\pm(z_0-z_1)+\epsilon\right]\left[\pm(z_1-\varphi_a)+\epsilon\right]} , \tag{5.4.16}$$

where a labels the single D3 brane that is located in the interval between the two $\mathrm{NS5}_+$ branes and the remaining $N-1$ D3s are between the inner-most $\mathrm{NS5}_-$ and the inner-most $\mathrm{NS5}_+$, see Figure 5.10-(ii). The bubbling factors for the different orderings of the monopole operators are obtained by evaluating this integral in the different FI chambers. The ordering of the operators is linked to the order of the NS5 branes, which affects the sign of the FI parameters and leads to the different chambers. In this case, there are two FI parameters, one for each $U(1)$ gauge node, which are given by

$$\xi_0 = x_1 - x_{-1} \ , \ \xi_1 = x_2 - x_1 \ , \tag{5.4.17}$$

where x_1, x_2 are the x^0 coordinates of the two $\mathrm{NS5}_+$ branes and x_{-1} of the inner $\mathrm{NS5}_-$. The outer $\mathrm{NS5}_-$ is a spectator and plays no role here.

By naively considering the order of these NS5 branes, one expects to find 6 chambers from the permutations of x_1, x_2, x_{-1}. However, there is a symmetry under the exchange of x_1 and x_2, which tells us that (ξ_1, ξ_0) is equivalent to $(-\xi_1, \xi_0 + \xi_1)$. Consequently, there are only 3 distinct chambers, which are illustrated in Figure 5.11, where:

- The $++-$ chamber satisfies the region $\xi_0 > 0, \xi_0 + \xi_1 > 0$.
- The $--+$ chamber satisfies the region $\xi_0 < 0, \xi_0 + \xi_1 < 0$.
- The final chamber, $+-+$, contains the remaining regions described by $\xi_1 >$

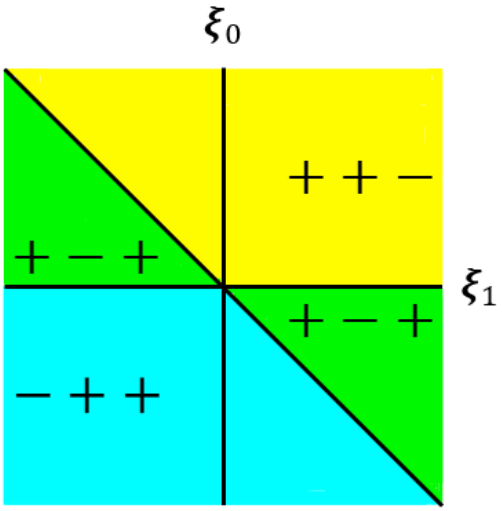

Figure 5.11: This figure illustrates how the 6 regions of the FI space (separated by the solid black lines) are grouped into 3 distinct chambers, due to the symmetry under the exchange of the two $NS5_+$ branes. Each chamber corresponds to a different ordering of the operators in the correlator (5.4.12).

$$0, \xi_0 < 0, \xi_0 + \xi_1 > 0 \text{ and } \xi_1 < 0, \xi_0 > 0, \xi_0 + \xi_1 < 0.$$

In general, for a correlator $\langle T\left((U_1^+)^A(U_1^-)^B\right)\rangle$ there will be $\frac{(A+B)!}{A!B!}$ inequivalent chambers, in correspondence to all the orderings of A U_1^+ operators and B U_1^- operators.

The JK prescription tells us that the multi-dimensional poles contributing to the JK integral in (5.4.16) are different in the different regions of the FI space. In Table 5.1 we list the poles contributing to the integral in each chamber. We apply the constructive definition of the JK residue from section 3.2.2, where each term in the sum of residues comes with the appropriate sign $\nu(F)$, see (3.2.10), which depends on the orientation of the ordered basis used to determine the order in which to perform the iterated residue for each pole. Evaluating (5.4.16) in each of the three

Region of FI space	Chamber	Sign of $\nu(F)$	Multi-dimensional Pole
$\xi_0 > 0$		$+$	$(z_1 = \varphi_a - \epsilon, z_0 = \varphi_a - 2\epsilon)$
$\xi_1 > 0$	$++-$	$+$	$(z_0 = \varphi_b - \epsilon, z_1 = \varphi_b - 2\epsilon)$
$\xi_0 + \xi_1 > 0$		$+$	$(z_1 = \varphi_a - \epsilon, z_0 = \varphi_b - \epsilon)$
$\xi_0 > 0$		$+$	$(z_0 = z_1 - \epsilon, z_1 = \varphi_a - \epsilon)$
$\xi_1 < 0$	$++-$	$-$	$(z_1 = z_0 + \epsilon, z_0 = \varphi_b - \epsilon)$
$\xi_0 + \xi_1 > 0$		$-$	$(z_0 = \varphi_b - \epsilon, z_1 = \varphi_a + \epsilon)$
$\xi_0 < 0$		$-$	$(z_1 = \varphi_a - \epsilon, z_0 = \varphi_a)$
$\xi_1 > 0$	$+-+$	$+$	$(z_1 = z_0 - \epsilon, z_0 = \varphi_b - \epsilon)$
$\xi_0 + \xi_1 > 0$		$-$	$(z_1 = \varphi_a - \epsilon, z_0 = \varphi_b + \epsilon)$
$\xi_0 > 0$		$-$	$(z_1 = \varphi_a + \epsilon, z_0 = \varphi_a)$
$\xi_1 < 0$	$+-+$	$+$	$(z_1 = z_0 + \epsilon, z_0 = \varphi_b + \epsilon)$
$\xi_0 + \xi_1 < 0$		$-$	$(z_1 = \varphi_a + \epsilon, z_0 = \varphi_b - \epsilon)$
$\xi_0 < 0$		$+$	$(z_1 = \varphi_a + \epsilon, z_0 = \varphi_a + 2\epsilon)$
$\xi_1 < 0$	$-++$	$+$	$(z_0 = \varphi_b + \epsilon, z_1 = \varphi_b + 2\epsilon)$
$\xi_0 + \xi_1 < 0$		$+$	$(z_1 = \varphi_a + \epsilon, z_0 = \varphi_b + \epsilon)$
$\xi_0 < 0$		$+$	$(z_0 = z_1 + \epsilon, z_1 = \varphi_a + \epsilon)$
$\xi_1 > 0$	$-++$	$-$	$(z_1 = z_0 - \epsilon, z_0 = \varphi_b + \epsilon)$
$\xi_0 + \xi_1 < 0$		$-$	$(z_0 = \varphi_b + \epsilon, z_1 = \varphi_a - \epsilon)$

Table 5.1: Multi-dimensional poles contributing to the integral (5.4.16) in each chamber, where a has a fixed value and $b = 1, \ldots, a-1, a+1, \ldots, N$.

chambers we find

$$Z_a^{++-} = \frac{(-1)^{N-1} P(\varphi_a - 2\epsilon)}{\prod\limits_{b\neq a} \left[(\varphi_{ab} - \epsilon)(\varphi_{ab} - 3\epsilon)\right]} + \sum_{b\neq a} \frac{2(-1)^{N-1} P(\varphi_b - \epsilon)}{(\varphi_{ab} - \epsilon)(\varphi_{ab} + 3\epsilon) \prod\limits_{\substack{c\neq b,a \\ b\neq a}} \left[\varphi_{bc}(\varphi_{bc} - 2\epsilon)\right]} \,, \tag{5.4.18}$$

$$Z_a^{+-+} = \frac{P(\varphi_a)}{\prod\limits_{b\neq a} \left[\pm\varphi_{ab} + \epsilon\right]} + \sum_{b\neq a} \left[\frac{(-1)^{N-1} P(\varphi_b + \epsilon)}{(\varphi_{ab} - \epsilon)(\varphi_{ab} - 3\epsilon) \prod\limits_{\substack{c\neq b,a \\ b\neq a}} \left[\varphi_{bc}(\varphi_{bc} + 2\epsilon)\right]} + (\epsilon \to -\epsilon) \right] , \tag{5.4.19}$$

$$Z_a^{--+} = \frac{(-1)^{N-1} P(\varphi_a + 2\epsilon)}{\prod\limits_{b\neq a} \left[(\varphi_{ab} + \epsilon)(\varphi_{ab} + 3\epsilon)\right]} + \sum_{b\neq a} \frac{2(-1)^{N-1} P(\varphi_b + \epsilon)}{(\varphi_{ab} + \epsilon)(\varphi_{ab} - 3\epsilon) \prod\limits_{\substack{c\neq b,a \\ b\neq a}} \left[\varphi_{bc}(\varphi_{bc} + 2\epsilon)\right]} \,, \tag{5.4.20}$$

where $P(x)$ is defined in (5.3.47). As expected, Z_a^{++-} and Z_a^{-++} are related by $\epsilon \to -\epsilon$, while Z_a^{+-+} is invariant.

Consequently, we find the following results for the correlator (5.4.12):

$$\begin{aligned}
\left\langle U_1^+ U_1^+ U_1^- \right\rangle &= \sum_{a\neq b} u_{2e_a-e_b} + \sum_a u_{e_a} Z_a^{++-} + \sum_{\substack{a\neq b,c \\ b\neq c}} u_{e_a+e_b-e_c} \frac{2}{(\pm\varphi_{ab}+2\epsilon)} \ , \\
\left\langle U_1^+ U_1^- U_1^+ \right\rangle &= \sum_{a\neq b} u_{2e_a-e_b} + \sum_a u_{e_a} Z_a^{+-+} + \sum_{\substack{a\neq b,c \\ b\neq c}} u_{e_a+e_b-e_c} \frac{2}{(\pm\varphi_{ab}+2\epsilon)} \ , \\
\left\langle U_1^- U_1^+ U_1^+ \right\rangle &= \sum_{a\neq b} u_{2e_a-e_b} + \sum_a u_{e_a} Z_a^{-++} + \sum_{\substack{a\neq b,c \\ b\neq c}} u_{e_a+e_b-e_c} \frac{2}{(\pm\varphi_{ab}+2\epsilon)} \ ,
\end{aligned} \tag{5.4.21}$$

where Z_a^{++-}, Z_a^{+-+}, and Z_a^{-++} are given in (5.4.18), (5.4.19), and (5.4.20), respectively. We have checked that these results agree with those obtained using (5.1.4) and the star product. These correlation functions are our 3d analogue of the results obtained in section 4.2.2 of [88]. The correlators of two minimal negative operators and one minimal positive operator can also be obtained from these results by sending $U_1^+ \leftrightarrow U_1^-$ and $e_a \leftrightarrow e_{-a}$.

We can now study the relationship between the results computed in the different chambers and wall-crossing. The jump between chamber $++-$ and $+-+$ is given by

$$\left\langle U_1^+ \left[U_1^+, U_1^-\right] \right\rangle = \sum_a u_{e_a} \left(Z_a^{++-}(\varphi, m, \epsilon) - Z_a^{+-+}(\varphi, m, \epsilon) \right) \ . \tag{5.4.22}$$

The difference between the SMM partition functions Z_a of (5.4.16) computed in the $++-$ and $+-+$ chambers is captured by the residue of a pole at infinity. To obtain Z_a^{+-+} from Z_a^{++-} there are two options. The first option involves setting $\xi_0 = 0$ and crossing the ξ_1 axis, see Figure 5.11. This corresponds to adding the contribution from the pole where z_1 is finite and $z_0 \to \infty$,

$$Z_a^{++-}(\varphi, m, \epsilon) - Z_a^{+-+}(\varphi, m, \epsilon) = -\operatorname*{Res}_{z_0=\infty} \operatorname*{Res}_{z_1=\varphi_a-\epsilon} I_a(z, \varphi, m, \epsilon) \ , \tag{5.4.23}$$

where $I_a(z, \varphi, m, \epsilon)$ is the integrand in (5.4.16). The second option involves crossing the line $\xi_0 + \xi_1 = 0$, which corresponds to adding the contribution from the pole

where $z_1 \to \infty, z_0 \to \infty$, with finite $z_1 - z_0$,

$$Z_a^{++-}(\varphi, m, \epsilon) - Z_a^{+-+}(\varphi, m, \epsilon) = -\operatorname*{Res}_{z_1=\infty} \operatorname*{Res}_{z_0=z_1-\epsilon} I_a(z, \varphi, m, \epsilon) \ . \tag{5.4.24}$$

These two options are identical, since the contributions from the poles at infinity obey the following relations,

$$\operatorname*{Res}_{z_0=\infty} \operatorname*{Res}_{z_1=\varphi_a-\epsilon} I_a = \operatorname*{Res}_{z_1=\varphi_a-\epsilon} \operatorname*{Res}_{z_0=\infty} I_a = \operatorname*{Res}_{z_1=\infty} \operatorname*{Res}_{z_0=z_1-\epsilon} I_a = -\operatorname*{Res}_{z_0=\infty} \operatorname*{Res}_{z_1=z_0+\epsilon} I_a \ . \tag{5.4.25}$$

Consequently, we can write

$$\left\langle U_1^+ \left[U_1^+, U_1^-\right]\right\rangle = -\sum_a u_{e_a} \operatorname*{Res}_{z_0=\infty} \operatorname*{Res}_{z_1=\varphi_a-\epsilon} I_a(z, \varphi, m, \epsilon) = -\sum_a u_{e_a} Z^\infty(\varphi - e_a\epsilon, m, \epsilon) \ , \tag{5.4.26}$$

which is obtained by evaluating the residue for the pole $z_1 = \varphi_a - \epsilon$, and then using the definition of $Z^\infty(\varphi, m, \epsilon)$ in (5.4.7).

This can be linked with our discussion of the star product by using the quantized abelian relations from section 5.2.1. In particular, using $u_{e_a} \cdot f(\varphi - e_a\epsilon) = u_{e_a} \star f(\varphi)$, we find

$$\left\langle U_1^+ \left[U_1^+, U_1^-\right]\right\rangle = \sum_a u_{e_a} \star [-Z^\infty(\varphi, m, \epsilon)] = \left\langle U_1^+\right\rangle \star \left\langle \left[U_1^+, U_1^-\right]\right\rangle \ , \tag{5.4.27}$$

where the last equality is obtained using the VEV of the commutator in (5.4.6).

Similarly, we find that the jump between chambers $+-+$ and $-++$ is

$$\begin{aligned} \left\langle \left[U_1^+, U_1^-\right] U_1^+\right\rangle = \sum_a u_{e_a} \left(Z_a^{+-+} - Z_a^{-++}\right) = & \ -Z^\infty(\varphi, m, \epsilon) \star \sum_a u_{e_a} \\ = & \left\langle \left[U_1^+, U_1^-\right]\right\rangle \star \left\langle U_1^+\right\rangle \ , \end{aligned} \tag{5.4.28}$$

after applying the relation $u_{e_a} \cdot f(\varphi + e_a\epsilon) = f(\varphi) \star u_{e_a}$ in (5.2.7). Lastly,

$$\langle [(U_1^+)^2, U_1^-]\rangle = \langle U_1^+ \left[U_1^+, U_1^-\right]\rangle + \langle \left[U_1^+, U_1^-\right] U_1^+\rangle = \sum_a u_{e_a} \left(Z_a^{++-} - Z_a^{-++}\right) \ , \tag{5.4.29}$$

which involves a sum of two commutators since to obtain Z_a^{-++} from Z_a^{++-} we must cross two codimension-one walls.

In this discussion we have not mentioned what happens when we set $\xi_1 = 0$ and cross

the ξ_0 axis. This situation corresponds to reversing the order of two NS5_+ branes. Hence, crossing the codimension-one wall given by $\xi_1 = 0$ is related to exchanging the two minimal positive operators in the correlator, which does not change the result since they obviously commute. We can also explain this by looking at the contribution from the appropriate pole at infinity. Crossing the ξ_0 axis corresponds to adding the contribution from the pole where z_0 is finite and $z_1 \to \infty$. Evaluating the residue of the integrand in (5.4.16) at this pole, we find zero.

Consequently, this analysis is consistent with the ordering of the NS5 branes described earlier, which explained how the 6 regions of FI space are actually grouped into only 3 inequivalent chambers, due to the symmetry under the exchange of the two NS5_+ branes. The difference in the ordering of the operators in the correlator is related to the signs and relevant magnitudes of the FI parameters. The codimension-one wall-crossing phenomenon is manifest when we exchange two operators of a different type, and the contribution from evaluating the residue of the appropriate pole at infinity is non-zero. The pole at infinity is specified entirely by crossing the codimension-one wall between the relevant chambers. When the contribution from a particular pole at infinity is zero, the correlator is unchanged, which corresponds to the exchange of two commuting (and in this case identical) operators.

5.4.3 Two Positive and Two Negative Minimal Monopole Operators

We finish our analysis by studying the correlator of the product of two minimal positive operators and two minimal negative operators, which is an example of a computation where a bubbling term with a non-abelian unitary gauge node emerges. Depending on the order of the operators, we obtain six different results. We require a set-up containing two NS5 pairs and we sum over configurations with four D1 strings, where a single string emanates from each of the NS5 branes.

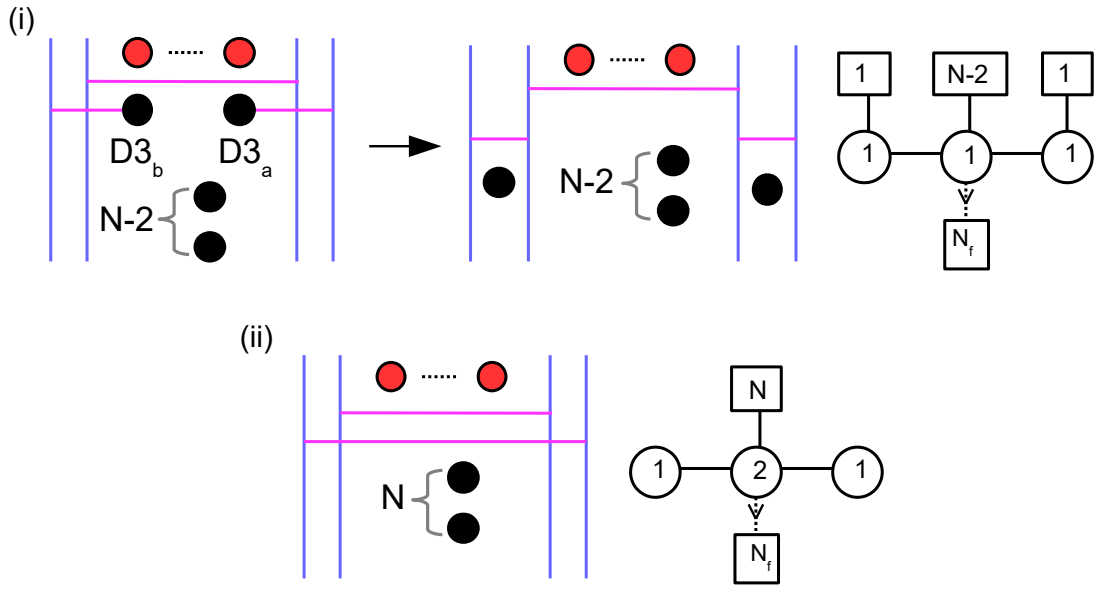

Figure 5.12: The brane configurations and associated SMMs for the chamber dependent terms that arise in the correlator $\left\langle T\left((U_1^+)^2(U_1^-)^2\right)\right\rangle$.

The correlator of the product of these monopole operators is given by

$$\begin{aligned}\left\langle T\left((U_1^+)^2(U_1^-)^2\right)\right\rangle = &\sum_{a,b} u_{2e_a-2e_b} + \sum_{a,b,c} u_{2e_a-e_b-e_c} Z_{bc}^- + \sum_{a,b,c} u_{-2e_a+e_b+e_c} Z_{bc}^+ \\ &+ \sum_{a,b,c,d} u_{e_a+e_b-e_c-e_d} Z_{ab,cd} + \sum_{a,b} u_{e_a-e_b} Z_{ab}(\xi) + Z(\xi)\ ,\end{aligned} \tag{5.4.30}$$

where $a, b, c, d = 1, \ldots, N$, and it is understood that all indices that are summed over are different. We have indicated explicitly the SMM partition functions that exhibit a non-trivial dependence on the FI parameters ξ, and the brane configurations for these two terms are illustrated in Figure 5.12.

The first term on the right hand side in the correlator, which has no monopole bubbling factor, arises from the configurations where one of the D3 branes, $\mathrm{D3}_a$, is connected to both $\mathrm{NS5}_+$, another D3, $\mathrm{D3}_b$, is connected to both $\mathrm{NS5}_-$ and $N-2$ D3s remain unconnected. The second term on the right hand side in (5.4.30) comes from the cases where both of the $\mathrm{NS5}_+$ are connected to the same D3, $\mathrm{D3}_a$, the two $\mathrm{NS5}_-$ are connected to different D3s, $\mathrm{D3}_b$ and $\mathrm{D3}_c$, and $N-3$ branes are unconnected.

The associated bubbling factor is computed as the SMM described by the quiver

$$\begin{bmatrix} 2 \\ \\ 1 \end{bmatrix} . \tag{5.4.31}$$

The partition function of this theory has already been computed previously and is

$$Z_{bc}^{-} = \oint_{\text{JK}} \frac{dz}{2\pi i} \frac{(2\epsilon)}{[\pm(z-\varphi_b)+\epsilon]\,[\pm(z-\varphi_c)+\epsilon]} = \frac{2}{(\pm\varphi_{bc}+2\epsilon)} , \tag{5.4.32}$$

where b and c are the D3 branes that are connected to the two NS5$_-$ in the construction. The third term in the correlator is given by a left-right mirror configuration, where both of the NS5$_-$ are connected to the same D3, D3$_a$, the two NS5$_+$ are connected to different D3s, D3$_b$ and D3$_c$, and $N-3$ branes remain unconnected. The bubbling factor is computed as the partition function of SMM described by the same quiver as (5.4.31). Its partition function is $Z_{bc}^{+} = Z_{bc}^{-}$, where now b and c represent the D3 branes that are connected to the two NS5$_+$ branes in the construction. The next term in (5.4.30) arises from the cases where all of the NS5 branes are connected to different D3s and $N-4$ D3s are unconnected. The resulting bubbling term factorises into a product of the two previous bubbling factors,

$$Z_{ab,cd} = Z_{ab}^{+} Z_{cd}^{-} = \frac{4}{(\pm\varphi_{ab}+2\epsilon)\,(\pm\varphi_{cd}+2\epsilon)} , \tag{5.4.33}$$

where a, b (c, d) denote the D3 branes that are connected to the NS5$_+$ (NS5$_-$).

All of the terms discussed so far are chamber independent. The different orderings of the operators in the correlator are encoded in the last two terms of (5.4.30), where the bubbling factors carry FI chamber dependence. The penultimate term in the correlator arises from the configurations where a single NS5$_+$ and a single NS5$_-$ are connected, and the other NS5$_+$ and NS5$_-$ are connected to different D3s, with $N-2$ D3s remaining unconnected, see Figure 5.12-(i). The bubbling factor is computed

as the SMM described by the quiver

$$\begin{bmatrix} 1 & N-2 & 1 \\ & & \\ 1 & \underline{1} & 1 \end{bmatrix} , \tag{5.4.34}$$

where again we underline the gauge node that is attached to the Fermi multiplets. The partition function of this theory is given by

$$Z_{ab}(\xi) = \oint_{\mathrm{JK}(\xi)} \frac{dz_{-1}dz_0dz_1}{(2\pi i)^3} \frac{(2\epsilon)^3 P(z_0)}{\Delta(z)} , \tag{5.4.35}$$

where

$$\Delta(z) = [\pm(z_{-1}-\varphi_b)+\epsilon]\,[\pm(z_1-\varphi_a)+\epsilon] \prod_{s=\pm 1} [\pm(z_{0s})+\epsilon] \prod_{c\neq a,b} [\pm(z_0-\varphi_c)+\epsilon] , \tag{5.4.36}$$

where a (b) denotes the single D3 brane that is connected to the $\mathrm{NS5}_+$ ($\mathrm{NS5}_-$), namely the D3 brane that is located in the interval between the two $\mathrm{NS5}_+$ ($\mathrm{NS5}_-$), after applying a Hanany-Witten transition. Finally, there is one configuration where all of the NS5s are connected by the D1 strings and N D3 branes remain unconnected, as shown in Figure 5.12-(ii). This gives the remaining bubbling factor, which is computed as the SMM described by the quiver

$$\begin{bmatrix} 0 & N & 0 \\ & & \\ 1 & \underline{2} & 1 \end{bmatrix} , \tag{5.4.37}$$

whose partition function is given by

$$Z(\xi) = \oint_{\mathrm{JK}(\xi)} \frac{dz_{-1}dz_1 \prod_{i=1}^{2} dz_{0,i}}{2(2\pi i)^4} \frac{(2\epsilon)^4\,[\pm z_{0,12}]\,[\pm z_{0,12}+2\epsilon] \prod_{i=1}^{2} P(z_{0,i})}{\prod_{i=1}^{2} \left[\prod_{s=\pm 1} [\pm(z_{0,i}-z_s)+\epsilon] \prod_{a=1}^{N} [\pm(z_{0,i}-\varphi_a)+\epsilon] \right]} . \tag{5.4.38}$$

All of the N D3 branes are located in the interval between the inner-most $\mathrm{NS5}_+$ and the inner-most $\mathrm{NS5}_-$. The explicit details of the computation of the monopole bubbling factors (5.4.35) and (5.4.38) has been relegated to appendix C.

The ordering of the NS5 branes affects the signs of the FI parameters, which leads

to the different chambers. In this case, there are three FI parameters given by

$$\xi_{-1} = x_{-1} - x_{-2} \ , \ \xi_0 = x_1 - x_{-1} \ , \ \xi_1 = x_2 - x_1 \ , \tag{5.4.39}$$

where x_1, x_2 are the x^0 coordinates of the two NS5$_+$ branes and x_{-1}, x_{-2} of the two NS5$_-$ branes. These FI parameters tell us that

$$\xi_{-1} + \xi_0 = x_1 - x_{-2} \ , \ \xi_0 + \xi_1 = x_2 - x_{-1} \ , \ \xi_{-1} + \xi_0 + \xi_1 = x_2 - x_{-2} \ . \tag{5.4.40}$$

By naively considering the order of these four NS5 branes, one expects to find 24 chambers from the permutations of x_{-2}, x_{-1}, x_1, x_2. However, there is a symmetry under the exchange of x_1 and x_2, and another symmetry under the exchange of x_{-1} and x_{-2}. Consequently, there are only 6 distinct chambers, which are given up to the aforementioned permutations by:

- $++--$ chamber: $x_{-2} < x_{-1} < x_1 < x_2$.
- $+-+-$ chamber: $x_{-2} < x_1 < x_{-1} < x_2$.
- $+--+$ chamber: $x_1 < x_{-2} < x_{-1} < x_2$.
- $--++$ chamber: $x_1 < x_2 < x_{-2} < x_{-1}$.
- $-+-+$ chamber: $x_1 < x_{-2} < x_2 < x_{-1}$.
- $-++-$ chamber: $x_{-2} < x_1 < x_2 < x_{-1}$.

For the chamber dependent SMM partition functions $Z_{ab}(\xi)$ and $Z(\xi)$ in (5.4.30), we will denote the chamber in which the partition function is computed by a superscript, *e.g.* Z_{ab}^{++--} is Z_{ab} evaluated in the $++--$ chamber.

We conclude our analysis by studying one example of wall-crossing between the results for (5.4.30) computed in two adjacent chambers, $++--$ and $+-+-$. Thus,

$$\left\langle U_1^+ \left[U_1^+, U_1^- \right] U_1^- \right\rangle = \sum_{a \neq b} u_{e_a - e_b} \left(Z_{ab}^{++--} - Z_{ab}^{+-+-} \right) + \left(Z^{++--} - Z^{+-+-} \right) \ . \tag{5.4.41}$$

Firstly, to obtain Z_{ab}^{+-+-} from Z_{ab}^{++--} we cross the plane $\xi_0 = 0$, which corresponds to adding the contribution from the pole where z_1 and z_{-1} are both finite, and $z_0 \to \infty$,

$$Z_{ab}^{++--} - Z_{ab}^{+-+-} = -\operatorname*{Res}_{z_0=\infty} \operatorname*{Res}_{z_1=\varphi_a-\epsilon} \operatorname*{Res}_{z_{-1}=\varphi_b-\epsilon} I_{ab} \ , \tag{5.4.42}$$

where I_{ab} is the integrand in (5.4.35). Analogously, to obtain Z^{+-+-} from Z^{++--} we must also cross $\xi_0 = 0$. Taking into account both the gauge and flavour symmetry, we find

$$Z^{++--} - Z^{+-+-} = -\sum_{a=1}^{N} \left(\operatorname*{Res}_{z_{0,1}=\infty} \operatorname*{Res}_{z_{-1}=\varphi_a-2\epsilon} \operatorname*{Res}_{z_1=\varphi_a-2\epsilon} \operatorname*{Res}_{z_{0,2}=\varphi_a-\epsilon} I + (z_{0,1} \leftrightarrow z_{0,2}) \right) \ , \tag{5.4.43}$$

where I is the integrand in (5.4.38). Due to the gauge symmetry, we find

$$\operatorname*{Res}_{z_{0,1}=\infty} \operatorname*{Res}_{z_{-1}=\varphi_a-2\epsilon} \operatorname*{Res}_{z_1=\varphi_a-2\epsilon} \operatorname*{Res}_{z_{0,2}=\varphi_a-\epsilon} I = \operatorname*{Res}_{z_{0,2}=\infty} \operatorname*{Res}_{z_{-1}=\varphi_a-2\epsilon} \operatorname*{Res}_{z_1=\varphi_a-2\epsilon} \operatorname*{Res}_{z_{0,1}=\varphi_a-\epsilon} I \ . \tag{5.4.44}$$

By evaluating the residues of the poles not at infinity and using our definition of Z^{∞} in (5.4.7), it is possible to write

$$\begin{aligned} \left\langle U_1^+ \left[U_1^+, U_1^- \right] U_1^- \right\rangle = &-\sum_{a\neq b}^{N} u_{e_a-e_b} Z^{\infty}(\varphi - (e_a+e_b)\epsilon, m, \epsilon) \\ &- \sum_{a=1}^{N} Z^{\infty}(\varphi - 2e_a\epsilon, m, \epsilon) \left[\frac{(-1)^{N-1} \prod_{k=1}^{N_f} [\varphi_a - m_k - \epsilon]}{\prod_{b\neq a} \varphi_{ab} \left(\varphi_{ab} - 2\epsilon\right)} \right] . \end{aligned} \tag{5.4.45}$$

Comparing with (5.2.8), we see that the final term in brackets is just $u_{e_a} \star u_{-e_a}$, and using our quantized abelian relations from section 5.2.1, along with (5.4.6), it is easy to see that

$$\left\langle U_1^+ \left[U_1^+, U_1^- \right] U_1^- \right\rangle = \left\langle U_1^+ \right\rangle \star \left\langle \left[U_1^+, U_1^- \right] \right\rangle \star \left\langle U_1^- \right\rangle \ , \tag{5.4.46}$$

showing agreement with the result expected from the star product.

To conclude, the non-commutativity of the monopole operators is tied to a wall-crossing phenomenon in the gauged SMM. The choice in the ordering of the monopole insertions along the line in $\mathbb{R} \times \mathbb{R}^2_\epsilon$ is directly related to a choice in the signs of the FI parameters in the SMM. When we reverse the order of two insertions, we cross a

codimension-one hyperplane, a wall, in the FI parameter space and the JK contour changes, instructing us to pick contributions at different poles. If the sign of the charge of the two monopole operators that are exchanged is the same, the partition function does not jump across the wall. However, every time we cross a wall at which two monopole operators of opposite charge (or equivalently an $NS5_+$ and an $NS5_-$ brane) change order, the partition function jumps. Hence, positively and negatively charged monopole operators generically do not commute. For the cases that we have discussed, we show that the commutators are simply related to the residues of poles at infinity in the matrix models.

Chapter 6

Concluding Remarks and Outlook

To conclude, we summarise the main points of this thesis and discuss the possible directions for future work.

After reviewing background material for two- and three-dimensional supersymmetric gauge theories in chapter 2, we discussed supersymmetric localization and the Jeffrey-Kirwan (JK) residue operation in chapter 3.

The technique of localization is useful to compute path integrals in supersymmetric field theories. The main point is summarised by emphasising that when the path integral is deformed by a Q-exact localizing action term, the semi-classical approximation is exact, and the path integral is localized to the fixed points of the Q-invariant field configurations given by solving $fermions = 0$ and $Q\,(fermions) = 0$. The localization procedure has been successfully applied to various supersymmetric field theories defined on curved spaces. We demonstrated this technique in an example by evaluating the exact two-sphere partition function of two-dimensional $\mathcal{N} = (2, 2)$ Landau-Ginzburg models with a twisted superpotential.

The JK residue is another useful tool in the analysis of exact results for supersymmetric gauge theories. Its definition was explained in section 3.2, and we also presented the explicit evaluation of a one- and two-dimensional JK integral. Both of these techniques, supersymmetric localization and the JK residue, were utilised in chapters 4 and 5 to obtain our results.

In chapter 4, by using the exact formula for the correlation functions of two-dimensional $\mathcal{N} = (2,2)$ Gauged Linear Sigma Models (GLSMs) on the Omega-deformed two-sphere background [74], we studied the computation of the correlators for the GLSM describing the non-compact orbifold $\mathbb{C}^3/Z_{(2N+1)(2,2,1)}$. With the Omega deformation turned off, we found that the result for the three-point correlators is ambiguous, since it depended on the twisted masses that were used to make the JK integral non-degenerate. We turned on the Omega deformation in an attempt to regulate the integral and repeated the computation. We found that the result for the three-point correlators matched the previous computation provided that the limits of vanishing twisted masses were taken in an appropriate fashion. In addition, we compared our results with the evaluation of these correlations functions in the literature. We clarified that the results obey the quantum cohomology relations in the massive theory but there is a mild violation, due to the three-point correlators, in the massless theory.

We examined in chapter 4 a single GLSM with a non-compact geometry, but it would be worthwhile to study other cases, including non-abelian models, to observe if the correlation functions for different non-compact geometries are ambiguous. It would also be interesting to investigate the connection between the contour integral of [20] and the A-model correlators formula of [74], see (4.2.21) and (4.1.19), respectively. A potential area for future research is the application of supersymmetric localization to B-twisted Landau-Ginzburg models on the Omega-deformed two-sphere. This would enable the computation of correlation functions to be compared using two-dimensional mirror symmetry.

In chapter 5 we computed correlators of monopole operators in three-dimensional $\mathcal{N} = 4$ $U(N)$ gauge theories in the $\mathbb{R} \times \mathbb{R}^2_\epsilon$ Omega background, using inputs from supersymmetry localization and the brane realisation of these operators in type IIB string theory. These correlators were written in terms of a sum containing products of abelian monopole variables and monopole bubbling factors. The abelian monopole variables, which are rational functions of the vacuum expectation values of complex

scalars in the vector multiplet, are well understood. On the other hand, the bubbling factors, which are the partition functions of zero-dimensional gauged Super-Matrix-Models (SMMs), are challenging to compute. These were realised as the theory living on the D1 strings in the brane construction and we explicitly computed them by applying the JK residue prescription. We found that the non-commutativity arising in the monopole operator insertions is related to wall-crossing phenomena in the FI parameter space of the SMM. Finally, we used the non-commutative Moyal (star) product and the action of PT symmetry as non-trivial consistency checks to successfully test our results.

The method discussed in chapter 5 has several advantages. Firstly, it is a direct approach, computing correlators from supersymmetric localization, so it does not rely on assumptions. It can also be applied for arbitrary gauge group rank. In addition, it provides evidence for the Moyal product realisation of the non-commutative product. Finally, in our method the physics of monopole bubbling is manifest, and importantly, the physics of the results is transparent.

This method also has some limitations. In particular, it requires a brane realisation of the 3d gauge theory, which is only available for quiver-like theories with classical gauge group factors. Even with a brane realisation, the method may become tedious for long quivers. However, one may argue that for complicated theories, any method will necessarily be tedious anyway. The significant remaining challenge is the computation of the matrix models Z_{SMM} at zero FI parameters, so called on-the-wall partition functions. When two adjacent NS5 branes (for example the inner-most NS5_+ and the inner-most NS5_-) share the same x^0 position, the corresponding FI parameter for the respective gauge node is zero, and the partition function cannot be computed using the JK residue prescription. This situation arises generically, pointing to the missing ingredient in our construction: the computation of Z_{SMM} on the FI walls. The SMM are readily evaluated when the FI parameters are non-zero, i.e. away from the chamber walls in the FI parameter space, which allowed us to compute the correlators of monopoles of minimal positive and negative charge

efficiently. On the other hand, the evaluation of the vacuum expectation values and correlators of higher charged monopoles crucially relies on the technical task of evaluating the matrix models on the FI space walls.

This work could be extended to study the quantized Coulomb branch of various 3d gauge theories (with brane realisations). Furthermore, the exact results for the correlators of Coulomb branch operators could be used to address various physics questions, in particular how to determine the quantized monopole relations and the precise map of operators under three-dimensional mirror symmetry. Finally, this analysis carried out using brane constructions has the potential to be extended to gauge theories with $\mathcal{N} < 4$ supersymmetry.

Appendix A

Mathematica Code for Performing the Jeffrey-Kirwan Residue

This appendix contains the Mathematica code used to compute the two-dimensional JK integral (3.2.16) in section 3.2.3.

JK Residue Computation Example

Integrand

e = epsilon

In[1]:=
```
Den1 = {z1 - z0 + e, -z1 + z0 + e, z2 - z3 + e, -z2 + z3 + e, z1 - z2 + e, -z1 + z2 + e}
Length[Den1]
listProduct[x_List] := Times @@ x
integrand = (2 e)^2 1/listProduct[Den1]
```

Out[1]= $\{e - z0 + z1,\ e + z0 - z1,\ e + z2 - z3,\ e - z2 + z3,\ e + z1 - z2,\ e - z1 + z2\}$

Out[2]= 6

Out[4]= $(4\,e^2) \,/\, ((e + z0 - z1)\,(e - z0 + z1)\,(e + z1 - z2)\,(e - z1 + z2)\,(e + z2 - z3)\,(e - z2 + z3))$

Charge Vectors

Define the charge vectors

In[5]:=
```
q[1] = {1, 0};
q[2] = {-1, 0};
q[3] = {0, 1};
q[4] = {0, -1};
q[5] = {1, -1};
q[6] = {-1, 1};
q[7] = {1, -1};
q[8] = {-1, 1};
```

Sum of two charges

In[13]:=
```
qsum2[i_, j_] := q[i] + q[j];
```

Poles

Associate the terms in the denominator of the integrand to the poles

In[14]:=
```
a = {1 → z1 → z0 - e, 2 → z1 → z0 + e, 3 → z2 → z3 - e, 4 → z2 → z3 + e,
   5 → z1 → z2 - e, 6 → z2 → z1 - e, 7 → z2 → z1 + e, 8 → z1 → z2 + e};
SelfReplace[rules_] := Map[Function[u, u[[1]] → (u[[2]] //. rules)], rules];
```

Find multidimensional poles and exclude the combinations that are not allowed

In[16]:=
```
d = Tuples[{{1, 2, 5, 8}, {3, 4, 6, 7}}];
Do[If[ContainsNone[d[[i]], {1, 2, 3, 4}] ||
    SubsetQ[d[[i]], {5, 6}] || SubsetQ[d[[i]], {5, 7}] || SubsetQ[d[[i]], {6, 8}] ||
    SubsetQ[d[[i]], {7, 8}], d[[i]] = 0,], {i, Length[d]}]
Length[d]
fieldswithconstraints = DeleteCases[d, 0]
Length[fieldswithconstraints]
```

Out[18]= 16

Out[19]=
```
{{1, 3}, {1, 4}, {1, 6}, {1, 7}, {2, 3},
 {2, 4}, {2, 6}, {2, 7}, {5, 3}, {5, 4}, {8, 3}, {8, 4}}
```

Out[20]= 12

Now use ‘a’ to change the numbers in the allowed combinations ‘fieldswithconstraints’ to the poles in terms of z’s and e. Use ‘SelfReplace’ to simplify the poles and check that all the poles are unique (no duplicates).

In[21]:=
```
dd = fieldswithconstraints /. a
tt = Table[SelfReplace[dd[[i]]], {i, 1, Length[dd]}]
compare = Table[Position[tt, tt[[k]]], {k, 1, Length[tt]}]
Do[If[Dimensions[compare[[i]]] ≠ {1, 1}, compare[[i]] = 0,], {i, 1, Length[compare]}]
unique = DeleteCases[compare, 0];
Length[tt]
Length[unique]
```

Out[21]=
```
{{z1 → -e + z0, z2 → -e + z3}, {z1 → -e + z0, z2 → e + z3}, {z1 → -e + z0, z2 → -e + z1},
 {z1 → -e + z0, z2 → e + z1}, {z1 → e + z0, z2 → -e + z3}, {z1 → e + z0, z2 → e + z3},
 {z1 → e + z0, z2 → -e + z1}, {z1 → e + z0, z2 → e + z1}, {z1 → -e + z2, z2 → -e + z3},
 {z1 → -e + z2, z2 → e + z3}, {z1 → e + z2, z2 → -e + z3}, {z1 → e + z2, z2 → e + z3}}
```

Out[22]=
```
{{z1 → -e + z0, z2 → -e + z3}, {z1 → -e + z0, z2 → e + z3}, {z1 → -e + z0, z2 → -2 e + z0},
 {z1 → -e + z0, z2 → z0}, {z1 → e + z0, z2 → -e + z3}, {z1 → e + z0, z2 → e + z3},
 {z1 → e + z0, z2 → z0}, {z1 → e + z0, z2 → 2 e + z0}, {z1 → -2 e + z3, z2 → -e + z3},
 {z1 → z3, z2 → e + z3}, {z1 → z3, z2 → -e + z3}, {z1 → 2 e + z3, z2 → e + z3}}
```

Out[23]=
```
{{{1}}, {{2}}, {{3}}, {{4}}, {{5}},
 {{6}}, {{7}}, {{8}}, {{9}}, {{10}}, {{11}}, {{12}}}
```

Out[26]= 12

Out[27]= 12

Good, now extract the unique allowed combinations and the unique poles. Separate the expressions on the left and on the right of the arrows in ‘unique’ into two separate lists, and check.

In[28]:=
```
uniquepoles = Table[Flatten[tt[[Flatten[unique[[i]]]]]], {i, 1, Length[unique]}]
uniquefields = Table[
  Flatten[fieldswithconstraints[[Flatten[unique[[i]]]]]], {i, 1, Length[unique]}]
pp = Table[Flatten[dd[[Flatten[unique[[i]]]]]], {i, 1, Length[unique]}]
up = Table[Last[pp[[k, i]]], {k, 1, Length[pp]}, {i, 1, Length[pp[[k]]]}]
zz = Table[First[pp[[k, i]]], {k, 1, Length[pp]}, {i, 1, Length[pp[[k]]]}]
Length[uniquepoles]
Length[uniquefields]
Length[up]
Length[zz]
unique[[4]]
uniquepoles[[4]]
uniquefields[[4]]
up[[4]]
zz[[4]]
```

Out[28]=
```
{{z1 → -e + z0, z2 → -e + z3}, {z1 → -e + z0, z2 → e + z3}, {z1 → -e + z0, z2 → -2 e + z0},
 {z1 → -e + z0, z2 → z0}, {z1 → e + z0, z2 → -e + z3}, {z1 → e + z0, z2 → e + z3},
 {z1 → e + z0, z2 → z0}, {z1 → e + z0, z2 → 2 e + z0}, {z1 → -2 e + z3, z2 → -e + z3},
 {z1 → z3, z2 → e + z3}, {z1 → z3, z2 → -e + z3}, {z1 → 2 e + z3, z2 → e + z3}}
```

Out[29]=
```
{{1, 3}, {1, 4}, {1, 6}, {1, 7}, {2, 3},
 {2, 4}, {2, 6}, {2, 7}, {5, 3}, {5, 4}, {8, 3}, {8, 4}}
```

Out[30]=
```
{{z1 → -e + z0, z2 → -e + z3}, {z1 → -e + z0, z2 → e + z3}, {z1 → -e + z0, z2 → -e + z1},
 {z1 → -e + z0, z2 → e + z1}, {z1 → e + z0, z2 → -e + z3}, {z1 → e + z0, z2 → e + z3},
 {z1 → e + z0, z2 → -e + z1}, {z1 → e + z0, z2 → e + z1}, {z1 → -e + z2, z2 → -e + z3},
 {z1 → -e + z2, z2 → e + z3}, {z1 → e + z2, z2 → -e + z3}, {z1 → e + z2, z2 → e + z3}}
```

Out[31]=
```
{{-e + z0, -e + z3}, {-e + z0, e + z3}, {-e + z0, -e + z1}, {-e + z0, e + z1},
 {e + z0, -e + z3}, {e + z0, e + z3}, {e + z0, -e + z1}, {e + z0, e + z1},
 {-e + z2, -e + z3}, {-e + z2, e + z3}, {e + z2, -e + z3}, {e + z2, e + z3}}
```

Out[32]=
```
{{z1, z2}, {z1, z2}, {z1, z2}, {z1, z2}, {z1, z2},
 {z1, z2}, {z1, z2}, {z1, z2}, {z1, z2}, {z1, z2}, {z1, z2}, {z1, z2}}
```

Out[33]= 12

Out[34]= 12

Out[35]= 12

Out[36]= 12

Out[37]= {{4}}

Out[38]= {z1 → -e + z0, z2 → z0}

Out[39]= {1, 7}

Out[40]= {-e + z0, e + z1}

Out[41]= {z1, z2}

Evaluate the iterated residue for each eta. Find the poles that contribute in each chamber, with their sign in the

iterated residue, and check that the final result is the same in all chambers.

JK parameters for each chamber.

In[42]:=
```
η = {{{1}, {2}}, {{2}, {1}}, {{2}, {-1}},
   {{1}, {-2}}, {{-1}, {-2}}, {{-2}, {1}}, {{-1}, {2}}};
Length[
 η]
```

Out[43]= 7

Check that these η are all unique.

In[44]:=
```
Table[η[[i]] === η[[j]], {i, 1, Length[η] - 1}, {j, i + 1, Length[η]}]
```

Out[44]=
```
{{False, False, False, False, False, False}, {False, False, False, False, False},
 {False, False, False, False}, {False, False, False}, {False, False}, {False}}
```

Good. Now for each of the chambers, find the poles that contribute in each chamber and follow the JK prescription to evaluate the iterated residue. Print the poles that contribute in each chamber and the final result.

```
In[45]:= For[ll = 1, ll < (Length[η] + 1), ll++,
 ww = 1;
 For[j = 1, j < (Length[uniquepoles] + 1), j++,
  pp = Table[Flatten[dd[[Flatten[unique[[i]]]]]], {i, 1, Length[unique]}];
  up = Table[Last[pp[[k, i]]], {k, 1, Length[pp]}, {i, 1, Length[pp[[k]]]}];
  zz = Table[First[pp[[k, i]]], {k, 1, Length[pp]}, {i, 1, Length[pp[[k]]]}];
  perm = Permutations[uniquefields[[j]]];
  Do[
   If[Solve[Transpose[{q[perm[[i, 1]]], qsum2[perm[[i, 1]], perm[[i, 2]]]}].{e, f} ==
        η[[ll]] && e ≥ 0 && f ≥ 0, {e, f}] == {}, perm[[i]] = 0,], {i, Length[perm]}];
  new = DeleteCases[perm, 0];
  If[new == {}, result[j] = 0,
   tt =
    Table[Position[uniquefields[[j]], new[[1, i]]], {i, 1, Dimensions[new][[2]]}];
   t = Flatten[tt];
   polefirst = zz[[j]][[t[[1]]]] → up[[j]][[t[[1]]]];
   rs1 = Residue[integrand, {zz[[j]][[t[[1]]]], up[[j]][[t[[1]]]]}];
   up[[j]] = up[[j]] /. {zz[[j]][[t[[1]]]] → up[[j]][[t[[1]]]]};
   polesecond = zz[[j]][[t[[2]]]] → up[[j]][[t[[2]]]];
   result[j] = Residue[rs1, {zz[[j]][[t[[2]]]], up[[j]][[t[[2]]]]}];
   up[[j]] = up[[j]] /. {zz[[j]][[t[[2]]]] → up[[j]][[t[[2]]]]};
   pol[ww] = {polefirst, polesecond};
   ww = ww + 1;
  ];
  If[new == {}, sig[j] = 0,
   ddd[j] = Det[Transpose[{q[uniquefields[[j]][[t[[1]]]]],
       qsum2[uniquefields[[j]][[t[[1]]]], uniquefields[[j]][[t[[2]]]]]}]];
   sig[j] = (Signature[t]) * (Sign[ddd[j]]);
  ];
  Clear[pp];
  Clear[up];
  Clear[zz];
 ];
 Print["In the chamber ", η[[ll]]];
 Print["The contributing poles are ", allpoles[ll] = Table[pol[y], {y, 1, ww - 1}]];
 Print["The total number of poles is ", Length[allpoles[ll]]];
 signs[ll] = DeleteCases[Table[sig[j], {j, 1, Length[uniquepoles]}], 0];
 Print["The sign in the iterated residue for each of these poles is ", signs[ll]];
 answer[ll] = Sum[sig[j] * result[j], {j, 1, Length[uniquepoles]}];
 Print["The result in this chamber is ", answer[ll]];
 Print["This result simplifies to ", FullSimplify[answer[ll]]];
 Print[];
 Clear[ww];
 Clear[result];
 Clear[pol];
 Clear[sig];
 Clear[ddd];
]
```

```
In the chamber {{1}, {2}}

The contributing poles are
 {{z2 → -e + z3, z1 → -e + z0}, {z1 → -e + z0, z2 → -2 e + z0}, {z2 → -e + z3, z1 → -2 e + z3}}

The total number of poles is 3
```

The sign in the iterated residue for each of these poles is {1, 1, 1}

The result in this chamber is

$$-\frac{1}{(e+z0-z3)\,(3e+z0-z3)}+\frac{1}{(e+z0-z3)\,(e-z0+z3)}-\frac{1}{(e-z0+z3)\,(3e-z0+z3)}$$

This result simplifies to $\frac{3}{(3e+z0-z3)\,(3e-z0+z3)}$

In the chamber {{2}, {1}}

The contributing poles are

{{z1 → −e + z0, z2 → −e + z3}, {z1 → −e + z0, z2 → −2 e + z0}, {z2 → −e + z3, z1 → −2 e + z3}}

The total number of poles is 3

The sign in the iterated residue for each of these poles is {1, 1, 1}

The result in this chamber is

$$-\frac{1}{(e+z0-z3)\,(3e+z0-z3)}+\frac{1}{(e+z0-z3)\,(e-z0+z3)}-\frac{1}{(e-z0+z3)\,(3e-z0+z3)}$$

This result simplifies to $\frac{3}{(3e+z0-z3)\,(3e-z0+z3)}$

In the chamber {{2}, {−1}}

The contributing poles are

{{z1 → −e + z0, z2 → e + z3}, {z1 → −e + z0, z2 → z0}, {z1 → −e + z2, z2 → −e + z3}}

The total number of poles is 3

The sign in the iterated residue for each of these poles is {−1, −1, 1}

The result in this chamber is

$$-\frac{1}{(e+z0-z3)\,(3e+z0-z3)}+\frac{1}{(e+z0-z3)\,(e-z0+z3)}-\frac{1}{(e-z0+z3)\,(3e-z0+z3)}$$

This result simplifies to $\frac{3}{(3e+z0-z3)\,(3e-z0+z3)}$

In the chamber {{1}, {−2}}

The contributing poles are

{{z2 → e + z3, z1 → −e + z0}, {z2 → e + z1, z1 → e + z0}, {z1 → −e + z2, z2 → e + z3}}

The total number of poles is 3

The sign in the iterated residue for each of these poles is {−1, 1, −1}

The result in this chamber is

$$-\frac{1}{(e+z0-z3)\,(3e+z0-z3)}+\frac{1}{(e+z0-z3)\,(e-z0+z3)}-\frac{1}{(e-z0+z3)\,(3e-z0+z3)}$$

This result simplifies to $\frac{3}{(3e+z0-z3)\,(3e-z0+z3)}$

In the chamber {{−1}, {−2}}

The contributing poles are

{{z2 → e + z3, z1 → e + z0}, {z1 → e + z0, z2 → 2 e + z0}, {z2 → e + z3, z1 → 2 e + z3}}

The total number of poles is 3

The sign in the iterated residue for each of these poles is {1, 1, 1}

The result in this chamber is

$$-\frac{1}{(e+z0-z3)\,(3e+z0-z3)}+\frac{1}{(e+z0-z3)\,(e-z0+z3)}-\frac{1}{(e-z0+z3)\,(3e-z0+z3)}$$

This result simplifies to $\frac{3}{(3e+z0-z3)\,(3e-z0+z3)}$

In the chamber {{−2}, {1}}

The contributing poles are

{{z1 → e + z0, z2 → −e + z3}, {z1 → e + z0, z2 → z0}, {z1 → e + z2, z2 → e + z3}}

The total number of poles is 3

The sign in the iterated residue for each of these poles is {−1, −1, 1}

The result in this chamber is

$$-\frac{1}{(e+z0-z3)\,(3e+z0-z3)}+\frac{1}{(e+z0-z3)\,(e-z0+z3)}-\frac{1}{(e-z0+z3)\,(3e-z0+z3)}$$

This result simplifies to $\frac{3}{(3e+z0-z3)\,(3e-z0+z3)}$

In the chamber {{−1}, {2}}

The contributing poles are

{{z2 → −e + z1, z1 → −e + z0}, {z2 → −e + z3, z1 → e + z0}, {z1 → e + z2, z2 → −e + z3}}

The total number of poles is 3

The sign in the iterated residue for each of these poles is {1, −1, −1}

The result in this chamber is

$$-\frac{1}{(e+z0-z3)\,(3e+z0-z3)}+\frac{1}{(e+z0-z3)\,(e-z0+z3)}-\frac{1}{(e-z0+z3)\,(3e-z0+z3)}$$

This result simplifies to $\frac{3}{(3e+z0-z3)\,(3e-z0+z3)}$

Good. Now verify that all of these results are the same.

In[46]:=
```
Do[Print[FullSimplify[answer[1] - answer[i]]], {i, 2, Length[η]}]
```

0

0

0

0

0

0

Good. Therefore, the chamber independent result is

In[47]:=
```
FullSimplify[answer[1]]
```

Out[47]=
$$\frac{3}{\left(3e+z0-z3\right)\,\left(3e-z0+z3\right)}$$

Appendix B

Computing Residues in Flavour Fugacities

In this appendix we explain how the partition function of the $T^{\sigma}_{\rho,L}[SU(N)]$ matrix model can be obtained from the partition function for the trivial D3 brane partition $\sigma = (1^N)$ by taking appropriate residues in the flavour fugacities, which have the effect of moving boxes in the Young tableaux associated to σ. We follow a related computation performed for Hilbert series in appendix C of [37].

Any partition σ of N can be obtained from $\sigma = (1^N)$ by repeatedly moving the last box to a previous row which is followed by rows of a single box only, so it is enough to consider the move[1]

$$\sigma = (\sigma_1, \ldots, \sigma_{d-h}, H, 1^h) \ \rightarrow \ \sigma' = (\sigma_1, \ldots, \sigma_{d-h}, H+1, 1^{h-1}) \ , \tag{B.0.1}$$

where the lengths of the partitions σ and σ' are $d+1$ and d, respectively. For brevity, we will denote $X = d - h + 1$, so that $\sigma_X = H$ and $\sigma'_X = H + 1$, where H is an integer greater than or equal to 1. We assume $\sigma_{X-1} > H$ so that the move is allowed.

[1] In the language of Kraft-Procesi transitions [95], in which moving a box up by k rows and to the right by one column is an A_k transition, whereas moving a box up by one row and to the right by l columns is an a_l transition, the move (B.0.1) realises an A_{h-1} transition followed by an a_{H-1} transition.

We claim that for such σ and σ',

$$\operatorname*{Res}_{z=0} Z_{T^{\sigma}_{\rho,L}[SU(N)]}\Big| = \frac{P(\varphi_X + (H-L)\epsilon)}{(H+1)(2\epsilon)\prod_{a=X+1}^{d}[\pm(\varphi_{Xa} + (H-1)\epsilon) + \epsilon]} Z_{T^{\sigma'}_{\rho,L}[SU(N)]}\ , \tag{B.0.2}$$

where $\Big|$ denotes the substitution $\varphi_X \to \varphi_X - (\epsilon - z), \varphi_{d+1} \to \varphi_X + H(\epsilon - z)$, and N_f fundamental Fermi multiplets are attached to gauge node L. For $L \leq H$, the term containing the Fermi multiplets is present since the rank of the gauge node attached to these multiplets reduces during the transition (B.0.1). In contrast, when $L > H$, the Fermi multiplets are unaffected by the transition and it is understood that $P\left(\varphi_X + (H-L)\epsilon\right) \to 1$ in (B.0.2).

To see this, recall that the quiver diagram of $T^{\sigma}_{\rho}[SU(N)]$ is represented by the matrix

$$\begin{bmatrix} 0 & h & 0 & \dots & 1 & M_{H+1} & \dots \\ 0 & N_1 & N_2 & \dots & N_H & N_{H+1} & \dots \end{bmatrix}\ , \tag{B.0.3}$$

where the first/second row in the matrix denotes the rank of a unitary flavour/gauge group, starting from nodes labelled by $i = 0$. In the case $L = H$, for example, the Fermi multiplets are attached to the $U(N_H)$ gauge group with a single flavour of fundamental hypermultiplets with mass parameter φ_X, which can be illustrated by underlining N_H in the matrix above. (B.0.3) is true for all $H > 1$, if we have $H = 1$ the quiver is instead given by the matrix

$$\begin{bmatrix} 0 & h+1 & M_2 & \dots \\ 0 & N_1 & N_2 & \dots \end{bmatrix}\ . \tag{B.0.4}$$

The matrix notation for $T^{\sigma'}_{\rho}[SU(N)]$ is given by

$$\begin{bmatrix} 1 & h-1 & 0 & \dots & 0 & M_{H+1}+1 & \dots \\ 0 & N_1 - 1 & N_2 - 1 & \dots & N_H - 1 & N_{H+1} & \dots \end{bmatrix}\ . \tag{B.0.5}$$

The ellipses on the right remain unchanged in the transition. In terms of these 0d quivers and their partition functions (5.3.15), we identify $\varphi_{d+1} = \tilde{\varphi}_{1,h}$ and $\varphi_X = \tilde{\varphi}_{H,1}$,

so φ_{d+1} is the mass parameter for one of the h fundamental hypermultiplets of gauge group 1 and φ_X is the mass parameter for the fundamental hypermultiplet of gauge group H.

The partition function in the left hand side of (B.0.2) has a simple pole at $z = 0$ if the term

$$\frac{1}{\varphi_{X,d+1} + (H+1)\epsilon} \ , \tag{B.0.6}$$

is present before the substitution.[2] This term appears if the abelian subquiver

$$\begin{bmatrix} 1 & 0 & \dots & 0 & 1 \\ \\ 1 & 1 & \dots & 1 & 1 \end{bmatrix} \ , \tag{B.0.7}$$

where the left/right flavour node has mass parameter φ_{d+1}/φ_X and the gauge nodes have parameters z_{i,N_i}, leads to a multi-dimensional pole in the SMM integral given by

$$z_{i,N_i} = \begin{cases} \varphi_{d+1} - i\epsilon \ , & 1 \leq i \leq a \ , \\ \\ \varphi_X + (H+1-i)\epsilon \ , & a+1 \leq i \leq H \ , \end{cases} \tag{B.0.8}$$

for some integer $a \in [0, H]$. This multi-dimensional pole of the partition function of the abelian subquiver can be illustrated diagrammatically by

$$\begin{array}{ccccccccc} \varphi_{d+1} & & & & & & & & \varphi_X \\ \uparrow & & & & & & & & \downarrow \\ \varphi_{d+1} - \epsilon & \leftarrow & \varphi_{d+1} - 2\epsilon & \dots & \leftarrow \varphi_{d+1} - a\epsilon & & \varphi_X + (H-a)\epsilon & \leftarrow \dots & \varphi_X + 2\epsilon \leftarrow \varphi_X + \epsilon \\ 1 & & 2 & \dots & a & & a+1 & \dots & H+1 \qquad H \end{array} \ , \tag{B.0.9}$$

where arrows indicate the chiral multiplets that contribute to the pole and the nodes have been replaced by their corresponding parameters. Due to the massive hypermultiplet associated to the missing link in the quiver (B.0.9), the residue of the

[2] Applying the substitution $\varphi_X \to \varphi_X - (\epsilon - z), \varphi_{d+1} \to \varphi_X + H(\epsilon - z)$ to (B.0.6) gives $(z(H+1))^{-1}$.

abelian subquiver partition function is $[\pm(\varphi_{X,d+1}+H\epsilon)+\epsilon]^{-1}$, which indeed contains the factor (B.0.6). Note that a pole of the type (B.0.9) for a certain value of a appears in any chamber: the relevant value of a is determined by $x_{a+1}=\max\{x_b\}_{b=1}^{H+1}$.[3]

If we now embed the abelian subquiver in the full non-abelian quiver and evaluate the integrals over z_{i,N_i} for $i=1,\ldots,H$ at the poles (B.0.8) in the full SMM partition function, the gauge group (B.0.3) of the original SMM reduces to the gauge group (B.0.5) of the new matrix model. Keeping track of the masses of the fields which enter the one-loop determinants and following several cancellations, it is then straightforward to obtain the right hand side of (B.0.2), where the new φ_X is now identified with an extra mass parameter for the flavour symmetry at node $H+1$, as expected. In the presence of Fermi multiplets, the poles (B.0.8) are unchanged since they depend only on the hypermultiplets. Thus, to take into account the factors that arise from the Fermi multiplets, we require the additional term in the numerator on the right hand side of (B.0.2).

As an example let us consider the transition $\sigma=(1^3)\to\sigma'=(2,1)$ with the NS5 brane partition $\rho=(1^3)$ and Fermi multiplets attached to the first gauge node. In the previous notation, $X=H=1$, $d=h=2$, and $L=1$. In the chamber described by the NS5 brane configuration $x_2<x_{-1}<x_1$,[4] the partition function of $T^{(1^3)}_{(1^3),1}[SU(3)]$ is

$$Z_{T_1^{(1^3)}[SU(3)]}=\frac{-1}{\varphi_{12}\varphi_{13}\varphi_{23}}\Bigg[\frac{P(\varphi_2+\epsilon)P(\varphi_3-\epsilon)}{(\varphi_{12}-2\epsilon)(\varphi_{13}+2\epsilon)(\varphi_{23}+2\epsilon)}$$
$$+\frac{P(\varphi_1+\epsilon)P(\varphi_2-\epsilon)}{(\varphi_{12}+2\epsilon)(\varphi_{13}+2\epsilon)(\varphi_{23}-2\epsilon)}+\frac{P(\varphi_1+\epsilon)P(\varphi_3-\epsilon)}{(\varphi_{12}+2\epsilon)(\varphi_{13}+2\epsilon)(\varphi_{23}+2\epsilon)}+(\epsilon\to-\epsilon)\Bigg]\,. \tag{B.0.10}$$

Performing the substitution $\varphi_1\to\varphi_1-(\epsilon-z)$, $\varphi_3\to\varphi_1+(\epsilon-z)$, and computing

[3] Recall that the FI parameter for the a-th gauge node is given by $x_{a+1}-x_a$.

[4] Using the map $\xi_0=x_1-x_{-1}$, $\xi_1=x_2-x_1$, this corresponds to the chamber $\xi_1<0,\xi_0>0,\xi_0+\xi_1<0$ in FI space.

the residue at $z = 0$ we find

$$\operatorname*{Res}_{z=0} Z_{T^{(1^3)}_{(1^3),1}[SU(3)]}\Big| = \frac{P(\varphi_1)}{2(2\epsilon)\left[\pm\varphi_{12}+\epsilon\right]} \times \left[\frac{P(\varphi_1)}{(\pm\varphi_{12}+\epsilon)} - \left(\frac{P(\varphi_2+\epsilon)}{(\varphi_{12}-\epsilon)\,(\varphi_{12}-3\epsilon)} + (\epsilon \to -\epsilon)\right)\right] . \tag{B.0.11}$$

According to the prescription (B.0.2), the term in brackets on the right hand side should be the partition function of $T^{(2,1)}_{(1^3),1}[SU(3)]$. Indeed, it matches the result for Z_1^{+-+} in (5.4.19) when $N = 2$, which was computed directly using the JK prescription.

Appendix C

More on the Computation of Monopole Bubbling Factors

In this appendix we state the results for the partition functions (5.4.35) and (5.4.38) in each of the 6 distinct chambers. These results have been computed by applying the JK prescription and have been verified by following the residues in the flavour fugacities procedure outlined in appendix B.

In Tables C.1 and C.2 we list the multi-dimensional poles contributing to (5.4.35) in one of the regions of FI space for each of the 6 inequivalent chambers. These poles are written in the order that the iterated residues are performed, from left to right, and the sign $\nu(F)$ that is associated to each pole is the sign used in the sum of the iterated residues, see (3.2.10) and (3.2.12).

Evaluating (5.4.35) in each of the six chambers we find

$$
\begin{aligned}
Z_{ab}^{++--}(\varphi,m,\epsilon) = & \left(\frac{(-1)^{N-1}\prod_{k=1}^{N_f}\left[\varphi_a - m_k - 2\epsilon\right]}{\varphi_{ab}\left(\varphi_{ab}-2\epsilon\right)\prod_{c\neq b,a}\left[\left(\varphi_{ac}-\epsilon\right)\left(\varphi_{ac}-3\epsilon\right)\right]} \right. \\
& \left. + \frac{(-1)^{N-1}\prod_{k=1}^{N_f}\left[\varphi_a - m_k - 2\epsilon\right]}{\left(\varphi_{ab}-2\epsilon\right)\left(\varphi_{ab}-4\epsilon\right)\prod_{c\neq b,a}\left[\left(\varphi_{ac}-\epsilon\right)\left(\varphi_{ac}-3\epsilon\right)\right]} + (a \leftrightarrow b) \right) \\
& + \sum_{c\neq b,a} \left[\frac{(-1)^{N-1}\prod_{k=1}^{N_f}\left[\varphi_c - m_k - \epsilon\right]}{\prod_{r=a,b}\left(\varphi_{rc}+\epsilon\right)\left(\varphi_{rc}+3\epsilon\right)\prod_{d\neq c,b,a}\varphi_{cd}\left(\varphi_{cd}-2\epsilon\right)} \right. \\
& + \frac{(-1)^{N-1}\prod_{k=1}^{N_f}\left[\varphi_c - m_k - \epsilon\right]}{\prod_{r=a,b}\left(\pm\varphi_{rc}+\epsilon\right)\prod_{d\neq c,b,a}\varphi_{cd}\left(\varphi_{cd}-2\epsilon\right)} \\
& \left. + \left(\frac{(-1)^{N}\prod_{k=1}^{N_f}\left[\varphi_c - m_k - \epsilon\right]}{\left(\pm\varphi_{ac}+\epsilon\right)\left(\varphi_{bc}+\epsilon\right)\left(\varphi_{bc}+3\epsilon\right)\prod_{d\neq c,b,a}\varphi_{cd}\left(\varphi_{cd}-2\epsilon\right)} + (a \leftrightarrow b) \right) \right] .
\end{aligned}
\tag{C.0.1}
$$

$$
\begin{aligned}
Z_{ab}^{--++}(\varphi,m,\epsilon) = & \left(\frac{(-1)^{N-1}\prod_{k=1}^{N_f}\left[\varphi_a - m_k + 2\epsilon\right]}{\varphi_{ab}\left(\varphi_{ab}+2\epsilon\right)\prod_{c\neq b,a}\left[\left(\varphi_{ac}+\epsilon\right)\left(\varphi_{ac}+3\epsilon\right)\right]} \right. \\
& \left. + \frac{(-1)^{N-1}\prod_{k=1}^{N_f}\left[\varphi_a - m_k + 2\epsilon\right]}{\left(\varphi_{ab}+2\epsilon\right)\left(\varphi_{ab}+4\epsilon\right)\prod_{c\neq b,a}\left[\left(\varphi_{ac}+\epsilon\right)\left(\varphi_{ac}+3\epsilon\right)\right]} + (a \leftrightarrow b) \right) \\
& + \sum_{c\neq b,a} \left[\frac{(-1)^{N-1}\prod_{k=1}^{N_f}\left[\varphi_c - m_k + \epsilon\right]}{\prod_{r=a,b}\left(\varphi_{rc}-\epsilon\right)\left(\varphi_{rc}-3\epsilon\right)\prod_{d\neq c,b,a}\varphi_{cd}\left(\varphi_{cd}+2\epsilon\right)} \right. \\
& + \frac{(-1)^{N-1}\prod_{k=1}^{N_f}\left[\varphi_c - m_k + \epsilon\right]}{\prod_{r=a,b}\left(\varphi_{rc}\pm\epsilon\right)\prod_{d\neq c,b,a}\varphi_{cd}\left(\varphi_{cd}+2\epsilon\right)} \\
& \left. + \left(\frac{(-1)^{N}\prod_{k=1}^{N_f}\left[\varphi_c - m_k + \epsilon\right]}{\left(\varphi_{ac}-\epsilon\right)\left(\varphi_{ac}-3\epsilon\right)\left(\pm\varphi_{bc}+\epsilon\right)\prod_{d\neq c,b,a}\varphi_{cd}\left(\varphi_{cd}+2\epsilon\right)} + (a \leftrightarrow b) \right) \right] .
\end{aligned}
\tag{C.0.2}
$$

$$Z_{ab}^{+-+-}(\varphi,m,\epsilon)=\left(\frac{(-1)^{N-1}\prod\limits_{k=1}^{N_f}\left[\varphi_a-m_k\right]}{\varphi_{ab}\left(\varphi_{ab}+2\epsilon\right)\prod\limits_{c\neq b,a}\left[\left(\varphi_{ac}-\epsilon\right)\left(\varphi_{ac}+\epsilon\right)\right]}\right.$$
$$\left.+\frac{(-1)^{N-1}\prod\limits_{k=1}^{N_f}\left[\varphi_a-m_k-2\epsilon\right]}{\left(\varphi_{ab}-2\epsilon\right)\left(\varphi_{ab}-4\epsilon\right)\prod\limits_{c\neq b,a}\left[\left(\varphi_{ac}-\epsilon\right)\left(\varphi_{ac}-3\epsilon\right)\right]}+(a\leftrightarrow b)\right)$$
$$+\sum_{c\neq b,a}\left[\left(\frac{(-1)^{N-1}\prod\limits_{k=1}^{N_f}\left[\varphi_c-m_k+\epsilon\right]}{\prod\limits_{r=a,b}\left(\varphi_{rc}-\epsilon\right)\left(\varphi_{rc}-3\epsilon\right)\prod\limits_{d\neq c,b,a}\varphi_{cd}\left(\varphi_{cd}+2\epsilon\right)}+(\epsilon\to-\epsilon)\right)\right.$$
$$\left.+\left(\frac{(-1)^{N}\prod\limits_{k=1}^{N_f}\left[\varphi_c-m_k-\epsilon\right]}{\left(\pm\varphi_{ac}+\epsilon\right)\left(\varphi_{bc}+\epsilon\right)\left(\varphi_{bc}+3\epsilon\right)\prod\limits_{d\neq c,b,a}\varphi_{cd}\left(\varphi_{cd}-2\epsilon\right)}+(a\leftrightarrow b)\right)\right]. \tag{C.0.3}$$

$$Z_{ab}^{-+-+}(\varphi,m,\epsilon)=\left(\frac{(-1)^{N-1}\prod\limits_{k=1}^{N_f}\left[\varphi_a-m_k\right]}{\varphi_{ab}\left(\varphi_{ab}-2\epsilon\right)\prod\limits_{c\neq b,a}\left[\left(\varphi_{ac}-\epsilon\right)\left(\varphi_{ac}+\epsilon\right)\right]}\right.$$
$$\left.+\frac{(-1)^{N-1}\prod\limits_{k=1}^{N_f}\left[\varphi_a-m_k+2\epsilon\right]}{\left(\varphi_{ab}+2\epsilon\right)\left(\varphi_{ab}+4\epsilon\right)\prod\limits_{c\neq b,a}\left[\left(\varphi_{ac}+\epsilon\right)\left(\varphi_{ac}+3\epsilon\right)\right]}+(a\leftrightarrow b)\right)$$
$$+\sum_{c\neq b,a}\left[\left(\frac{(-1)^{N-1}\prod\limits_{k=1}^{N_f}\left[\varphi_c-m_k+\epsilon\right]}{\prod\limits_{r=a,b}\left(\varphi_{rc}-\epsilon\right)\left(\varphi_{rc}-3\epsilon\right)\prod\limits_{d\neq c,b,a}\varphi_{cd}\left(\varphi_{cd}+2\epsilon\right)}+(\epsilon\to-\epsilon)\right)\right.$$
$$\left.+\left(\frac{(-1)^{N}\prod\limits_{k=1}^{N_f}\left[\varphi_c-m_k+\epsilon\right]}{\left(\varphi_{ac}-\epsilon\right)\left(\varphi_{ac}-3\epsilon\right)\left(\pm\varphi_{bc}+\epsilon\right)\prod\limits_{d\neq c,b,a}\varphi_{cd}\left(\varphi_{cd}+2\epsilon\right)}+(a\leftrightarrow b)\right)\right]. \tag{C.0.4}$$

$$
\begin{aligned}
Z_{ab}^{+-+-}(\varphi,m,\epsilon) = & \frac{(-1)^{N-1}\prod_{k=1}^{N_f}[\varphi_a - m_k]}{\varphi_{ab}\left(\varphi_{ab}-2\epsilon\right)\prod_{c\neq b,a}\left[\left(\varphi_{ac}-\epsilon\right)\left(\varphi_{ac}+\epsilon\right)\right]} \\
& + \frac{(-1)^{N-1}\prod_{k=1}^{N_f}[\varphi_b - m_k + 2\epsilon]}{\left(\varphi_{ab}-2\epsilon\right)\left(\varphi_{ab}-4\epsilon\right)\prod_{c\neq b,a}\left[\left(\varphi_{bc}+\epsilon\right)\left(\varphi_{bc}+3\epsilon\right)\right]} \\
& + \sum_{c\neq b,a}\frac{(-1)^{N-1}2\prod_{k=1}^{N_f}[\varphi_c - m_k + \epsilon]}{\left(\varphi_{ac}-\epsilon\right)\left(\varphi_{ac}-3\epsilon\right)\left(\varphi_{bc}+\epsilon\right)\left(\varphi_{bc}-3\epsilon\right)\prod_{d\neq c,b,a}\varphi_{cd}\left(\varphi_{cd}+2\epsilon\right)} \\
& + (\epsilon\to-\epsilon)\ .
\end{aligned}
\tag{C.0.5}
$$

$$
\begin{aligned}
Z_{ab}^{-++-}(\varphi,m,\epsilon) = & \frac{(-1)^{N-1}\prod_{k=1}^{N_f}[\varphi_b - m_k]}{\varphi_{ab}\left(\varphi_{ab}-2\epsilon\right)\prod_{c\neq b,a}\left[\left(\varphi_{bc}-\epsilon\right)\left(\varphi_{bc}+\epsilon\right)\right]} \\
& + \frac{(-1)^{N-1}\prod_{k=1}^{N_f}[\varphi_a - m_k - 2\epsilon]}{\left(\varphi_{ab}-2\epsilon\right)\left(\varphi_{ab}-4\epsilon\right)\prod_{c\neq b,a}\left[\left(\varphi_{ac}-\epsilon\right)\left(\varphi_{ac}-3\epsilon\right)\right]} \\
& + \sum_{c\neq b,a}\frac{(-1)^{N-1}2\prod_{k=1}^{N_f}[\varphi_c - m_k - \epsilon]}{\left(\varphi_{ac}-\epsilon\right)\left(\varphi_{ac}+3\epsilon\right)\left(\varphi_{bc}+\epsilon\right)\left(\varphi_{bc}+3\epsilon\right)\prod_{d\neq c,b,a}\varphi_{cd}\left(\varphi_{cd}-2\epsilon\right)} \\
& + (\epsilon\to-\epsilon)\ .
\end{aligned}
\tag{C.0.6}
$$

As expected from the action of PT symmetry, see section 5.2.2, these results satisfy

$$
\begin{aligned}
Z_{ab}^{++--}(\varphi,m,\epsilon) = Z_{ab}^{--++}(\varphi,m,-\epsilon) \quad , \quad Z_{ab}^{+-+-}(\varphi,m,\epsilon) \ &= Z_{ab}^{-+-+}(\varphi,m,-\epsilon)\ , \\
Z_{ab}^{+--+}(\varphi,m,\epsilon) = Z_{ab}^{+--+}(\varphi,m,-\epsilon) \quad , \quad Z_{ab}^{-++-}(\varphi,m,\epsilon) \ &= Z_{ab}^{-++-}(\varphi,m,-\epsilon)\ .
\end{aligned}
\tag{C.0.7}
$$

In addition, the correlator (5.4.30) is invariant under a charge conjugation C that reverses the sign of the charge of the monopole operators (and of the abelian monopole variables) and sends $\epsilon\to-\epsilon$. This symmetry manifests itself in the identities

$$
\begin{aligned}
Z_{ab}^{++--}(\varphi,m,\epsilon) &= Z_{ba}^{--++}(\varphi,m,-\epsilon)\ , \\
Z_{ab}^{+-+-}(\varphi,m,\epsilon) &= Z_{ba}^{-+-+}(\varphi,m,-\epsilon)\ , \\
Z_{ab}^{+--+}(\varphi,m,\epsilon) &= Z_{ba}^{-++-}(\varphi,m,-\epsilon)\ .
\end{aligned}
\tag{C.0.8}
$$

All of these 6 results agree when $N_f = 0, 1, \ldots, 2N-2$, in which case the bubbling factor is no longer chamber dependent.

In Tables C.3 and C.4 we list the poles that give a non-zero contribution to (5.4.38) in one of the regions of FI space for each of the 6 distinct chambers.

Evaluating (5.4.38) in each of the six chambers we find

$$\begin{aligned} Z^{++--}(\varphi, m, \epsilon) = &\sum_{a=1}^{N} \frac{\prod_{k=1}^{N_f} \left[(\varphi_a - m_k - \epsilon)(\varphi_a - m_k - 3\epsilon)\right]}{\prod_{b\neq a} \left[\varphi_{ab}(\varphi_{ab} - 2\epsilon)^2(\varphi_{ab} - 4\epsilon)\right]} \\ &+ \sum_{a\neq b} \frac{2\prod_{k=1}^{N_f} \left[(\varphi_a - m_k - \epsilon)(\varphi_b - m_k - \epsilon)\right]}{\varphi_{ab}(\varphi_{ab} + 2\epsilon)^2(\varphi_{ab} - 2\epsilon) \prod_{c\neq a,b} \prod_{r=a,b} \varphi_{rc}(\varphi_{rc} - 2\epsilon)} \,. \end{aligned} \tag{C.0.9}$$

$$\begin{aligned} Z^{--++}(\varphi, m, \epsilon) = &\sum_{a=1}^{N} \frac{\prod_{k=1}^{N_f} \left[(\varphi_a - m_k + \epsilon)(\varphi_a - m_k + 3\epsilon)\right]}{\prod_{b\neq a} \left[\varphi_{ab}(\varphi_{ab} + 2\epsilon)^2(\varphi_{ab} + 4\epsilon)\right]} \\ &+ \sum_{a\neq b} \frac{2\prod_{k=1}^{N_f} \left[(\varphi_a - m_k + \epsilon)(\varphi_b - m_k + \epsilon)\right]}{\varphi_{ab}(\varphi_{ab} - 2\epsilon)^2(\varphi_{ab} + 2\epsilon) \prod_{c\neq a,b} \prod_{r=a,b} \varphi_{rc}(\varphi_{rc} + 2\epsilon)} \,. \end{aligned} \tag{C.0.10}$$

$$\begin{aligned} Z^{+-+-}(\varphi, m, \epsilon) = &\sum_{a=1}^{N} \frac{\prod_{k=1}^{N_f} (\varphi_a - m_k - \epsilon)^2}{\prod_{b\neq a} \left[\varphi_{ab}^2(\varphi_{ab} - 2\epsilon)^2\right]} \\ &+ \sum_{a\neq b} \frac{\prod_{k=1}^{N_f} \left[(\varphi_a - m_k - \epsilon)(\varphi_b - m_k + \epsilon)\right]}{\varphi_{ab}(\varphi_{ab} - 2\epsilon)^2(\varphi_{ab} - 4\epsilon) \prod_{c\neq a,b} \left[\varphi_{ac}\varphi_{bc}(\varphi_{ac} - 2\epsilon)(\varphi_{bc} + 2\epsilon)\right]} \\ &+ \sum_{a\neq b} \frac{\prod_{k=1}^{N_f} \left[(\varphi_a - m_k - \epsilon)(\varphi_b - m_k - \epsilon)\right]}{\varphi_{ab}^2(\varphi_{ab} \pm 2\epsilon) \prod_{c\neq a,b} \left[\varphi_{ac}\varphi_{bc}(\varphi_{ac} - 2\epsilon)(\varphi_{bc} - 2\epsilon)\right]} \,. \end{aligned} \tag{C.0.11}$$

$$
\begin{aligned}
Z^{-+-+}(\varphi,m,\epsilon) = &\sum_{a=1}^{N} \frac{\prod_{k=1}^{N_f} (\varphi_a - m_k + \epsilon)^2}{\prod_{b\neq a} \left[\varphi_{ab}^2 (\varphi_{ab}+2\epsilon)^2\right]} \\
&+ \sum_{a\neq b} \frac{\prod_{k=1}^{N_f} \left[(\varphi_a - m_k + \epsilon)(\varphi_b - m_k - \epsilon)\right]}{\varphi_{ab}(\varphi_{ab}+2\epsilon)^2(\varphi_{ab}+4\epsilon) \prod_{c\neq a,b} \left[\varphi_{ac}\varphi_{bc}(\varphi_{ac}+2\epsilon)(\varphi_{bc}-2\epsilon)\right]} \\
&+ \sum_{a\neq b} \frac{\prod_{k=1}^{N_f} \left[(\varphi_a - m_k + \epsilon)(\varphi_b - m_k + \epsilon)\right]}{\varphi_{ab}^2(\varphi_{ab}\pm 2\epsilon) \prod_{c\neq a,b} \left[\varphi_{ac}\varphi_{bc}(\varphi_{ac}+2\epsilon)(\varphi_{bc}+2\epsilon)\right]} \,.
\end{aligned}
\tag{C.0.12}
$$

$$
\begin{aligned}
Z^{+--+}(\varphi,m,\epsilon) = &\sum_{a=1}^{N} \frac{\prod_{k=1}^{N_f} (\varphi_a - m_k \pm \epsilon)}{\prod_{b\neq a} \left[\varphi_{ab}^2 (\varphi_{ab}\pm 2\epsilon)\right]} \\
&+ \sum_{a\neq b} \frac{2\prod_{k=1}^{N_f} \left[(\varphi_a - m_k - \epsilon)(\varphi_b - m_k + \epsilon)\right]}{\varphi_{ab}^2(\varphi_{ab}-2\epsilon)(\varphi_{ab}-4\epsilon) \prod_{c\neq a,b} \left[\varphi_{ac}\varphi_{bc}(\varphi_{ac}-2\epsilon)(\varphi_{bc}+2\epsilon)\right]} \,.
\end{aligned}
\tag{C.0.13}
$$

$$
\begin{aligned}
Z^{-++-}(\varphi,m,\epsilon) = &\sum_{a=1}^{N} \frac{\prod_{k=1}^{N_f} (\varphi_a - m_k \pm \epsilon)}{\prod_{b\neq a} \left[\varphi_{ab}^2 (\varphi_{ab}\pm 2\epsilon)\right]} \\
&+ \sum_{a\neq b} \frac{2\prod_{k=1}^{N_f} \left[(\varphi_a - m_k + \epsilon)(\varphi_b - m_k - \epsilon)\right]}{\varphi_{ab}^2(\varphi_{ab}+2\epsilon)(\varphi_{ab}+4\epsilon) \prod_{c\neq a,b} \left[\varphi_{ac}\varphi_{bc}(\varphi_{ac}+2\epsilon)(\varphi_{bc}-2\epsilon)\right]} \,.
\end{aligned}
\tag{C.0.14}
$$

These results also transform appropriately under the discrete symmetries PT and C, which manifest themselves in identities identical to (C.0.7) and (C.0.8) with a and b removed. We have also checked that the chamber dependence disappears when $N_f = 0, 1, \ldots, 2N-2$, as expected from (5.4.8) and the Moyal product.

Region of FI Space	Sign of $\nu(F)$	Multi-dimensional Pole
$++--$ Chamber	$+$	$(z_{-1}=\varphi_b-\epsilon, z_0=\varphi_c-\epsilon, z_1=\varphi_a-\epsilon)$
$\xi_1>0$	$+$	$(z_0=\varphi_c-\epsilon, z_{-1}=\varphi_c-2\epsilon, z_1=\varphi_a-\epsilon)$
$\xi_0>0$	$+$	$(z_{-1}=\varphi_b-\epsilon, z_0=\varphi_b-2\epsilon, z_1=\varphi_a-\epsilon)$
$\xi_{-1}>0$	$+$	$(z_{-1}=\varphi_b-\epsilon, z_1=\varphi_a-\epsilon, z_0=\varphi_a-2\epsilon)$
$\xi_1+\xi_0>0$	$+$	$(z_1=\varphi_a-\epsilon, z_0=\varphi_a-2\epsilon, z_{-1}=\varphi_a-3\epsilon)$
$\xi_0+\xi_{-1}>0$	$+$	$(z_{-1}=\varphi_b-\epsilon, z_0=\varphi_c-\epsilon, z_1=\varphi_c-2\epsilon)$
$\xi_1+\xi_0+\xi_{-1}>0$	$+$	$(z_0=\varphi_c-\epsilon, z_{-1}=\varphi_c-2\epsilon, z_1=\varphi_c-2\epsilon)$
	$+$	$(z_{-1}=\varphi_b-\epsilon, z_0=\varphi_b-2\epsilon, z_1=\varphi_b-3\epsilon)$
$+-+-$ Chamber	$+$	$(z_{-1}=z_0-\epsilon, z_0=\varphi_c-\epsilon, z_1=\varphi_a-\epsilon)$
$\xi_1>0$	$-$	$(z_{-1}=\varphi_b-\epsilon, z_1=\varphi_a-\epsilon, z_0=\varphi_c+\epsilon)$
$\xi_0<0$	$+$	$(z_1=\varphi_a-\epsilon, z_{-1}=z_0-\epsilon, z_0=\varphi_a-2\epsilon)$
$\xi_{-1}>0$	$-$	$(z_{-1}=\varphi_b-\epsilon, z_1=\varphi_a-\epsilon, z_0=\varphi_b)$
$\xi_1+\xi_0>0$	$-$	$(z_{-1}=\varphi_b-\epsilon, z_1=\varphi_a-\epsilon, z_0=\varphi_a)$
$\xi_0+\xi_{-1}>0$	$+$	$(z_{-1}=\varphi_b-\epsilon, z_1=z_0-\epsilon, z_0=\varphi_c-\epsilon)$
$\xi_1+\xi_0+\xi_{-1}>0$	$+$	$(z_0=\varphi_c-\epsilon, z_{-1}=\varphi_c-2\epsilon, z_1=\varphi_c-2\epsilon)$
	$+$	$(z_{-1}=\varphi_b-\epsilon, z_1=z_0-\epsilon, z_0=\varphi_b-2\epsilon)$
$+--+$ Chamber	$-$	$(z_1=\varphi_a-\epsilon, z_0=\varphi_c+\epsilon, z_{-1}=\varphi_b-\epsilon)$
$\xi_1>0$	$-$	$(z_1=\varphi_a-\epsilon, z_0=\varphi_c+\epsilon, z_{-1}=\varphi_c)$
$\xi_0<0$	$+$	$(z_1=\varphi_a-\epsilon, z_0=z_{-1}+\epsilon, z_{-1}=\varphi_b+\epsilon)$
$\xi_{-1}>0$	$-$	$(z_1=\varphi_a-\epsilon, z_0=\varphi_a, z_{-1}=\varphi_b-\epsilon)$
$\xi_1+\xi_0>0$	$-$	$(z_1=\varphi_a-\epsilon, z_0=\varphi_a, z_{-1}=\varphi_a-\epsilon)$
$\xi_0+\xi_{-1}<0$	$+$	$(z_1=z_0-\epsilon, z_0=\varphi_c-\epsilon, z_{-1}=\varphi_b-\epsilon)$
$\xi_1+\xi_0+\xi_{-1}>0$	$+$	$(z_1=z_0-\epsilon, z_0=\varphi_c-\epsilon, z_{-1}=\varphi_c-2\epsilon)$
	$+$	$(z_1=z_0-\epsilon, z_{-1}=\varphi_b-\epsilon, z_0=\varphi_b-2\epsilon)$

Table C.1: Poles contributing to the integral (5.4.35) in the $++--$, $+-+-$, and $+--+$ chambers, where a, b are fixed and $c \neq b, a$.

Region of FI Space	Sign of $\nu(F)$	Multi-dimensional Pole
$--++$ Chamber	$-$	$(z_0 = \varphi_c + \epsilon, z_{-1} = \varphi_b - \epsilon, z_1 = \varphi_a - \epsilon)$
$\xi_1 > 0$	$-$	$(z_0 = \varphi_c + \epsilon, z_{-1} = \varphi_c, z_1 = \varphi_a - \epsilon)$
$\xi_0 < 0$	$+$	$(z_0 = z_{-1} + \epsilon, z_{-1} = \varphi_b + \epsilon, z_1 = \varphi_a - \epsilon)$
$\xi_{-1} > 0$	$+$	$(z_0 = z_1 + \epsilon, z_1 = \varphi_a + \epsilon, z_{-1} = \varphi_b - \epsilon)$
$\xi_1 + \xi_0 < 0$	$+$	$(z_0 = z_1 + \epsilon, z_{-1} = z_1, z_1 = \varphi_a + \epsilon)$
$\xi_0 + \xi_{-1} < 0$	$-$	$(z_0 = \varphi_c + \epsilon, z_{-1} = \varphi_b - \epsilon, z_1 = \varphi_c)$
$\xi_1 + \xi_0 + \xi_{-1} < 0$	$-$	$(z_{-1} = z_0 - \epsilon, z_1 = z_0 - \epsilon, z_0 = \varphi_c + \epsilon)$
	$+$	$(z_0 = z_{-1} + \epsilon, z_1 = z_{-1}, z_{-1} = \varphi_b + \epsilon)$
$-+-+$ Chamber	$-$	$(z_0 = \varphi_c + \epsilon, z_1 = \varphi_a - \epsilon, z_{-1} = \varphi_b - \epsilon)$
$\xi_1 > 0$	$-$	$(z_1 = \varphi_a - \epsilon, z_{-1} = z_0 - \epsilon, z_0 = \varphi_c + \epsilon)$
$\xi_0 < 0$	$+$	$(z_0 = z_{-1} + \epsilon, z_1 = \varphi_a - \epsilon, z_{-1} = \varphi_b + \epsilon)$
$\xi_{-1} > 0$	$-$	$(z_{-1} = z_0 - \epsilon, z_1 = \varphi_a - \epsilon, z_0 = \varphi_a)$
$\xi_1 + \xi_0 < 0$	$+$	$(z_0 = z_1 + \epsilon, z_{-1} = \varphi_b - \epsilon, z_1 = \varphi_a + \epsilon)$
$\xi_0 + \xi_{-1} < 0$	$+$	$(z_1 = z_0 - \epsilon, z_{-1} = z_0 - \epsilon, z_0 = \varphi_c - \epsilon)$
$\xi_1 + \xi_0 + \xi_{-1} > 0$	$-$	$(z_1 = z_0 - \epsilon, z_{-1} = \varphi_b - \epsilon, z_0 = \varphi_c + \epsilon)$
	$-$	$(z_1 = z_0 - \epsilon, z_0 = z_{-1} + \epsilon, z_{-1} = \varphi_b - \epsilon)$
$-+-+$ Chamber	$+$	$(z_{-1} = z_0 - \epsilon, z_0 = \varphi_c - \epsilon, z_1 = \varphi_a - \epsilon)$
$\xi_1 > 0$	$-$	$(z_{-1} = \varphi_b - \epsilon, z_0 = \varphi_c + \epsilon, z_1 = \varphi_a - \epsilon)$
$\xi_0 < 0$	$+$	$(z_{-1} = z_0 - \epsilon, z_1 = \varphi_a - \epsilon, z_0 = \varphi_a - 2\epsilon)$
$\xi_{-1} > 0$	$-$	$(z_0 = z_{-1} + \epsilon, z_{-1} = \varphi_b - \epsilon, z_1 = \varphi_a - \epsilon)$
$\xi_1 + \xi_0 < 0$	$+$	$(z_{-1} = \varphi_b - \epsilon, z_0 = z_1 + \epsilon, z_1 = \varphi_a + \epsilon)$
$\xi_0 + \xi_{-1} > 0$	$+$	$(z_{-1} = z_0 - \epsilon, z_0 = \varphi_c - \epsilon, z_1 = \varphi_c - 2\epsilon)$
$\xi_1 + \xi_0 + \xi_{-1} > 0$	$-$	$(z_{-1} = \varphi_b - \epsilon, z_1 = z_0 - \epsilon, z_0 = \varphi_c + \epsilon)$
	$-$	$(z_{-1} = \varphi_b - \epsilon, z_1 = z_0 - \epsilon, z_0 = \varphi_b)$

Table C.2: Poles contributing to the integral (5.4.35) in the $--++$, $-+-+$, and $-+-+$ chambers, where a, b are fixed and $c \neq b, a$.

Region of FI space	Sign of $\nu(F)$	Multi-dimensional Pole
$++--$ Chamber	$+$	$(z_{0,1}=\varphi_a-\epsilon, z_1=\varphi_a-2\epsilon,$
$\xi_{-1}>0$		$z_{-1}=\varphi_a-2\epsilon, z_{0,2}=\varphi_a-3\epsilon)$
$\xi_0>0,\ \xi_1>0$	$+$	$(z_{0,1}=\varphi_a-\epsilon, z_1=\varphi_a-2\epsilon,$
$\xi_{-1}+\xi_0>0$		$z_{0,2}=\varphi_b-\epsilon, z_{-1}=\varphi_a-2\epsilon)$
$\xi_1+\xi_0>0$	$+$	$(z_{0,2}=\varphi_b-\epsilon, z_1=\varphi_b-2\epsilon,$
$\xi_{-1}+\xi_0+\xi_1>0$		$z_{0,1}=\varphi_a-\epsilon, z_{-1}=\varphi_a-2\epsilon)$
$+-+-$ Chamber	$-$	$(z_{0,1}=\varphi_a-\epsilon, z_1=\varphi_a-2\epsilon,$
$\xi_{-1}>0$		$z_{-1}=\varphi_a-2\epsilon, z_{0,2}=\varphi_a-\epsilon)$
$\xi_0<0,\ \xi_1>0$	$-$	$(z_{0,1}=\varphi_a-\epsilon, z_1=\varphi_a-2\epsilon,$
$\xi_{-1}+\xi_0>0$		$z_{-1}=\varphi_a-2\epsilon, z_{0,2}=\varphi_b+\epsilon)$
$\xi_0+\xi_1>0$	$+$	$(z_1=z_{0,2}-\epsilon, z_{0,2}=\varphi_b-\epsilon,$
$\xi_{-1}+\xi_0+\xi_1>0$		$z_{-1}=z_{0,1}-\epsilon, z_{0,1}=\varphi_a-\epsilon)$
$+--+$ Chamber	$+$	$(z_{-1}=z_{0,1}-\epsilon, z_{0,2}=z_1+\epsilon,$
$\xi_{-1}>0$		$z_{0,1}=\varphi_a-\epsilon, z_1=\varphi_a)$
$\xi_0<0,\ \xi_1>0$	$-$	$(z_{-1}=z_{0,1}-\epsilon, z_{0,1}=\varphi_a-\epsilon,$
$\xi_{-1}+\xi_0<0$		$z_{0,2}=\varphi_b+\epsilon, z_1=\varphi_a-2\epsilon)$
$\xi_1+\xi_0>0$	$-$	$(z_{-1}=z_{0,1}-\epsilon, z_{0,1}=\varphi_a-\epsilon,$
$\xi_{-1}+\xi_0+\xi_1>0$		$z_1=z_{0,2}-\epsilon, z_{0,2}=\varphi_b+\epsilon)$

Table C.3: Poles contributing to the integral (5.4.38) in the $++--$, $+-+-$, and $+--+$ chambers, where $a=1,\ldots,N$ and $b=1,\ldots,a-1,a+1,\ldots,N$. In this table we only list half of the poles contributing in each chamber, we also need to include the poles obtained from $z_{0,1}\leftrightarrow z_{0,2}$.

Region of FI space	Sign of $\nu(F)$	Multi-dimensional Pole
$--++$ Chamber	$-$	$(z_{0,1}=\varphi_a+\epsilon, z_{0,2}=z_1+\epsilon,$
$\xi_{-1}>0$		$z_{-1}=z_1, z_1=\varphi_a+2\epsilon)$
$\xi_0<0,\ \xi_1>0$	$+$	$(z_{0,2}=\varphi_b+\epsilon, z_1=z_{0,1}-\epsilon,$
$\xi_{-1}+\xi_0<0$		$z_{-1}=z_{0,1}-\epsilon, z_{0,1}=\varphi_a+\epsilon)$
$\xi_1+\xi_0<0$	$+$	$(z_{0,1}=\varphi_a+\epsilon, z_1=z_{0,2}-\epsilon,$
$\xi_{-1}+\xi_0+\xi_1<0$		$z_{0,2}=\varphi_b+\epsilon, z_{-1}=\varphi_a)$
$-+-+$ Chamber	$+$	$(z_1=z_{0,2}-\epsilon, z_{0,1}=\varphi_a+\epsilon,$
$\xi_{-1}>0$		$z_{-1}=\varphi_a, z_{0,2}=\varphi_a+\epsilon)$
$\xi_0<0,\ \xi_1>0$	$-$	$(z_{0,2}=\varphi_b+\epsilon, z_{-1}=z_{0,1}-\epsilon,$
$\xi_{-1}+\xi_0<0$		$z_1=z_{0,1}-\epsilon, z_{0,1}=\varphi_a-\epsilon)$
$\xi_1+\xi_0<0$	$+$	$(z_{-1}=z_{0,1}-\epsilon, z_1=z_{0,2}-\epsilon,$
$\xi_{-1}+\xi_0+\xi_1>0$		$z_{0,1}=\varphi_a+\epsilon, z_{0,2}=\varphi_b+\epsilon)$
$-++-$ Chamber	$+$	$(z_1=z_{0,1}-\epsilon, z_{0,2}=z_{-1}+\epsilon,$
$\xi_{-1}>0$		$z_{0,1}=\varphi_a-\epsilon, z_{-1}=\varphi_a)$
$\xi_0<0,\ \xi_1>0$	$-$	$(z_1=z_{0,1}-\epsilon, z_{0,1}=\varphi_a-\epsilon,$
$\xi_{-1}+\xi_0>0$		$z_{0,2}=\varphi_b+\epsilon, z_{-1}=\varphi_a-2\epsilon)$
$\xi_1+\xi_0<0$	$-$	$(z_1=z_{0,2}-\epsilon, z_{0,2}=\varphi_b-\epsilon,$
$\xi_{-1}+\xi_0+\xi_1>0$		$z_{-1}=z_{0,1}-\epsilon, z_{0,1}=\varphi_a+\epsilon)$

Table C.4: Poles contributing to the integral (5.4.38) in the $--++$, $-+-+$, and $-++-$ chambers, where $a=1,\dots,N$ and $b=1,\dots,a-1,a+1,\dots,N$. In this table we only list half of the poles contributing in each chamber, we also need to include the poles obtained from $z_{0,1}\leftrightarrow z_{0,2}$.

Bibliography

[1] R. Haag, J. T. Łopuszanski and M. Sohnius, *All Possible Generators of Supersymmetries of the S-Matrix*, *Nucl. Phys.* **B88** (1975) 257–274.

[2] S. R. Coleman and J. Mandula, *All Possible Symmetries of the S Matrix*, *Phys. Rev.* **159** (1967) 1251–1256.

[3] J. Wess and B. Zumino, *Supergauge Transformations in Four-Dimensions*, *Nucl. Phys.* **B70** (1974) 39–50.

[4] B. Assel, S. Cremonesi and M. Renwick, *Quantized Coulomb Branches, Monopole Bubbling and Wall-Crossing Phenomena in 3d $\mathcal{N} = 4$ Theories*, *JHEP* **04** (2020) 213, [1910.01650].

[5] E. Witten, *Phases of N=2 theories in two dimensions*, *Nucl. Phys.* **B403** (1993) 159–222, [hep-th/9301042].

[6] A. Hanany and E. Witten, *Type IIB superstrings, BPS monopoles, and three-dimensional gauge dynamics*, *Nucl. Phys.* **B492** (1997) 152–190, [hep-th/9611230].

[7] J. Wess and J. Bagger, *Supersymmetry and supergravity.* Princeton University Press, Princeton, NJ, USA, 1992.

[8] A. Bilal, *Introduction to Supersymmetry*, hep-th/0101055.

[9] K. Hori et al., *Mirror symmetry*, vol. 1 of *Clay mathematics monographs.* AMS, Providence, USA, 2003.

[10] L. J. Dixon, *Summer Workshop in High-energy Physics and Cosmology: Superstrings, Unified Theories and Cosmology*, 1987.

[11] W. Lerche, C. Vafa and N. P. Warner, *Chiral Rings in N=2 Superconformal Theories*, *Nucl. Phys.* **B324** (1989) 427–474.

[12] E. Witten, *Topological Quantum Field Theory*, *Commun. Math. Phys.* **117** (1988) 353–386.

[13] E. Witten, *Mirror manifolds and topological field theory*, *AMS/IP Stud. Adv. Math.* **9** (1998) 121–160, [hep-th/9112056].

[14] K. Hori and C. Vafa, *Mirror Symmetry*, hep-th/0002222.

[15] K. Hori, *Trieste Lectures on Mirror Symmetry*, *ICTP Lect. Notes Ser.* **13** (2003) 109–202.

[16] R. K. Gupta and S. Murthy, *Squashed toric sigma models and mock modular forms*, 1705.00649.

[17] D. R. Morrison and M. R. Plesser, *Summing the Instantons: Quantum Cohomology and Mirror Symmetry in Toric Varieties*, *Nucl. Phys.* **B440** (1995) 279–354, [hep-th/9412236].

[18] K. Hori and A. Kapustin, *Duality of the Fermionic 2D Black Hole and $\mathcal{N} = 2$ Liouville Theory as Mirror Symmetry*, *JHEP* **08** (2001) 045, [hep-th/0104202].

[19] I. V. Melnikov and M. R. Plesser, *The Coulomb Branch in Gauged Linear Sigma Models*, *JHEP* **06** (2005) 013, [hep-th/0501238].

[20] I. V. Melnikov and M. R. Plesser, *A-Model Correlators from the Coulomb Branch*, *JHEP* **02** (2006) 044, [hep-th/0507187].

[21] J. Caldeira, T. Maxfield and S. Sethi, *(2,2) Geometry from Gauge Theory*, *JHEP* **11** (2018) 201, [1810.01388].

[22] K. Hori and D. Tong, *Aspects of Non-Abelian Gauge Dynamics in Two-Dimensional $\mathcal{N} = (2, 2)$ Theories*, *JHEP* **05** (2007) 079, [hep-th/0609032].

[23] R. Donagi and E. Sharpe, *GLSM's for Partial Flag Manifolds*, *J. Geom. Phys.* **58** (2008) 1662–1692, [0704.1761].

[24] K. A. Intriligator and N. Seiberg, *Mirror Symmetry in Three Dimensional Gauge Theories*, *Phys. Lett.* **B387** (1996) 513–519, [hep-th/9607207].

[25] P. C. Argyres, M. R. Plesser and N. Seiberg, *The Moduli Space of Vacua of N=2 SUSY QCD and Duality in N=1 SUSY QCD*, *Nucl. Phys.* **B471** (1996) 159–194, [hep-th/9603042].

[26] N. J. Hitchin, A. Karlhede, U. Lindstrom and M. Rocek, *Hyperkähler Metrics and Supersymmetry*, *Commun. Math. Phys.* **108** (1987) 535–589.

[27] J. de Boer, K. Hori, H. Ooguri and Y. Oz, *Mirror Symmetry in Three-Dimensional Gauge Theories, Quivers and D-branes*, *Nucl. Phys.* **B493** (1997) 101–147, [hep-th/9611063].

[28] J. de Boer, K. Hori, H. Ooguri, Y. Oz and Z. Yin, *Mirror Symmetry in Three-Dimensional Theories, SL(2,Z) and D-brane Moduli Spaces*, *Nucl. Phys.* **B493** (1997) 148–176, [hep-th/9612131].

[29] V. Borokhov, A. Kapustin and X.-k. Wu, *Monopole Operators and Mirror Symmetry in Three Dimensions*, *JHEP* **12** (2002) 044, [hep-th/0207074].

[30] G. 't Hooft, *On the Phase Transition Towards Permanent Quark Confinement*, *Nucl. Phys.* **B138** (1978) 1–25.

[31] V. Borokhov, *Monopole Operators in Three-Dimensional $\mathcal{N} = 4$ SYM and Mirror Symmetry*, *JHEP* **03** (2004) 008, [hep-th/0310254].

[32] M. Bullimore, T. Dimofte and D. Gaiotto, *The Coulomb Branch of 3d $\mathcal{N} = 4$ Theories*, *Commun. Math. Phys.* **354** (2017) 671–751, [1503.04817].

[33] S. Cremonesi, A. Hanany and A. Zaffaroni, *Monopole operators and Hilbert series of Coulomb branches of 3d $\mathcal{N} = 4$ gauge theories*, *JHEP* **01** (2014) 005, [1309.2657].

[34] S. Cremonesi, A. Hanany, N. Mekareeya and A. Zaffaroni, *Coulomb branch Hilbert series and Hall-Littlewood polynomials*, *JHEP* **09** (2014) 178, [1403.0585].

[35] S. Cremonesi, A. Hanany, N. Mekareeya and A. Zaffaroni, *Coulomb branch Hilbert series and Three Dimensional Sicilian Theories*, *JHEP* **09** (2014) 185, [1403.2384].

[36] S. Cremonesi, G. Ferlito, A. Hanany and N. Mekareeya, *Coulomb Branch and The Moduli Space of Instantons*, *JHEP* **12** (2014) 103, [1408.6835].

[37] S. Cremonesi, A. Hanany, N. Mekareeya and A. Zaffaroni, T_ρ^σ *(G) theories and their Hilbert series*, *JHEP* **01** (2015) 150, [1410.1548].

[38] S. Cremonesi, *The Hilbert series of 3d* $\boldsymbol{\mathcal{N}} = 2$ *Yang–Mills theories with vectorlike matter*, *J. Phys.* **A48** (2015) 455401, [1505.02409].

[39] S. Cremonesi, N. Mekareeya and A. Zaffaroni, *The moduli spaces of 3d* $\mathcal{N} \geq 2$ *Chern-Simons gauge theories and their Hilbert series*, *JHEP* **10** (2016) 046, [1607.05728].

[40] S. Cremonesi, *3d supersymmetric gauge theories and Hilbert series*, *Proc. Symp. Pure Math.* **98** (2018) 21–48, [1701.00641].

[41] B. Assel and S. Cremonesi, *The Infrared Physics of Bad Theories*, *SciPost Phys.* **3** (2017) 024, [1707.03403].

[42] B. Assel and S. Cremonesi, *The Infrared Fixed Points of 3d* $\mathcal{N} = 4$ $USp(2N)$ *SQCD Theories*, *SciPost Phys.* **5** (2018) 015, [1802.04285].

[43] D. Gaiotto and E. Witten, *S-Duality of Boundary Conditions In* $\mathcal{N} = 4$ *Super Yang-Mills Theory*, *Adv. Theor. Math. Phys.* **13** (2009) 721–896, [0807.3720].

[44] H. Nakajima, *Towards a mathematical definition of Coulomb branches of* 3*-dimensional* $\mathcal{N} = 4$ *gauge theories, I*, *Adv. Theor. Math. Phys.* **20** (2016) 595–669, [1503.03676].

[45] A. Braverman, M. Finkelberg and H. Nakajima, *Towards a mathematical definition of Coulomb branches of* 3*-dimensional* $\mathcal{N} = 4$ *gauge theories, II*, *Adv. Theor. Math. Phys.* **22** (2018) 1071–1147, [1601.03586].

[46] A. Braverman, M. Finkelberg and H. Nakajima, *Coulomb branches of* $3d$ $\mathcal{N} = 4$ *quiver gauge theories and slices in the affine Grassmannian*, *Adv. Theor. Math. Phys.* **23** (2019) 75–166, [1604.03625].

[47] H. Nakajima, *Introduction to a provisional mathematical definition of Coulomb branches of* 3*-dimensional* $\mathcal{N} = 4$ *gauge theories*, 1706.05154.

[48] A. Braverman and M. Finkelberg, *Coulomb Branches of 3-Dimensional Gauge Theories and Related Structures*, *Lect. Notes Math.* **2248** (2019) 1–52, [1807.09038].

[49] B. Assel, *Ring Relations and Mirror Map from Branes*, *JHEP* **03** (2017) 152, [1701.08766].

[50] B. Assel, *The Space of Vacua of 3d* $\mathcal{N} = 3$ *Abelian Theories*, *JHEP* **08** (2017) 011, [1706.00793].

[51] L. C. Jeffrey and F. C. Kirwan, *Localization for Nonabelian Group Actions*, *Topology* **34** (1995) 291–327, [alg-geom/9307001].

[52] F. Benini, R. Eager, K. Hori and Y. Tachikawa, *Elliptic Genera of 2d* $\mathcal{N} = 2$ *Gauge Theories*, *Commun. Math. Phys.* **333** (2015) 1241–1286, [1308.4896].

[53] S. Cremonesi, *An Introduction to Localisation and Supersymmetry in Curved Space*, *PoS* **Modave2013** (2013) 002.

[54] J. J. Duistermaat and G. J. Heckman, *On the Variation in the cohomology of the symplectic form of the reduced phase space*, *Invent. Math.* **69** (1982) 259–268.

[55] N. Berline and M. Vergne, *Classes caractéristiques équivariantes. Formule de localisation en cohomologie équivariante*, *C. R. Acad. Sci. Paris* **295** (1982) 539–541.

[56] M. F. Atiyah and R. Bott, *The moment map and equivariant cohomology*, *Topology* **23** (1984) 1–28.

[57] N. A. Nekrasov, *Seiberg-Witten Prepotential from Instanton Counting*, *Adv. Theor. Math. Phys.* **7** (2003) 831–864, [hep-th/0206161].

[58] V. Pestun, *Localization of Gauge Theory on a Four-Sphere and Supersymmetric Wilson Loops*, *Commun. Math. Phys.* **313** (2012) 71–129, [0712.2824].

[59] A. Kapustin, B. Willett and I. Yaakov, *Exact Results for Wilson Loops in Superconformal Chern-Simons Theories with Matter*, *JHEP* **03** (2010) 089, [0909.4559].

[60] D. L. Jafferis, *The Exact Superconformal R-Symmetry Extremizes Z*, *JHEP* **05** (2012) 159, [1012.3210].

[61] N. Hama, K. Hosomichi and S. Lee, *Notes on SUSY Gauge Theories on Three-Sphere*, *JHEP* **03** (2011) 127, [1012.3512].

[62] F. Benini and S. Cremonesi, *Partition Functions of $\mathcal{N} = (2, 2)$ Gauge Theories on S^2 and Vortices*, *Commun. Math. Phys.* **334** (2015) 1483–1527, [1206.2356].

[63] N. Doroud, J. Gomis, B. Le Floch and S. Lee, *Exact Results in D=2 Supersymmetric Gauge Theories*, *JHEP* **05** (2013) 093, [1206.2606].

[64] J. Gomis and S. Lee, *Exact Kähler Potential from Gauge Theory and Mirror Symmetry*, *JHEP* **04** (2013) 019, [1210.6022].

[65] F. Benini and B. Le Floch, *Supersymmetric localization in two dimensions*, *J. Phys.* **A50** (2017) 443003, [1608.02955].

[66] D. S. Park, *Recent developments in 2d $\mathcal{N} = (2, 2)$ supersymmetric gauge theories*, *Int. J. Mod. Phys.* **A31** (2016) 1630045, [1608.03607].

[67] F. Benini, *Localization in supersymmetric field theories*, 2016.

[68] V. Pestun et al., *Localization techniques in quantum field theories*, *J. Phys.* **A50** (2017) 440301, [1608.02952].

[69] A. Alekseev, *Notes on Equivariant Localization*, *Lect. Notes Phys.* **543** (2000) 1–24.

[70] G. Festuccia and N. Seiberg, *Rigid Supersymmetric Theories in Curved Superspace*, *JHEP* **06** (2011) 114, [1105.0689].

[71] C. Closset and S. Cremonesi, *Comments on $\mathcal{N} = (2, 2)$ Supersymmetry on Two-Manifolds*, *JHEP* **07** (2014) 075, [1404.2636].

[72] E. Witten, *Two dimensional gauge theories revisited*, *J. Geom. Phys.* **9** (1992) 303–368, [hep-th/9204083].

[73] F. Benini and A. Zaffaroni, *A topologically twisted index for three-dimensional supersymmetric theories*, *JHEP* **07** (2015) 127, [1504.03698].

[74] C. Closset, S. Cremonesi and D. S. Park, *The equivariant A-twist and gauged linear sigma models on the two-sphere*, *JHEP* **06** (2015) 076, [1504.06308].

[75] L. Ferro, T. Łukowski and M. Parisi, *Amplituhedron meets Jeffrey–Kirwan Residue*, *J. Phys.* **A52** (2019) 045201, [1805.01301].

[76] Y. Honma and M. Manabe, *Local B-model Yukawa couplings from A-twisted correlators*, *PTEP* **2018** (2018) 073A03, [1805.02661].

[77] A. Szenes and M. Vergne, *Toric reduction and a conjecture of Batyrev and Materov*, *Invent. Math.* **158** (2004) 453–495, [math/0306311].

[78] K. Hori, H. Kim and P. Yi, *Witten Index and Wall Crossing*, *JHEP* **01** (2015) 124, [1407.2567].

[79] F. Englert and P. Windey, *Quantization Condition for 't Hooft Monopoles in Compact Simple Lie Groups*, *Phys. Rev.* **D14** (1976) 2728.

[80] P. Goddard, J. Nuyts and D. I. Olive, *Gauge Theories and Magnetic Charge*, *Nucl. Phys.* **B125** (1977) 1–28.

[81] A. Kapustin, *Wilson-'t Hooft operators in four-dimensional gauge theories and S-duality*, *Phys. Rev.* **D74** (2006) 025005, [hep-th/0501015].

[82] T. Okuda and Y. Yoshida, *SUSY localization for Coulomb branch operators in omega-deformed 3d N=4 gauge theories*, 1910.01802.

[83] N. Nekrasov and E. Witten, *The Omega Deformation, Branes, Integrability, and Liouville Theory*, *JHEP* **09** (2010) 092, [1002.0888].

[84] Y. Ito, T. Okuda and M. Taki, *Line operators on $S^1 \times \mathbb{R}^3$ and quantization of the Hitchin moduli space*, *JHEP* **04** (2012) 010, [1111.4221].

[85] A. Kapustin and E. Witten, *Electric-Magnetic Duality And The Geometric Langlands Program*, *Commun. Num. Theor. Phys.* **1** (2007) 1–236, [hep-th/0604151].

[86] D. Tong, *The Holographic Dual of $AdS_3 \times S^3 \times S^3 \times S^1$*, *JHEP* **04** (2014) 193, [1402.5135].

[87] T. D. Brennan, A. Dey and G. W. Moore, *'t Hooft Defects and Wall Crossing in SQM*, *JHEP* **10** (2019) 173, [1810.07191].

[88] H. Hayashi, T. Okuda and Y. Yoshida, *Wall-crossing and operator ordering for 't Hooft operators in $\mathcal{N} = 2$ gauge theories*, *JHEP* **11** (2019) 116, [1905.11305].

[89] C.-K. Chang, H.-Y. Chen, D. Jain and N. Lee, *Connecting Localization and Wall-Crossing via D-Branes*, *Nucl. Phys.* **B932** (2018) 298–322, [1512.02645].

[90] T. D. Brennan, A. Dey and G. W. Moore, *On 't Hooft Defects, Monopole Bubbling and Supersymmetric Quantum Mechanics*, *JHEP* **09** (2018) 014, [1801.01986].

[91] T. D. Brennan, *Monopole Bubbling via String Theory*, *JHEP* **11** (2018) 126, [1806.00024].

[92] B. Assel and A. Sciarappa, *On Monopole Bubbling Contributions to 't Hooft Loops*, *JHEP* **05** (2019) 180, [1903.00376].

[93] F. Benini, R. Eager, K. Hori and Y. Tachikawa, *Elliptic genera of two-dimensional N=2 gauge theories with rank-one gauge groups*, *Lett. Math. Phys.* **104** (2014) 465–493, [1305.0533].

[94] C. Closset, W. Gu, B. Jia and E. Sharpe, *Localization of twisted $\mathcal{N} = (0, 2)$ gauged linear sigma models in two dimensions*, *JHEP* **03** (2016) 070, [1512.08058].

[95] S. Cabrera and A. Hanany, *Branes and the Kraft-Procesi Transition*, *JHEP* **11** (2016) 175, [1609.07798].